Chapter 2
Direct, Mold-Less Production Systems

Reinhart Poprawe, Wolfgang Bleck, Frank Thomas Piller, Günther Schuh, Sebastian Barg, Arne Bohl, Sebastian Bremen, Jan Bültmann, Christian Hinke, Ruth Jiang, Robin Kleer, Simon Merkt, Ulrich Prahl, Michael Riesener, Johannes Schrage, Christian Weller and Stephan Ziegler

Contents

R. Poprawe (✉)
Fraunhofer Institute for Laser Technology (ILT), Steinbachstraße 15, 52074 Aachen, Germany
e-mail: reinhart.poprawe@ilt.fraunhofer.de

W. Bleck · J. Bültmann · U. Prahl
Department of Ferrous Metallurgy (IEHK), RWTH Aachen University, Intzestr. 1, 52072 Aachen, Germany
e-mail: wolfgang.bleck@iehk.rwth-aachen.de

F.T. Piller · R. Jiang · R. Kleer · C. Weller
Research Area Technology, Innovation, Marketing, Entrepreneurship (TIME), RWTH Aachen University, Kackertstr. 7, 52072 Aachen, Germany
e-mail: piller@time.rwth-aachen.de

G. Schuh
Laboratory for Machine Tools and Production Engineering (WZL), RWTH Aachen University, Steinbachstraße 19, 52074 Aachen, Germany
e-mail: G.Schuh@wzl.rwth-aachen.de

C. Brecher and D. Özdemir (eds.), *Integrative Production Technology*,
DOI 10.1007/978-3-319-47452-6_2

2.1 Summary

"What would you make if you had a machine that could make everything?" (Lipson and Kurman 2013). This quote refers to additive manufacturing (AM), or colloquially 3D printing, which seems to offer unlimited possibilities and with that boundless opportunity. AM is defined as "[…] the process of joining materials to make objects from 3D model data, usually layer upon layer […]" (ASTM International 2015). This cutting-edge technology has made leaps and bounds over the course of the last decade, and while some limitations still exist, many expect AM to be a game changer in the way we manufacture products. In the last couple of years, AM has gained tremendous public attention and sparked public interest. The highest profile endorsement came when the President of the USA, Barack Obama, mentioned 3D printing in his 2013 State of the Union address, saying that "3D

S. Barg · A. Bohl · M. Riesener
Laboratory for Machine Tools and Production Engineering (WZL),
RWTH Aachen University, Steinbachstr. 53B, 52074 Aachen, Germany
e-mail: s.barg@wzl.rwth-aachen.de

S. Bremen
Fraunhofer Institute for Laser Technology (ILT), Steinbachstr. 15,
52074 Aachen, Germany
e-mail: sebastian.bremen@ilt.fraunhofer.de

C. Hinke · S. Merkt · J. Schrage · S. Ziegler
Chair for Laser Technology (LLT), RWTH Aachen University,
Steinbachstr. 15, 52074 Aachen, Germany
e-mail: christian.hinke@llt.rwth-aachen.de

printing […] has the potential to revolutionize the way we make almost everything" (Forbes 2013). While AM has been hailed as the future of production and referred to as a technology with the potential of paving the path toward a new industrial revolution (and certainly has a lot of promise), it is important to understand the current possibilities and limitations of AM technology.

Therefore, this chapter highlights the AM technology's potential of

i. Creating a value increment when offering highly customized products,
ii. Enhancing MC offerings from a modular choice to continuous adjustments in a product's solution space,
iii. Facilitating an enhanced market segmentation strategy,
iv. Disrupting cost paradigms of conventional manufacturing systems, and
v. Changing market structures and increasing available product variety

These seven propositions are derived within this study that build an impetus for future research and point out how firms and individuals can benefit from AM's capabilities.

All in all, we identified the effects AM has on consumer's willingness to pay (WTP) (and, thus, the value increment of AM), on market segmentation and a firm's payoff function. In our research, mass customization (MC) literature is enriched with empirical evidence on AM's value creation potential when enhancing customizability of products from a modular approach to full customization with stepless adjustments of product design attributes (Weller et al. 2015b). Moreover, we established economic market structure models extended to capture AM technology's specific characteristics (Weller et al. 2015a).

Based on the implications resulting from the integration of AM technologies like selective laser melting (SLM) into manufacturing, the product production system (PPS) developed by Bohl (2015) is revised regarding these influences. The factors determine the formalizations to describe the characteristic curves, which in turn define the isoquants of equivalent operating points in the PPS. In the following, the main formalizations of the four dimensions of the PPS are presented in the four conflict fields "Product Program," "Product Architecture," "Production Structure" and "Supply Chain."

Today's cost drivers of SLM-manufactured parts are the machine costs. In this chapter, the influence of the workpiece dimensions, the filling degree of workpiece envelope, the build envelope dimension, the number and output power of lasers and the number of scanner systems on the unit costs are examined systematically. For instance, this work reveals that a parallelization of the SLM process by means of two lasers and two scanner systems by keeping the total laser power constant can be favorable from an economic point of view. From these results, new machine concepts are developed and presented.

As a result for the process development for high-power selective laser melting (HP SLM), it can be observed that increased laser power up to P_L = 2 kW can be used to significantly increase the productivity of the SLM process. Overall, the theoretical build-up rate is increased up to $\dot{V} = 27$ mm^3/s, which is an increase by a factor of nine in comparison with the SLM state-of-the-art process for the tool steel 1.2709. In addition, the mechanical properties for conventional and HP SLM-manufactured test specimen are analyzed. The results show that by adapting the heat treatment the reference for the tool steel 1.2709 can be attained while increasing the theoretical build-up rate significantly.

The qualification of lattice structures for custom part properties is performed on two different types of structures: type f2cc,z, and hollow-sphere structures. Different laser exposure strategies and their influence on the microstructure and mechanical properties of the lattice structures are examined experimentally. The development of scaling laws is based on a large number of different types and configurations of lattice structures (e.g., the specific energy absorption in dependence of the cell width of the structures). A databank is developed that provides an interface to a design engineer to find suitable structures regarding concrete requirements based on the above-presented scaling laws. Based on these results, a design methodology is proposed that systemizes the process of designing function components with custom part functions by integrating lattice structures to functional components.

Characterizing and qualifying of the high-manganese steel X30Mn22 for the SLM process was done by developing process parameters for SLM manufacturing of fully dense test samples. Furthermore, the microstructures of the samples were analyzed and tensile tests of test samples were determined experimentally. Furthermore, SLM scanning strategies for the reduction of distortion of test specimen out of X30Mn22 were developed. Those scanning strategies make it possible to build complex part geometries with less support structures.

2.2 Motivation and Research Question

The overall objective of the research area “Mold-less Production Systems” is the resolution of the dichotomy between scale and scope—that is, manufacturing products at mass production costs with a maximum fit to customer needs or functional requirements. The emerging AM technologies like SLM provide great potential for solving this dilemma. Due to technology-intrinsic advantages like one-piece-flow capability and almost infinite freedom of design, AM was recently even described as “the manufacturing technology that will change the world” (The Economist 2011) and several international research groups are working on this topic (Lindemann et al. 2006; Hopkinson et al. 2006; Gibson et al. 2015).

Due to the complex nature of production systems, the technological potential of AM can only be realized by a holistic comprehension of the complete value creation chain, especially the interdependency between products and production processes. In order to enable AM for industrial serial production, the production efficiency of AM systems has to be further increased. This leads to the following research question:

> How can product and process structures for direct, mold-less production systems be harmonized in order to significantly increase the production efficiency of individual products, fulfilling customer needs?

2.2.1 *Objectives and Measures for the Second Funding Period*

The focus of the research area "Direct, mold-less Production Systems" is on the development, implementation and validation of mold-less production systems, based on mold-less manufacturing technologies developed in the first funding period, see Schuh et al. (2012). AM technologies in general and in particular SLM are characterized by a fundamentally different relation of cost, lot size and product complexity compared to conventional manufacturing processes (see Fig. 2.1). There is no increase of costs for small lot sizes (in contrast to mold-based technologies), and implementing high-speed additive manufacturing technologies like HP SLM machines allows for cost reduction up to higher lot sizes (Schleifenbaum et al. 2011) (see Fig. 2.1, left). Due to no increase of costs for shape complexity (in contrast to subtractive technologies), innovative products with enhanced functionality can be manufactured in the first place and furthermore at a low cost effort (see Fig. 2.1, right).

Thus, only the holistic development of a direct, mold-less production system, taking into account all relevant interdependencies along the product creation chain, provides the full economic, ecologic and social benefits of AM technologies in future production.

Main objective is analyzing and modeling the interdependencies between each individual item in the whole AM ecosystem. Figure 2.2 illustrates the AM ecosystem with all its entities. This reference architecture allows for the systematic design of products and direct, mold-less production systems, fulfilling partly opposing and continuously changing requirements from economics (e.g., lot size, costs), ecology (e.g., resource consumption, weight) and society (e.g., grade of individualization, grade of customer interaction, purchase experience) at its optimum.

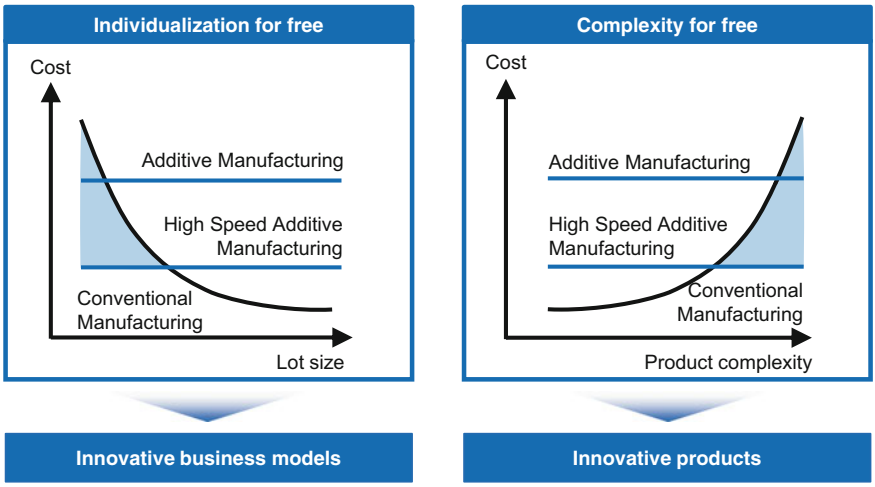

Fig. 2.1 Innovative business models and innovative products enabled by direct, mold-less production technologies

In parallel with the development of the required deterministic and cybernetic models (see Sects. 2.3.2.2 and 2.4.1), a high-performance SLM production system is realized and *validated* (see Sect. 2.4.3.11). This SLM production system increases the performance in terms of productivity (e.g., build-up rate, scanning strategy) and scalability (e.g., build platform size, architecture of optical system, number of beam sources, automation strategy for 100 % laser on time) to a holistic production system for individualized industrial serial production. The deep holistic comprehension resulting from methodical and experimental research will allow for a continuous stream of new, innovative products (number of variants) and business models (see Sect. 2.4.1) (e.g., value co-creation, grade of customer interaction, grade of individualization) in the following high-wage country relevant fields: (i) lightweight components, enabled by new topology optimization methods (regarding the shape and geometric features), simultaneously providing functional (e.g., load, heat transfer) optimization while taking into account technology (SLM)-specific restrictions and potential (see Sect. 2.4.5), (ii) highly functional integrated components, enabled by new SLM-specific design guidelines for complex multi-part constructions (see Sect. 2.4.5) (e.g., assembly strategy, strength, surface roughness), (iii) highly customized products, enabled by new interactive product design tools, simultaneously providing new ways of customer inclusion (e.g., experience design, generative design) while taking into account technology (SLM)-specific restrictions and potential (see Sects. 2.4.1 and 2.4.5) and (iv) high-performance SLM production systems for industrial individualized serial production (see Sect. 2.4.3.11), enabled by the developed reference architecture for direct, mold-less production systems.

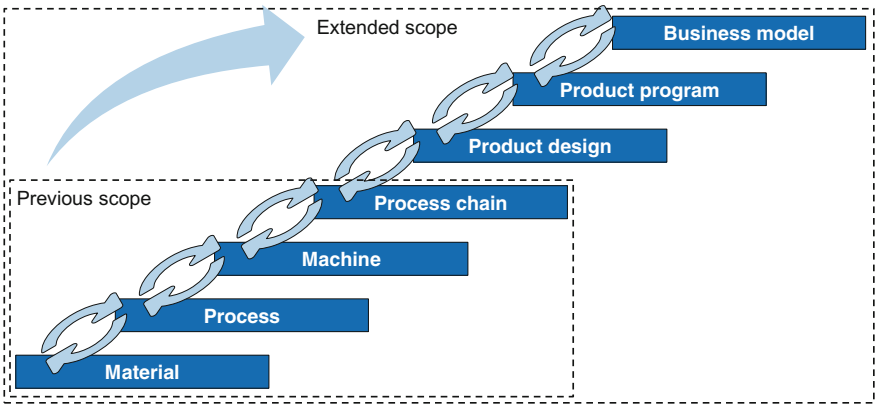

Fig. 2.2 Schematic illustration of the complete AM ecosystem

The main objectives of phase 2 are as follows:

1. Development of a reference architecture for direct, mold-less production systems applied on selective laser melting (SLM) production systems
2. Implementation and validation of a SLM production system as a representative one-piece-flow production system with high product diversity

These two objectives can be expressed by the following research questions, resolved into the single projects. They will be detailed and answered in the following sections.

Research question regarding the Product Production System (PPS)

- "How does the complexity-based behavior of a product production system (PPS) look like when implementing new production technologies like SLM?"

Research question regarding the machine-specific cost drivers

- "What are the main machine-specific cost drivers of SLM machines that influence SLM manufactured parts?"
- "How does a machine architecture have to look like in order to achieve a maximum productivity at lowest product costs?"

Research questions regarding the business model:

- "What are AM technology's characteristics that influence value creation activities of firms and economic interactions between firms and individuals? How can firms and individuals benefit from AM technology's capabilities?"

- "What economic theories are suitable to assess the implications of AM technology for theory development and managerial practice?"
- "How can we empirically measure the performance implications of AM technology?"

Research questions regarding the high-power selective laser melting (HP SLM):

- "Can the increased laser power up to $P_L \leq 2$ kW be transferred into an increased theoretical build-up rate for the tool steel 1.2709 and how is the process efficiency influenced?"
- "What impact does the increased laser power $P_L \leq 2$ kW and the adaption of process parameters have on the microstructure and the mechanical properties according to the employed heat treatment?"

Research questions regarding the qualification of lattice structures manufacturing by SLM:

- "How can the macroscopic behavior of lattice-integrated customized parts be modeled?"
- "What are the mechanical properties of SLM-manufactured lattice structures and lattice-integrated parts?"
- "How does a design methodology for components with customized part functions look like?"

Research questions regarding the use of steels in SLM

- "Which mechanical properties and which microstructure can be achieved by processing the high-manganese steel X30Mn22 with SLM?"

2.3 State of the Art

2.3.1 Value Creation with Customized Products for the Case of Additive Manufacturing (AM)

Throughout the twentieth century, mass production dominated economic thinking as companies tried to offer goods and services at low prices to reach as many people as possible. For the longest time, the Pareto principle, sometimes called the 80/20 rule, which states that 20 % of the products are responsible for 80 % of sales, applied to almost all products (Anderson 2008). The most successful companies were the ones that provided products for the lowest prices; now, this thought process might not be valid anymore. Thinking has shifted toward mass customization. Companies offer goods and services in variations to ensure that nearly everyone finds exactly what they want (Pine 1993). Currently, companies try to understand customer needs and offer a broader spectrum of products to meet those

exact desires. For example, most major sports apparel companies have already created Web sites where customers can choose different colors and styles to individualize their equipment. These changes in offering have already made an impact on economic theory as classical modes and principles no longer apply. Now, offering a multitude of products is the norm and offerings expanded massively so that consumers can buy exactly the products that they actually want, creating the long tail of products that cannot be found in traditional retail stores. This has also enabled consumers to change behavior: they now actively seek niche products that are not offered in traditional stores, causing the Pareto principle to lose relevance as a more diversified range of products is sold and revenue is spread over a larger number of items (see Fig. 2.3). The overall trend toward a more diversified product range results in greater sales generated from niche products, creating the so-called long tail (Brynjolfsson et al. 2011). The customer's shift away from already successful products reduces the concentration of sales on only a few items. Instead, customers focus their attention on a broader spectrum of items, resulting in a more diverse range of products that is being sold by companies.

2.3.1.1 Value and Customer Benefits of Customized Products: The Mass Customization Approach

Instead of fighting over market shares with stiff competition and participating in price wars, many companies turn away from the strategy of mass production and opt instead for the principle of mass customization (Anderson 2008). There are several advantages to product customization. Primarily, individually customizing products leads to higher customer satisfaction (Coelho and Henseler 2012). Furthermore, the customization process typically increases customer involvement with the product and results in increasing customer loyalty (Piller and Schoder 1999). Both effects can be turned into higher revenues. Currently, mass customized products are made by mass manufacturing several modular elements, which can then be assembled in different combinations. This method limits the true

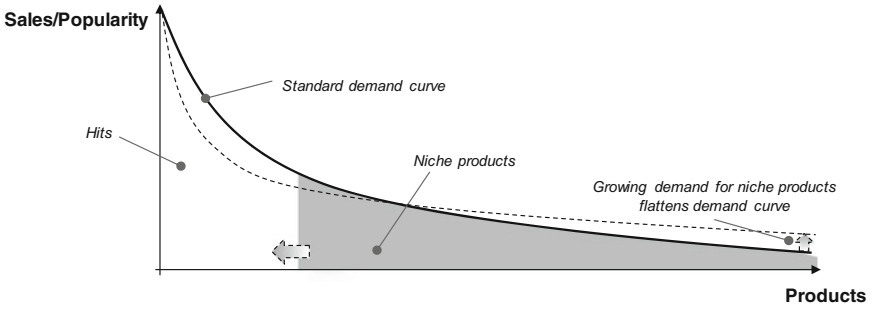

Fig. 2.3 Long tail of product demand (Elberse 2008)

individuality of the product and, accordingly, the benefits that come with mass customization (Wang et al. 2014). AM, with its advantages, allows the fabrication of truly customized products as consumers do not have to make any compromises regarding product design. Consumers can customize product attributes to a point where the product meets their exact wishes. All of this can be achieved without increasing the production costs for the manufacturer while maximizing the benefits of customization. The above-mentioned effects only describe and explain the consumers' demand side factors that contribute to the "long tail."

While Internet technology enables retailers to reduce costs through cheaper storage and shipping methods, producers so far have not been able to adapt to this new trend on a large scale. Lampel and Mintzberg (1996) defined five stages of customization from full standardization, for which design, fabrication, assembly and distribution are completely standardized to full customization, where all of those steps are completely customized (Lampel and Mintzberg 1996). Figure 2.4 illustrates the segments in between full standardization and full customization: segmented standardization, where only distribution is customizable by the consumer; mass customization, where the design and fabrication are done on a standardized level, but also leave the customer the liberty of customizing the assembly, which basically amounts to letting the customer choose from several modules; and tailored customization, a step in between mass customization and full customization. Here, fabrication can be customized to match a specific consumer demand, but the customer cannot influence the original design. This can only be done with full customization, where every step of the process can be altered or adjusted to ensure that customers get exactly what they want. Full customization can only be achieved by letting customers actively participate in the design process.

This is where AM technology has the chance to revolutionize production. Modeling software enables customers to print their own designs, while only marginally increasing production costs. As customers become more involved with a product by taking part in the customization process, their perceived product value as well as the probability of purchase increases. As consumers and producers design a product together, they are learning from one another and producers can use that knowledge to further address a customer's need in the future.

Currently, mass customization is restricted to giving consumers the option of picking from a few shapes or colors, thereby severely limiting the customization options, and the benefits that come with it (Weller et al. 2015b).

Producers attempt to increase the customizability of their product while still sticking to the concept of mass customization by analyzing consumer needs and allowing consumers to alter those aspects that are most important to them. This process is called "solution space development" (Piller 2004). Companies attempt to limit additional costs by maximizing the solution space to provide greater variety in their products without having to make major changes. Finding the equilibrium of an

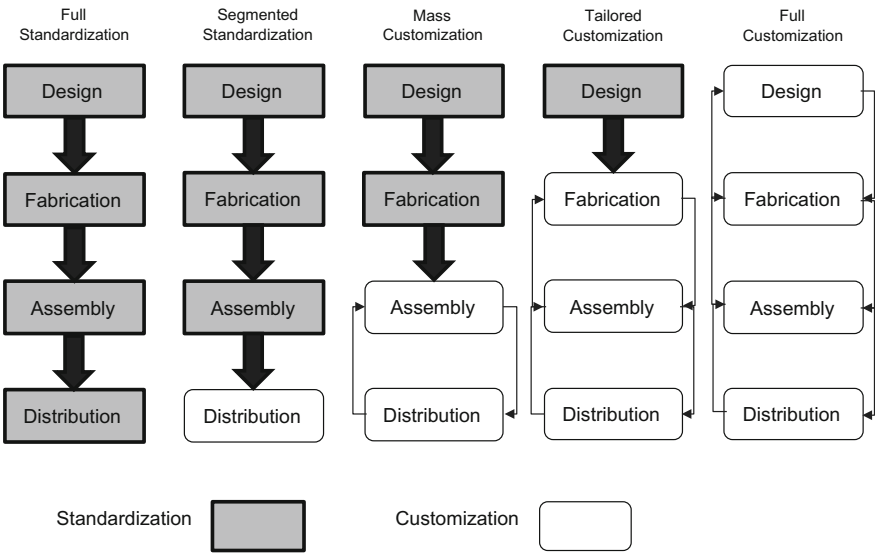

Fig. 2.4 Stages of customization (Lampel and Mintzberg 1996)

acceptable solution space and an efficient production system in order to be able to offer mass customized products is the biggest challenge that producers face.

Furthermore, producers have to choose between modular and continuous approaches to mass customization (Steiner 2014). While modular approaches can be implemented by conventional machinery, it limits the consumer to predetermined options, which are each mass produced to generate economies of scale. The continuous, true full customization approach, on the other hand, can be realized by AM technology, which has no limitations or dependencies regarding production capabilities and can be offered for competitive prices (Gebhardt 2012; Berman 2012; Lipson and Kurman 2013). Products made using AM technology can be produced using a single machine in a single-step production process, completely independent from the laws of production that have shaped our society since the industrial revolution. While there are already several existing companies that offer fully customized printed products, such as jewelry or small pieces of art, the market is still emerging and the potential is perceived to be high.

Figure 2.5 shows four diagrams representing product demand, mass production, mass customization and full customization, respectively.

The x and y axes represent two product attributes which outline the solution space. The concentric circles describe consumer demand for a combination of the two attributes. The highest demand is depicted with the innermost circle, while each larger circle shows a decrease in demand. Mass producers focus their production on

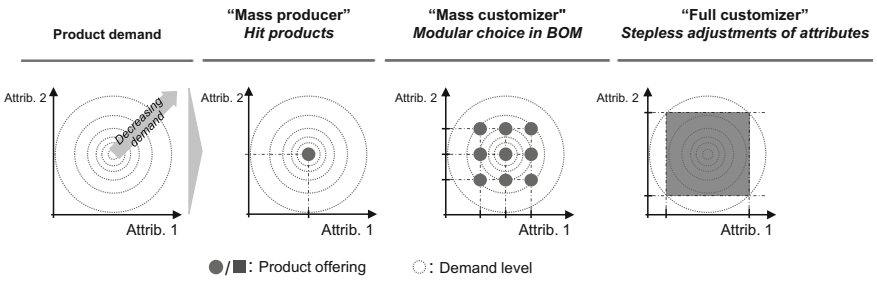

Fig. 2.5 Mass production versus full customization (Weller et al. 2015b)

a standardized product, which combines the two attributes in a way to attract the most demand, expecting to maximize their sales by producing the product that is the most sought after. A mass customization approach offers predefined combinations of attributes, leaving consumers to select the combination that appeals to them the most. The diagram on the far right depicts the full customization approach, where instead of covering certain combinations, the consumer can steplessly create any combination of the two attributes within certain boundaries. Consumers can combine both attributes freely to create an infinite amount of different outcomes, inevitably finding exactly what they are looking for (Schreier 2006; Franke and Piller 2004).

2.3.2 *Complementation of Manufacturing with SLM Technologies*

In the recent literature, the influences of complementing manufacturing with AM technologies are discussed extensively. Regarding the integration of SLM in manufacturing, the approach of Weller et al. (2015a) indicates a significant increase in product variety in the product program due to a nearly cost-free product configuration. According to Bechthold et al. (2015), the possibility of manufacturing several components within one process step as a result of geometrical flexibility can have enormous impacts on the flexibility of the product architecture. Moreover, Thomas and Gilbert (2014) and Baumers et al. (2016) made relevant contributions to the effects of AM technologies on the supply chain and the production structure. Thereafter, the reduced production process enables a decentralization of manufacturing locations as a possible innovation to shorten supply chains, open up distant markets and guarantee an increasing manufacturing flexibility.

From a technological point of view, various high-potential mold-less processes have been developed to encounter shortening development times and therefore allow highly iterative product development (Gebhardt 2013; Gibson et al. 2015). To satisfy the requirements of mass production, SLM turned out to be the most suitable technology regarding material, time of production as well as precision and quality (Bechthold et al. 2015; Eisenhut and Langefeld 2013; Gobrecht 2009). At this stage of the technological development, SLM is experiencing ongoing optimizations regarding the process and product characteristics to enhance itself as a future enabling technology (Berman 2012). Therefore, Bremen et al. (2011) presented an approach to further developing the laser and process speed as well as the build-up rate.

2.3.2.1 The Product Production System (PPS)

In order to cope with the increasing complexity of products and hence the increasing complexity of the production process due to the individualization of demand, it requires an integrative view of the overall value-added chain. Therefore, Schuh et al. (2012) developed a methodology for the complexity-oriented controlling of manufacturing firms and the assessment of the strategic fit between the product and its production. The methodology's objective is to enable the derivation of operating points regarding the optimum number of variants within the product program.

The approach divides the overall system into the four subsystems: Product Program, Product Architecture, Production Structure and Supply Chain. Each of the subsystems is defined by two conflicting dimensions described with key performance indicators (KPIs). Factors that cause an increase in complexity interact not only on a subsystem level, but rather have a complex impact on the overall system. By controlling the complexity in the product and its manufacturing process with the assistance of the presented KPIs, the operating point of a manufacturing firm can be ascertained and evaluated. The reference figure of the operating point is the number of external product variants offered. Within the PPS, equivalent operating points are defined by the isoquants in the form of characteristic curves. Since the interdependencies are of nonlinear and multi-dimensional nature, alterations generally have far-reaching effects. For example, complications in the production process can have a decisive influence on the compliance with specified delivery deadlines and hence on the supply chain. The overall PPS is shown in Fig. 2.6.

Although this methodology addresses the regarded internal scale-scope dilemma, it does not suit the requirements of modern companies that supplement production with SLM technologies. Therefore, the methodology is further developed as presented in the following.

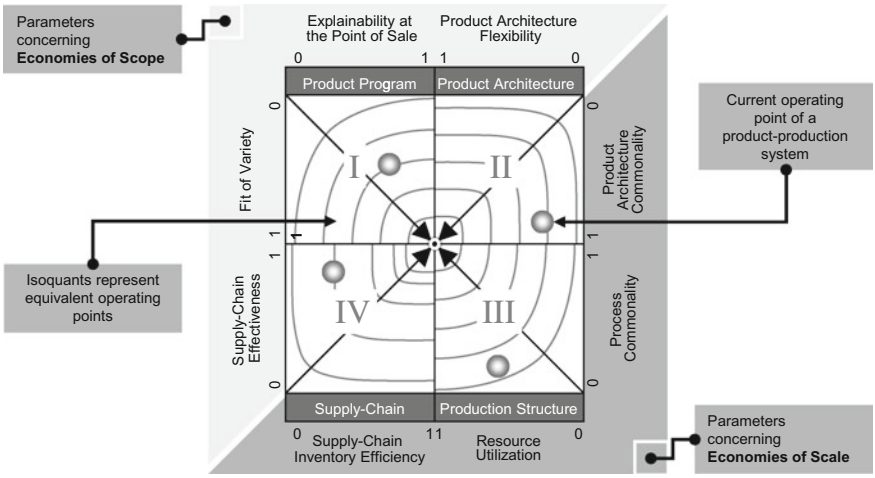

Fig. 2.6 Product production system (PPS) (Schuh et al. 2013)

2.3.2.2 Influences on the Product Production System (PPS) from Integrating SLM Technologies into Manufacturing

With respect to the complex interdependencies within the dimensions of a PPS, all state-of-the-art studies mentioned in Sect. 2.3.2 lack an integrative view of the consequences of integrating SLM technologies into manufacturing. The recent literature is singularly focused on describing impact on one particular conflict field only. Hence, the approach described in the following offers an integrative view. Therefore, the influences of integrating SLM technologies into the PPS are described in order to derive the revised PPS in consideration of changing circumstances in a manufacturing firm. In the following, the main influences on all of the four dimensions Product Program, Product Architecture, Supply Chain and Production Structure are presented.

Influences on the Conflict Field "Product Program"

With regard to the product program, the integration of SLM into manufacturing is likely to increase the number of offered product variants significantly. The conflict field in the dimension Product Program is defined by the factors "Explainability at the Point of Sale" and "Individualization of the Product Portfolio" (Bohl 2015). Compared to the traditional PPS, which lacks of the consequences of integrating SLM into manufacturing, the degree of customer interaction needs to be considered within the dimension "Explainability at the Point of Sale." This consideration takes into account that the integration of SLM into manufacturing enables the customer to interact during the development process, e.g., in terms of 3D-CAD data. Therefore, the possibility of maximum customer-individualized components or product variants arises. Those variants are better explained by the sales department as the customer already interacted during product development (Bogers et al. 2016; Rayna

and Striukova 2014). On the contrary, the increasing complexity in processes and documentation needs to be considered. Hence, product programs realized through modular product platforms need to be optimized to the effect of maximum individualization without increasing the internal complexity significantly. Besides this, SLM technologies enable the possibility for an economic production of lot size 1 product variants, since no tools or molds are necessary anymore (Kieviet 2015; Rayna and Striukova 2016).

Altogether, the integration of SLM into manufacturing enables the realization of a higher degree of individualization within the product program. To keep the explainability at the point of sale, companies should take the opportunity of increased possibilities of interaction with the customer.

Influences on the Conflict Field "Product Architecture"
In terms of the product architecture, the integration of SLM into manufacturing redefines the reallocation of modules and increases the complexity of the product architecture. Therefore, the importance of standardized interfaces arises. The conflict field is defined with the contradictory dimensions "Product Architecture Flexibility" and "Product Architecture Commonality." With SLM-complemented manufacturing, the influences of the degree of customer integration, the degree of dynamic adaption and the degree of integration of SLM components need to be considered. By enabling customer interactions during product development and manufacturing, the degree of dynamic adaption arises. This leads to the effect that the product architecture becomes more flexible by enabling fast shipment of customer-specific variants. In addition, SLM parts enable the focus on component functionality due to fewer restrictions in terms of manufacturability (Gibson et al. 2015; Wohlers 2015). Moreover, different functionalities and parts can be integrated in single SLM parts due to the possibility of realizing complex structures and facing less manufacturing restrictions. In contrast, the integration of SLM components negatively affects the commonality of modules and components in the product architecture. Summarizing the effects on the product architecture, the flexibility is likely to steepen due to a faster and more intense customer interaction, while the commonality of the product architecture seems to decrease. However, this decrease is less relevant due to the diminution of the significance of scale effects.

Influences on the Conflict Field "Production Structure"
Efficiency in terms of manufacturing is realized by low idle times of manufacturing resources and optimized processes. Integrating SLM technologies affects both dimensions significantly. The conflict field on the production structure reaches in two dimensions: "Process Commonality in Manufacturing" and "Resource Utilization in Manufacturing". In particular, the process commonality is affected by integrating SLM into manufacturing due to a significantly lower number of material flow relationships resulting from one-step processes for components manufactured with SLM technologies (Gebhardt 2013). Due to the possibility of integrating functionality within one SLM part, less handling is needed. Therefore, the influences depending on the share of SLM technologies in manufacturing need to be considered. Moreover, the degree of dynamic adaption correlates negatively with

the resource utilization. The dynamic adaption is more likely to be faster with low resource utilization since the availability of (SLM) resources will be more flexible.

Influences on the Conflict Field "Supply Chain"
Along with the integration of SLM technologies, a lot of expectations are to be found regarding the supply chain. These expectations result from the incident that a higher degree of SLM integration enhances inventory efficiency since components are produced on request and therefore overcapacity due to extended production can be avoided.

The dimension of the supply chain is defined by the conflicting factors "Supply-Chain Effectiveness" and "Supply-Chain Inventory Efficiency". When complementing the PPS of Bohl (2015) with SLM technologies, additional influences need to be considered. The degree of decentralization takes into account that manufacturing components with SLM diminishes the different resource types needed. Moreover, the share of AM technologies influences the supply-chain inventory efficiency indirectly by reducing the amount of stocked components and products. Due to the independence of SLM resources, one main potential of integrating SLM into manufacturing is the prospect of intensified decentralization of production to open up new markets, minimize inventory and serve customer requirements with shortened delivery times.

2.3.3 Machine-Specific Cost Drivers in Additive Manufacturing (AM) Technologies like Selective Laser Melting (SLM)

2.3.3.1 Current SLM Machines

The market for commercial SLM systems is characterized by a high degree of innovation and wide dynamics. Numerous providers offer SLM systems for professional end users to build complex functional components. The well-known representatives of the first hour include SLM Solutions Group (headquarters: Lübeck, Germany), EOS GmbH (headquarters: Krailling near Munich, Germany), Concept Laser GmbH (headquarters: Lichtenfels, Germany), Realizer GmbH (headquarters: Borchen, Germany) and Trumpf AG (headquarters: Ditzingen near Stuttgart, Germany). Trumpf AG stopped the production of SLM systems after the first generation founded a joint venture with the Italian company Sisma [headquarters: Piovene Rocchette (VI) Italy], to re-enter the market for SLM machines. International providers of SLM machines are Renishaw (headquarters: Gloucestershire, UK) and 3D Systems with LayerWise (headquarters: Leuven, Belgium).

Commercial systems differ in five points: the powder application mechanism, the laser and scanner system, the available build envelope, the inert gas flow and the system peripherals. Figure 2.7 shows a typical SLM machine on the example of a

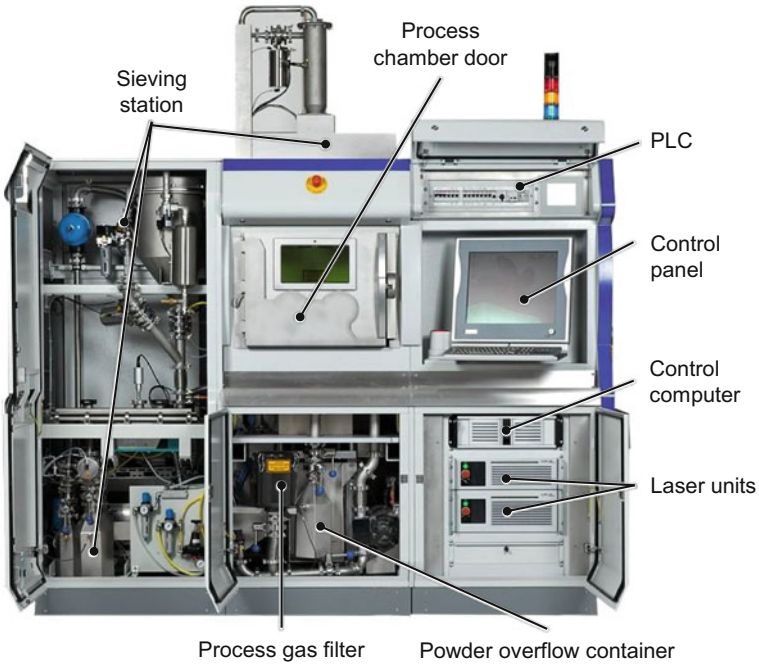

Fig. 2.7 SLM machine using the example of a SLM280HL (photograph by SLM Solutions)

SLM machine by SLM Solutions. This SLM machine is equipped with two fiber lasers with an output power from 400 W up to 700 W and a build envelope of $250 \times 250 \times 300$ mm^3. The powder application is typically done with the aid of a brush, a roller or a silicone lip (see Fig. 2.8). One powder layer thickness can be varied between 20 and 200 µm and is done by the downward movement of the build platform. High laser powers can be used to increase the build-up rate and thus increase the productivity.

The protective gas flow is an important and necessary function of SLM machines to remove splashes and vapors from the surrounding components and the coupling window from contamination that may adversely affect the laser radiation. Typical protective gases used in SLM machines are argon and nitrogen. Typically, the protective gas flow is applied from one platform side over the build platform and is sucked on the other side (see Fig. 2.8, left). The gas is filtered in a gas filter system to remove spatters and solid waste out of the shielding gas. Some SLM machines comprise a recirculating air filter system with an automatic self-cleaning function of the filter to ensure a long lifetime of the filter elements.

The SLM machine manufacturers typically use their own data formats for transferring the prepared CAD data to their machines. Materialise (headquarters: Leuven, Belgium) develops and distributes the preprocessing software Magics (including Marcam Autofab). This software allows for support structure generation,

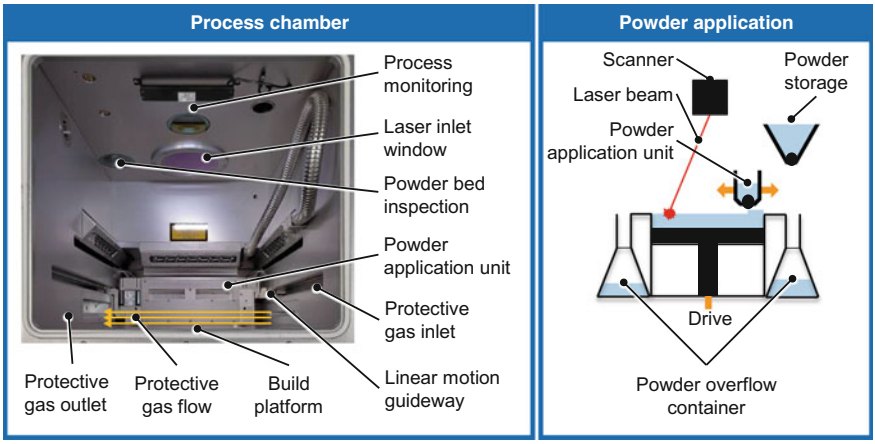

Fig. 2.8 Photograph of process chamber (*left*) and schematic illustration of the powder application process (*right*) (photograph by SLM solutions, illustration by Fraunhofer ILT)

virtual positioning of the workpieces in the build envelope, slicing the CAD data into the single layers and transferring the build data to the SLM machine. SLM-processible materials on commercial systems include stainless steels, aluminum alloys, nickel-based alloys, titanium alloys and pure titanium.

Current trends in SLM machine development are multi-scanner systems, which allow the simultaneous exposure of the powder bed with multiple lasers. Thus, the main time of the process can be reduced and larger components are manufactured economically by linking individual scan fields. The greatest build envelope in a SLM machine can be found in the SLM machine X line 2000R® with a size of $800 \times 400 \times 500$ mm^3. This machine is equipped with two laser beam sources with 1 kW output power (each). One special feature of this SLM machine is the two build chambers placed on a rotating platform. This allows for simultaneous producing in one build chamber during the pre- or postprocessing in the second one. The downtime of the machine during the workpiece change and machine setup can be reduced.

Both the parallelization of the SLM processes and the parallelization of machine setup increase total machine productivity, but will take significantly larger capital expenditures for additional laser and scanner systems.

Therefore, it is necessary to examine the components and assemblies of SLM machines that represent the cost drivers in the SLM production process.

2.3.3.2 Current Cost Models

In the literature, several approaches for the description and calculation of manufacturing costs of SLM-manufactured components exist.

Rickenbacher et al. (2013) described a cost model for determining the SLM manufacturing costs of one single part per build job and also a mixed build job (Rickenbacher et al. 2013). The determined costs are factored in: preparing CAD data (supports attachment, of which expenditure depends on the component geometry and its complexity), preparation of the build job (virtual part orientation, of which expenditure depends on the number of components), preparation of the machine and the build job process time (the build job time is estimated based on 24 build jobs, doing a linear regression analysis), powder removal, component removal of the substrate plate, component finishing.

The study conducted by Roland Berger Strategy Consultants divided the SLM manufacturing costs into direct costs (e.g., for material expenses) and indirect costs (energy, labor, machining and overhead costs) (Roland Berger Strategy Consultants 2013). In this study, the key assumptions were made with a fixed machine price (machine purchase price of € 500,000), a machine operating time of eight years, machine utilization of 83 % and a constant build-up rate of 10 cm^3/h. The powder price was assumed with € 89/kg for stainless steel powder. The outcome is that the SLM manufacturing costs are dominated by approximately 50 % of the machine costs, 26 % material costs, while labor costs account for 21 %.

Baumers presented a methodology for the quantitative analysis of the shape complexity, the build time, the process energy flows and financial costs of SLM-manufactured workpieces applied (Baumers 2012). Results indicate that—at least for the technology variant electron beam melting (EBM)—shape complexity may be realized at zero marginal energy consumption and cost. Furthermore, the combined estimator of build time, energy consumption and cost suggests that AM process efficiency is independent of production volume. Rather, this thesis argues that the key to efficient AM operation lies in the user's ability to exhaust the available build space.

Baumers et al. (2016) compared the cost performance of two different AM systems for EBM and direct metal laser sintering (DMLS). High specific costs, measured at £ 2.39 and £ 6.18 per one cubic centimeter of material deposited, are identified. The research demonstrated differing levels of system productivity, suggesting that the observed deposition rates are not sufficient for the adoption of EBM and DMLS in high-volume manufacturing applications. Despite the absence of amortizable tooling costs, the analysis also revealed that economies of scale are achievable in AM.

The mentioned approaches differ significantly in terms of the level of detail of their analyses. But no present approach focuses on the integrated machine assemblies and components (e.g., number of laser beam sources and laser output power, build envelope size) in order to derive SLM machine optimization measures.

2.3.4 High-Power Selective Laser Melting (HP SLM)

One of the most important topics to pave the way for SLM to series production is the increase of the productivity (Gausemeier 2013). In order to increase the productivity of the SLM process, it is necessary to increase the theoretical build-up rate

$$\dot{V} = D_S \cdot \Delta y_S \cdot v_S, \tag{2.1}$$

which is calculated by the factors scan line spacing Δy_s, layer thickness D_S and scanning speed v_s, see Eq. (2.1) (Schleifenbaum 2012).

In addition to the productivity, the efficiency of the SLM process is an important value. This means how efficiently the employed laser power can be transferred into an increased theoretical build-up rate. A parameter to quantify the efficiency of the SLM process is the volume energy

$$E_V = \frac{P_L}{D_S \cdot \Delta y_S \cdot v_S}, \tag{2.2}$$

which is calculated according to Eq. (2.2) (Meiners 1999).

For the use of SLM in series production, a trade-off between increase of the productivity and increase of efficiency has to be investigated.

According to the current state of the art, two general principles to increase the theoretical build-up rate exist in commercial available machines (SLM Solutions Group AG 2015; EOS GmbH 2015; Concept Laser GmbH 2015). The first principle is to use up to four laser sources parallel in the SLM process. By the use of this principle, the theoretical build-up rate can be linear increased by the number of laser sources used. However, each optical system, consisting of a scanning and focusing unit, needs a separate scanning field and an overlap between these scanning fields in order to assure a mechanical bonding for overlapping parts. Therefore, the platform size has to be increased by each additional laser source. The advantage of this principle is that the beam diameter and beam profile are not changed compared to the conventional SLM ($P_L \leq 400$ W, $d_s \approx 100$ µm). For this reason, the process parameters scanning speed v_s, scan line spacing Δy_s and layer thickness D_S do not have to be adjusted (Fig. 2.9).

In contrast, the second principle to increase the productivity of the SLM process is the use of increased laser power up to $P_L = 1$ kW and the adaption of process parameters. This principle is generally defined as high-power selective laser melting (HP SLM) and is one of the key results of the first phase of the Cluster of Excellence "Integrative Production Technology for High-Wage countries" (Brecher 2012). Increasing the laser power and keeping the beam diameter stable leads to an increased intensity in the interaction zone between powder material and laser. In particular, materials with lower heat conductivity show evaporation, spattering and deep welding effects by increasing the intensity, in which a stable and reproducible process is not possible.

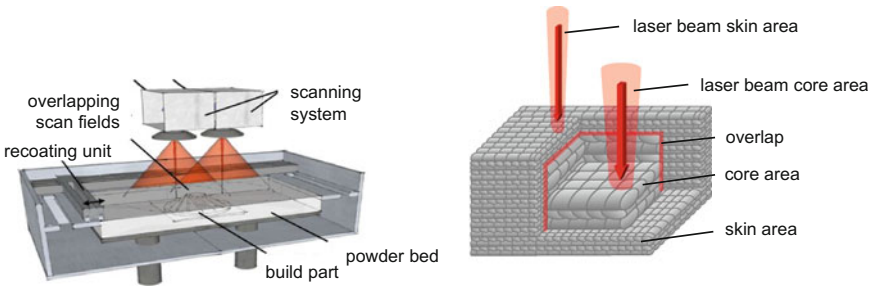

Fig. 2.9 Principles to increase productivity of the SLM process

In order to prevent these effects, the beam diameter is increased to decrease the intensity in the interaction zone—although the detailed resolution and surface roughness are negatively influenced. The so-called skin–core strategy offers the potential to combine high productivity and an adequate surface roughness by dividing the part into the two areas: skin and core. The skin is processed with a layer thickness D_S = 30–50 µm, a laser power of $P_L \leq 400$ W and a beam diameter of $d_s \leq 100$ µm with the aim to achieve a comparable surface roughness in comparison with conventional SLM ($P_L \leq 400$ W, $d_s \approx 100$ µm). For the core area, an increased beam diameter d_s = 500–1000 µm, a layer thickness D_S = 50–200 µm and a laser power $P_L \leq 1$ kW are used to increase the theoretical build-up rate.

Due to the use of an increased beam diameter, the scanning speed is especially decreased, which results in a significant change of the cooling and solidification behavior in the SLM process. The cooling and solidification behavior directly influences the microstructure and the mechanical properties. According to the current state of the art, there are no fundamental studies on the influence of HP SLM on the resulting microstructure and the mechanical properties for tool steels.

Therefore, research with different beam diameters (d_S = 70 µm and d_S = 720 µm), beam profiles (Gaussian and top hat), laser power ($P_L \leq 2$ kW) and process parameters (Δy_s, D_S, v_s) is carried out for the maraging tool steel X3NiCoMoTi18-9-5 (1.2709) to answer the aforementioned research questions.

2.3.5 *Qualification of Lattice Structures Manufactured by Selective Laser Melting (SLM) for Custom Part Properties*

The integration of lattice structures in functional components is one of the most promising approaches to exploit the full technology potential of the SLM process. The main advantages of cellular materials are a great stiffness-to-weight ratio and great energy absorption and damping capabilities. In addition to these advantages,

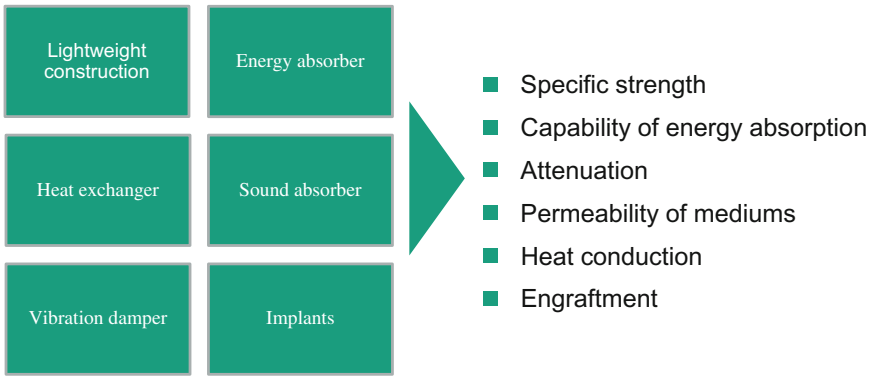

Fig. 2.10 Applications and derived part functions of cellular material

process time can be reduced by substituting solid material by lattice structures in areas of lower stress. Moreover, SLM allows modifying the part functions—such as stiffness—locally by an adjustment of the geometric parameters of the lattice structures.

Currently, cellular materials are used in various fields such as lightweight construction, as energy and sound absorbers, vibration dampers, in-heat exchangers and implants. Within these domains cellular materials fulfill different tasks through their specific properties, which can be derived from their applications. The main applications and derived functions are shown in Fig. 2.10 (Ashby 2006; Gibson and Ashby 1999; Rehme 2009).

Several researchers are examining the unique capability of manufacturing lattice structures with SLM (Rehme 2007, 2009, 2011; Gümrük and Mines 2013; Shen et al. 2012; Hao et al. 2012). The overall goal to effectively make use of the unique properties of lattice structures in real parts is illustrated in Fig. 2.11. Depending on the stress or on particular functions of part areas, lattice structures are substituting solid material. This combination of lattice structures and solid material results in extreme lightweight parts with customized part functions which cannot be built by conventional manufacturing technologies such as casting or cutting (see Fig. 2.11, top pictures). The main challenges in designing these types of customized parts are the intricate modeling of the macroscopic behavior, the mostly unknown mechanical properties and the absence of a design methodology for components with customized part functions (see also Fig. 2.11).

Rehme (2009) analyzed the properties of cubic lattice structures in detail and suggested a classification in analogy to crystallography (see Fig. 2.12). To manufacture these types of structures, Rehme (2009) introduced the so-called point-like exposure, a special scanning strategy. Structure types with horizontal struts were not considered by Rehme (2009) due to the overhang restriction of SLM process. In his research, various lattice structure blocks with a constant strut diameter of approximately 500 µm were manufactured in different relative densities. The relative density

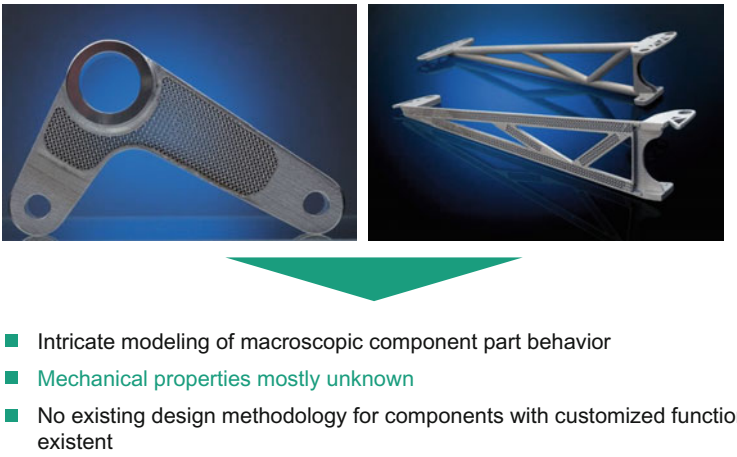

Fig. 2.11 Vision and main challenges to resolve (Merkt 2016)

of the cell types varied, with different cell widths from 1.5 to 6 mm. The mechanical properties of the lattice structures were determined in tensile, compression and shear tests. If one considered the specific mechanical properties (MPa per kg), structure type f2cc,z showed the overall best performance of all structure types (Rehme 2009).

One requirement to consider is that this structure type shows a highly anisotropic behavior and may not be built in any build-up direction. Nevertheless, cubic lattice structures are the most analyzed type of lattice structures, and the first scaling laws to describe the mechanical properties of these structures independent of geometric parameters were developed by Rehme (2009). The functional behavior of lattice structure can usually be described in good accordance with the following exponential Eq. (2.3) (Rehme 2009):

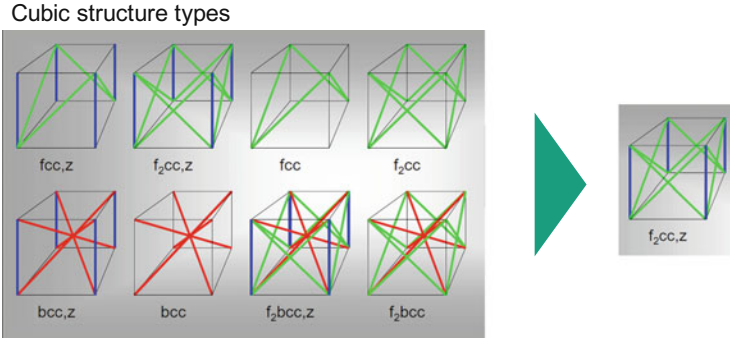

Fig. 2.12 Classification of cubic lattice structures according to Rehme (2009)

$$\frac{K^*}{K_{\text{solid}}} = C * \left(\frac{\rho^*}{\rho_{\text{solid}}}\right)^n; \tag{2.3}$$

K^* Property of cellular material;
K_{solid} Property of solid material;
C Constant of proportionality;
ρ^* Density of cellular material;
ρ_{solid} Density of solid material.

The lack of scaling laws to describe the mechanical properties of lattice structures, the absence of isotropic structure types and the limited understanding of the influence of different scanning strategies on the mechanical properties currently hinders the further distribution of lattice structure designs.

2.3.6 Steels in the Selective Laser Melting (SLM) Process

2.3.6.1 Results of the First Phase

In the first phase of the Cluster of Excellence, the primarily examined materials were the hot working steel X38CrMo5-1 (material number 1.2343) and the stainless steel X2CrNiMo17-12-2 (material number 1.4404 or AISI 316L). The main goal was to influence the melt pool dynamics by adding alloying elements to achieve a more stable process and produce a surface with reduced roughness. The X38CrMo5-1 was additionally alloyed with 0.4 wt% of carbon in a first step and 0.4 wt% of carbon plus 2 wt% of copper in a second step. The X2CrNiMo17-12-2 was compared with an X3CrNiCuMo17-11-3-2 stainless steel (material number 1.4578 or AISI 316 K) because of its 3 wt% of copper. To quantify the influence of the alloying elements on the surface roughness of the samples produced by means of SLM, the side surfaces were examined with respect to their surface topography and roughness. Regarding the hot working steel, the X38CrMo5-1+C featured significantly reduced roughness and the X38CrMo5-1+C+Cu even more. So the carbon and copper had a positive influence. On the other hand, the stainless steels both had similar roughness values. A positive effect of the copper was not measurable.

In the second phase, the focus of the research was shifted to the mechanical properties of the processed steels. Analyzing the mechanical properties of lattice structures made of X2CrNiMo17-12-2 stainless steel, adapting the postprocess heat treatment of the X3NiCoMoTi18-9-5 maraging steel for better mechanical properties, and introducing and characterizing the high-manganese steel X30Mn22 to the SLM process.

2.3.6.2 Mechanical Properties of Steels Processed by Selective Laser Melting (SLM)

Selective Laser Melting might be able to process every material that can be molten and solidified again. So every steel should be processible, but the list of already processed steels is short. And the list of processed steels with published mechanical properties like tensile tests is even shorter. The mechanical properties from tensile tests of two different tool steels, a hot-working tool steel and a maraging steel, four different stainless steels and two high-manganese steels found in the literature are shown in Fig. 2.13. They are indicated with a letter for the different steels and a number for the different sources and additionally with the angle of the build direction if stated in the literature. In this case, 0° is a sample that was built lying on the substrate plate which leads to tensile testing direction and scanning layers to be parallel. A standing sample with tensile testing direction perpendicular to the scanning layers is indicated with 90°. The values for ultimate tensile strength, uniform elongation and/or total elongation, depending on what was shown in the literature, are averaged for each source (see Table 2.1).

The mechanical properties differ vastly even for the same steel due to different material conditions like various postprocess heat treatments or as-built, meaning without any heat treatment after the SLM process at all. In particular, mechanical properties of the tool steels are depending on the heat treatment performed after the SLM process. But the SLM process parameters themselves—for example, laser power, scanning speed, scanning strategies—have a high influence on the mechanical properties, not only because of imperfections but also because of the microstructure and the surface of the sample. Another influence on the differing

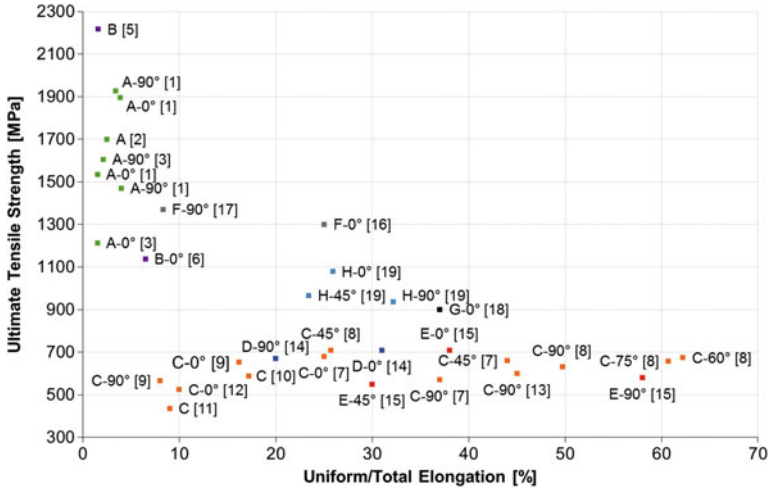

Fig. 2.13 Mechanical properties of steels processed by SLM with build direction, if stated in the literature

Table 2.1 Steels processed by SLM with their literature with indication used for Fig. 2.13

Indication	Steel	Source
A	X38CrMoV5-1 hot-working tool steel	1. Schleifenbaum (2012)
		2. Over (2003)
		3. Holzweissig et al. (2015)
B	X3NiCoMoTi18-9-5 maraging steel	4. see Sect. 2.4.4
		5. Yasa et al. (2010)
		6. Casalino et al. (2015)
C	X2CrNiMo17-12-2 stainless steel	7. Merkt (2016)
		8. Shifeng et al. (2014)
		9. Mertens et al. (2014)
		10. Wei et al. (2015)
		11. Yadroitsev and Smurov (2010)
		12. Zhang et al. (2013)
		13. Bültmann et al. (2015)
D	X10CrNiTi18-9 stainless steel	14. Ma et al. (2015)
E	X5CrNi18-10 stainless steel	15. Guan et al. (2013)
F	X5CrNiCuNb16-4 stainless steel	16. Mohles et al. (2010)
		17. Murr et al. (2012)
G	X60Mn22 high-manganese steel	18. Niendorf and Brenne (2013)
H	X30Mn22 High-manganese steel	19. see Sect. 2.4.6

results potentially is different sample geometries and tensile test conditions, from mini tensile test specimens to larger regular samples.

Uniform or total elongation was used depending on what was shown in the literature. Different mechanical properties of the same steel may occur due to different sample geometries, scanning strategies, process parameters, and material conditions like as-built or heat-treated (for the list of steels and literature sources, see Table 2.1).

2.4 Results

2.4.1 Value Creation with Customized Products for the Case of Additive Manufacturing (AM)

2.4.1.1 Value Dimensions of Customized Products

Several studies regarding mass customization have linked customization to an increase in perceived product value (Franke and Piller 2004; Schreier 2006; Franke and Schreier 2010). In order for that to be the case, the consumer needs to benefit from either the final product or the process of designing it to a greater extent than

the process-caused effort (Schreier 2006; Franke and Schreier 2010). To put these terms into perspective, mass customization research has developed specific categories which describe and categorize them (Franke and Schreier 2010; Schreier 2006; Merle et al. 2010; Ulrich 2011; Franke et al. 2009):

i. Preference fit: product-related utilitarian benefit that customers perceive when a product's characteristics (design, features) match their individual requirements.
ii. Uniqueness value and pride of ownership: product-related hedonic benefits that customers perceive when a customized product constitutes a piece of differentiation and makes the customer pride of being the creator of the customized product.
iii. Process enjoyment: process-related hedonic benefit customers perceive when the co-designing activity of customizing a product constitutes an enjoyable, rewarding and fun activity (the so-called I designed it myself effect).
iv. Reduction of process complexity, effort and risk: process-related utilitarian benefit that customers perceive when the co-design process reduces search and evaluation costs related to the product choice.

The above-mentioned criteria all affect consumers' perceived value of a product. A brief analysis of the four categories preference fit, uniqueness value and pride of ownership, reduction of process complexity, and process enjoyment helps to demonstrate why AM technology leads to a higher WTP. In general, higher customer perceived value is derived directly from the benefits a customer experiences through the product itself or the process of creating it. The preference fit category describes how higher customer benefit directly correlates with the degree the customers' demands are met. Since products produced through AM have the highest variation potential, they are highly likely to be the most beneficial to the customer. Uniqueness and value of ownership increases with individuality of the product. AM allows the creation of truly original, one-of-a-kind products that maximize customer benefits. While some might argue that the process enjoyment of co-designing a product is not really measurable, many consumers find the idea of creating something themselves exhilarating (Franke et al. 2010). AM technology allows customers not just to obtain a customized product, but also lets the customer become deeply involved in the designing process. The "I designed it myself effect" is not to be underestimated in its effects on the perceived value of a product (Franke et al. 2010).

2.4.1.2 Involvement and Perceived Product Value

Consumers' perceived product value is a complex composition of several factors and difficult to exactly pinpoint how certain attributes affect customers' WTP. However, several studies have shown that product involvement is a key element in perceived product value (Franke et al. 2010; Gordon et al. 1998).

Product involvement describes a customer's perceived personal relevance of the product based on attributes such as inherent needs, values and interests (Zaichkowsky 1985). Accordingly, products that initiate high involvement in consumers tend to be of great value or relevance to the consumer.

It is therefore logical that customers who are deeply involved with a product are more likely to have concrete ideas as to what the product should look like or be able to do and are subsequently more interested in customization (Franke et al. 2009). Consumers who display high product involvement are also less willing to accept compromises of product features, which is an argument for AM technology, since consumers can design their own product without any compromises regarding preference fit.

Despite all the headway mass customization has made over the last years, it still has not spread to most aspects of everyday life. There are several reasons for why the concept has not "taken off" yet, and while Piller (2004) discusses all of them, we will only mention the most relevant ones here. For the longest time, manufacturers were not able to produce truly customized products at competitive prices. AM has the potential of changing that. But the biggest hurdle for producers are consumers themselves: Few have made real experience with mass customization, and while this number will have increased significantly since the article in 2004, mass customization still attracts a rather small target group (Piller 2004).

2.4.1.3 Cognitive Costs of Product Customization

Cognitive costs of product customization are described as the indirect costs that arise with customization, in addition to the potential price premiums a customer has to pay (Piller 2004). These costs can significantly influence a consumer's benefit from a product, thus altering his or her perceived product value. Research has shown that customers who are more interested in or have a positive attitude toward customization activities are generally less likely to see the co-designing process as a chore or an unpleasant experience. Accordingly, customers who lack a positive attitude toward customization often find the co-designing process tedious, resulting in higher cognitive costs and hence a reduced overall benefit from customization.

Since the cognitive costs may negate the positive effects gained from customization, the overall effect of customization has to be re-evaluated. This effect, dubbed "mass confusion" by Huffman and Kahn (1998), is mainly the result of the so-called burden of choice (Piller 2004). The burden of choice is based on the realization that customers generally seek quick and simple solutions for their needs. When a product or process becomes too complex or the variety is too large, the customer might be overwhelmed by all the information and refuse to make a decision, or feel unhappy about his choice later (Franke et al. 2009; Schreier 2006). Additionally, many consumers are either unsure about what they really want or not able to describe their needs using product attributes, making it nearly impossible to create a product with a high preference fit, potentially negating the positive benefits of AM technology (Piller 2004). As a result, consumers who show low product

involvement tend to avoid customization activities that require too much effort (Weller et al. 2015b).

In conclusion, consumers who display low product involvement could bear cognitive costs while simultaneously profiting less from product customization. Our studies' aim was therefore to evaluate whether customers nowadays are willing to pay a price premium for individually customized products despite higher effort and cognitive costs.

2.4.1.4 The Value of Higher Co-Design Freedom

Focusing on the question of whether AM can be a source of value creation, we analyzed the case of full customization. Thus, we compared it to conventional (modular) mass customization offerings and assessed consumers' perceived product value in two studies. We further identified drivers of perceived product value.

In a first study, we assessed the value increment of enhanced customization in a simulated online buying process of customizable espresso cups. Round about 360 participants of every age set were present in equal measures. Online participants were exposed to three different treatments in random order: Treatment 1: a standard product with no self-designing option where they made a choice out of a predefined range of espresso cups; Treatment 2: a modularly customizable product with various product design configurations for color scheme, size and shape; and Treatment 3: a continuously customizable product with the option to edit product design steplessly representing the highest degree of product co-design freedom; this product design was enabled by using AM technology. This scenario gave the participants the following options to choose from: Treatment 1 offered twelve different standard product variants, whereas Treatments 2 and 3 allowed the participants to change the shape of the espresso cup by adjusting the height, weight, surface smoothness and color through a mock-up of an online toolkit. The research question was whether an additional degree of customization enabled by AM (Treatment 3) led to an overall higher perceived product value compared to conventional customization options. The general aim was to identify a value increment by comparing the WTP for all three treatments (see Fig. 2.14).

The result of the first study was that the delta between WTP for a highly customizable product (Treatment 3) and a standard product (Treatment 1) reached a value of +189 %, whereas the WTP for a highly customizable product (Treatment 3) is 50 % higher when compared to the modular approach in Treatment 2. Due to these findings, we started a second study which shifted the focus on the trend of increasing perceived product value for higher co-design freedom in customization offerings, comparing the modularly customizable approach to the continuously customizable approach with AM.

In a second study, we again let consumers state their perceived product value for an espresso cup with different degrees of customizability, but this time in a real experimental setup with a binding WTP measure (i.e., a lottery approach). Participants were, again, exposed to alternatives with different degrees of

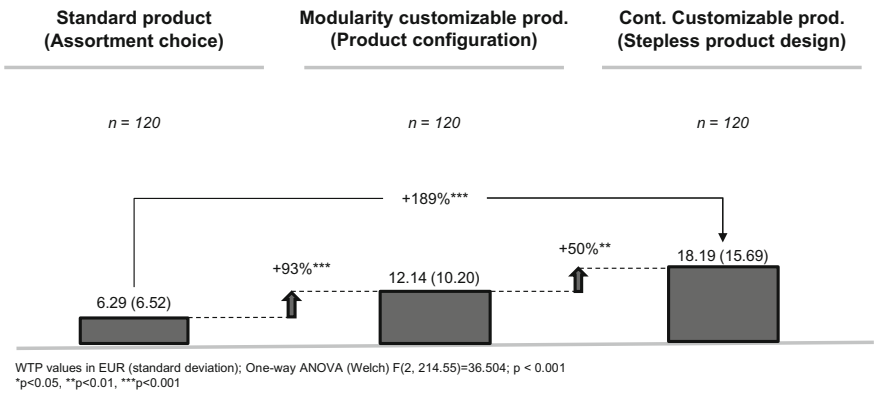

Fig. 2.14 Comparison of WTP (Weller et al. 2015b)

customization. This time around the comparison was about WTP in two treatments —that is, modularly customizable product attributes and continuously adjustable product attributes. The experiment was conducted with functional online toolkits in a laboratory environment. The number of participants reached a total amount of 66. Like before, participants were able to co-design their individually customized espresso cups with an online toolkit that was especially programmed for this purpose. In order to capture the most realistic and most probable price participants were truly willing to pay, they were asked for their binding WTP. In the end, participants received a 3D-printed copy of their self-designed espresso cup and had to pay for it. The aim here was to gather additional insights for explaining the trend observed in the previous study, meaning the increase of perceived product value from a modular (Treatment 1) to a full customization approach (Treatment 2) while making use of AM technology.

Overall, we found that full customization leads to a significant value upside in Studies 1 and 2. When steplessly adjusting product attributes, WTP was between 50 and 68 % higher than for the conventional MC offerings at an aggregated level. We could identify the driver of "perceived co-design freedom" that explained (part) of this value increment. Moreover, we found that participants' characteristics largely influenced WTP [for a more detailed view on the study, see Weller et al. (2015b)].

2.4.1.5 Product Customization and Perceived Product Value

To assess the value creation potential of enhanced product customizability further from an attribute perspective, comparing form versus function properties, we carried out another study. Here, we portrayed a simulated online buying process of a customizable ceramic knife. Within this attribute-related study, we designed two online surveys with German consumers. In the course of the survey, consumers were treated with two non-functional mock-ups of an online buying process for the

ceramic kitchen knife. The mock-ups represented online toolkits with different degrees of available product customization. The treatments were shown randomly, and participants had to answer a short survey on their own perceived value, purchase intent and WTP.

In the first survey, we assessed the value of customizing style-related/aesthetic (e.g., color) product design parameters, while fit-related parameters, such as the kitchen knife handle in this case, were focused on in the second survey. When consumers could customize aesthetic attributes in the first survey, we found that differences in perceived product value were insignificant. Contrarily, when consumers customized fit-related attributes in the second survey, there was a significant value upside for full customization.

We revealed that both product involvement and attitude toward customization influenced WTP positively and identified different value drivers for customization offerings, i.e., process enjoyment, uniqueness value and pride of ownership as well as the attitude toward customization. Our main goal was to assess the value creation potential of AM from a consumer's perspective by assessing the perceived value of a higher degree of product customization. The results show that consumers are willing to pay more for highly customizable products—in particular in the case of fit-related customization in the second survey. There was a small but significant value increase of 7 % at an aggregated level. A cluster analysis performed (see Fig. 2.15) showed that an upside in WTP of 50–60 % should be possible when targeting niches. Specifically, we show in Fig. 2.6 that participants in Cluster 4 ("highly involved customizers") valued customizable products the most; participants clustered into Cluster 1 "uninterested" had the lowest WTP (for detailed information, see (Weller 2015)). These results show that (i) it is important to target

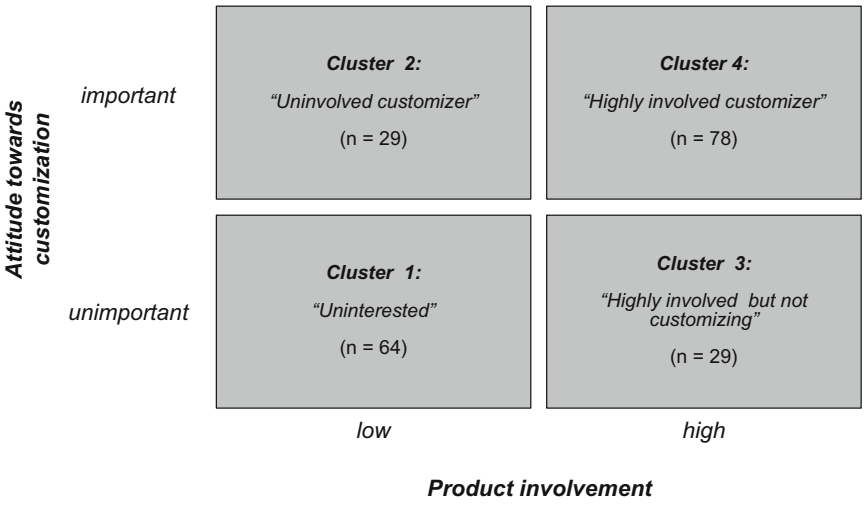

Fig. 2.15 Cluster analysis structure (Weller 2015)

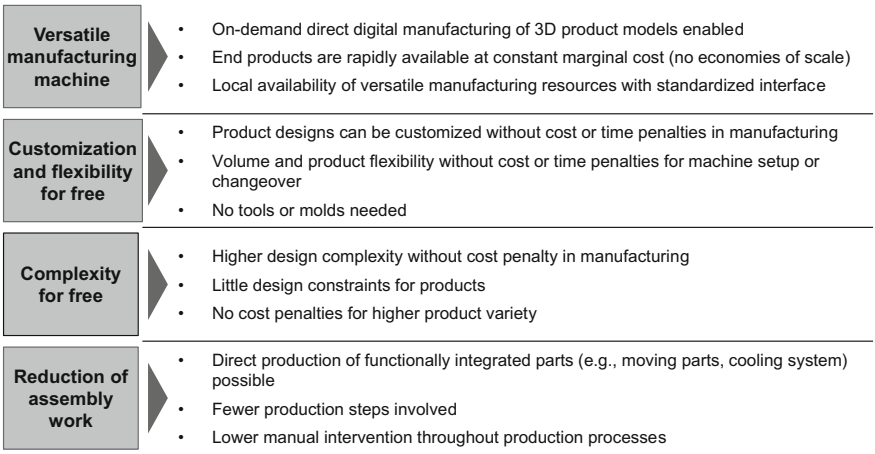

Fig. 2.16 Key principles of production with AM technology (Weller et al. 2015a)

niches with customizable offerings and (ii) it is very important to choose the product to customize carefully.

In particular, when comparing the results of the espresso cup study and this second study, it becomes obvious that in the espresso cup case, customers were willing to pay more for customized form factors in contrast to the kitchen knife. Here, only functional customization options generated higher WTP.

2.4.1.6 Implications of AM on the Manufacturing Firm and the Market

To be able to answer the research question on what economic theories are suitable to assess the implications of AM technology, we discussed the impact of AM technology at both firm and industry levels in Weller et al. (2015a).

Taking a production economics perspective, we discuss implications on a firm's payoff function and potential market structure effects. We first identified the economic and technological characteristics of AM and highlighted four key principles relevant to manufacturers at the firm level (see Fig. 2.16). First of all, AM technology is a "versatile manufacturing machine" with the capability of transforming digital 3D models directly into physical products. Second, AM offers "customization and flexibility for free," meaning that it does not require additional tools or molds for the start of production. Also, because sequence and volume of products can be altered without cost penalties manufacturing flexibility is high. Third, AM offers "complexity for free"—it allows more complex products and large variety of products with no increase in manufacturing costs. Fourth, integrated functional designs in one step are possible, reducing assembly (Weller et al. 2015a).

After having emphasized the above-mentioned effects, we critically assessed those effects of AM at the industry level by analyzing the validity of production costs-related assumptions on the firm's payoff function and in established economic market models when these four principles of AM technology apply. We based the analysis of the payoff function on Milgrom and Roberts (1990) as theoretical foundation and applied AM's key principles here as well as on market structure models outlined in the literature. In doing so, we derived a set of seven propositions providing an impetus for future research.

In particular, we proposed that a monopolist that adopts AM could increase profits by capturing consumer surplus when flexibly producing customized products. In competitive markets, competition is spurred as AM may lower barriers to market entry and offers the ability to serve multiple markets at once.

This should ultimately result in lower prices for consumers. More generally, our analysis allows us to point out markets where AM technology may be adopted first: markets with overall lower economies of scale, a higher demand for individualized products and a need for more complex designs. Markets for AM could hence be characterized by four patterns: (i) small production output, (ii) high product complexity, (iii) high demand for customized products tailored to individual customers' needs and (iv) spatially remote demand for products. For a more detailed look into these propositions, see Weller et al. (2015a).

2.4.2 The SLM-Complemented Product Production System (PPS)

Based on the implications resulting from the integration of SLM manufacturing technologies, the PPS is revised regarding these influences. The factors determine the formalizations to describe the characteristic curves that in turn define the isoquants of equivalent operating points in the PPS. In the following, the main formalizations of the four dimensions of the PPS are presented.

2.4.2.1 Conflict Field "Product Program"

As described in Sect. 2.3.2.2, the conflict field Product Program is characterized by the dimensions "Individualization of the Product Program" and "Explainability at the Point of Sale". In comparison with the formalization of the dimension within a PPS considering traditional manufacturing technologies only and although the individualization of the product program is likely to be extensively higher, the quantitative formalization of this dimension stays untouched. Bohl (2015) formalized the "Individualization of the Product Program" as follows:

$$\mathrm{IV_{PP}} = \frac{n_{\mathrm{sold}}}{n_{\mathrm{sold}} + S_{\mathrm{max}} - S_{\mathrm{min}}}; \tag{2.4}$$

$\mathrm{IV_{PP}}$ Individualization of the Product Program;
n_{sold} Number of product variants sold;
S_{max} Sales of product variant with highest turnover;
S_{min} Sales of product variant with lowest turnover.

Based on the maximization of individualization and modification possibilities for components or product variants as a result of SLM-complemented manufacturing, the customer is more likely to create his/her own individual product variants. When strengthening the integration of the customer into development and production process as described in Sect. 2.3.2.2, the effort needed to explain the product program by sales descends. This effect results from the fact that product variants or components configured by the customer are not likely to be explained by sales to the same extent anymore. Therefore, the formalization of the "Explainability at the Point of Sale" according to Bohl (2015) is extended to the following:

$$\mathrm{EV_{PP}} = \frac{1}{v * n_{off}} * \left(\sum_{i=1}^{v} n_{\mathrm{expl}_i} + \sum_{j=0}^{w} n_{\mathrm{conf}_j} \right); \tag{2.5}$$

$\mathrm{EV_{PP}}$ Explainability at the Point of Sale;
v Number of sales employees;
n_{off} Number of product variants offered;
n_{expl_i} Number of product variants explainable by sales employee i;
n_{conf_j} Number of product variants configured by customer j.

The revised formalization takes the number of product variants configured by the customer into account. Under the assumption that customers will take advantage of the opportunity to interact during product development, the explainability at the point of sale is unlikely to fall to zero.

2.4.2.2 Conflict Field "Product Architecture"

The conflict field Product Architecture is characterized by the conflicting dimensions "Product Architecture Flexibility" and "Product Architecture Commonality". When trying to realize mass customization with economies of scale due to standardized modules, the realization of economies of scope in terms of a flexible product architecture is essential. Therefore, the possibility to change the upfront-defined product architecture regarding individual customer needs is described as the flexibility of the product architecture. Accordingly, the "Product Architecture Flexibility" is formalized as follows (Bohl 2015):

$$FL_{PA} = 1 - \frac{n_{Ftr\,Strd}}{n_{Ftr\,var}}; \tag{2.6}$$

FL_{PA} Flexibility of the Product Architecture;
$n_{Ftr\,Strd}$ Number of variable features within the standardized product architecture;
$n_{Ftr\,var}$ Total number of varied features.

When integrating SLM technologies into manufacturing, the degree of customer interaction arises. Therefore, the product architecture flexibility is likely to increase due to possibilities of interaction during product development. Moreover, the number of standardized modules is likely to decrease. Altogether, the integration of SLM technologies increases the flexibility of the product architecture. The needed commonality of the product architecture to achieve economies of scale can be formulated according to Bohl (2015) as follows:

$$CM_{PA} = \sqrt{4}{\frac{1}{m}} \sum_{i=1}^{m} w_i \cdot \frac{q_i}{q_{ges}} \approx \sqrt{4}{\frac{1}{m^2}} \cdot \sum_{i=1}^{m} \frac{q_i}{q_{ges}} = \sqrt{\frac{1}{m}}; \tag{2.7}$$

CM_{PA} Product Architecture Commonality;
m Number of component variants used in product architecture [1; ∞[;
w_i Value share of component variant i of total value of all component variants [0; 1];
q_i Output of component variant i [1 pcs.; ∞ pcs.[;
q_{ges} Total output of all component variants [pcs.].

Under the assumption that the value shares and the outputs are not correlated, the commonality of the product architecture is dependent on the number of component variants used in product architecture m only, which can be determined as follows (Bohl 2015):

$$m = n^{1-c_{WV}} \cdot k; \tag{2.8}$$

m Number of component variants used in product architecture;
n Number of module variants used [1; ∞[;
c_{WV} Parameter of reuse of component variants [0; 1];
k Average number of components per module [1; ∞[.

When integrating SLM technologies into manufacturing, the number of module variants used is likely to increase. Hence, the commonality of the product architecture decreases. In contrary, the average number of components per module is likely to decrease due to the possibilities of functionality integration within SLM parts. Altogether, the dichotomy between the flexibility and the commonality of the product architecture persists even when using SLM technologies in manufacturing.

2.4.2.3 Conflict Field "Production Structure"

The conflict field product structure is defined via the dimensions "Resource Utilization in Manufacturing" and "Process Commonality in Manufacturing." Due to the possibilities of realizing complex structures and integrated functionalities with SLM components, the resource utilization takes the influences of integrating SLM technologies into manufacturing into account:

$$\mathrm{RU_{PS}} = \frac{1}{Q_{\mathrm{PS}}} \cdot \sum_{i=1}^{r} T_{gi} = \frac{t_b \cdot v_t + t_{ba} \cdot v_a}{Q_{\mathrm{PS}}}; \tag{2.9}$$

$\mathrm{RU_{PS}}$ Resource Utilization in Manufacturing;
t_b Average basic time per unit conventionally manufactured [0h; ∞h[;
v_t Total quantity of conventionally manufactured units [0 pcs.; ∞ pcs.[;
t_{ba} Average basic time per unit manufactured with SLM technologies [0h; ∞h[;
v_a Total quantity of units manufactured with SLM technologies [0 pcs.; ∞ pcs.[;
Q_{PS} Total capacity of all resources considered within a specified time interval [h].

With the factors t_{ga} and v_a, the revised formulization explicitly takes the SLM resources into consideration. When integrating SLM technologies into manufacturing, the total quantity of conventionally manufactured units is likely to decrease. Hence, the number of material flow relationships decreases, which is taken into account in the formulization of the "Process Commonality in Manufacturing" (Bohl 2015):

$$\mathrm{PC_{PS}} = \frac{r-1}{f}; \tag{2.10}$$

$\mathrm{PC_{PS}}$ Process Commonality in Manufacturing;
r Number of resources in manufacturing;
f Number of material flow relationships.

Due to the increasing number of resources in manufacturing and the anticipated decrease of material flow relationships, the process commonality in manufacturing is likely to increase when integrating SLM technologies into manufacturing.

2.4.2.4 Conflict Field "Supply Chain"

The supply chain is defined by the conflicting factors "Supply-Chain Inventory Efficiency" and "Supply-Chain Effectiveness." The inventory efficiency is the result of the ratio between different types of stock and the revenue achieved equivalent to the priced sales volume.

$$\mathrm{IE_{SC}} = 1 - \frac{S_{\mathrm{Pd}} + S_{\mathrm{Ct}} \cdot \frac{1}{m_0} + S_{\mathrm{WIP}} \cdot \frac{C_{\mathrm{WW}}}{m_0}}{\mathrm{Rev_{ttl}} \cdot (1 + C_{\mathrm{GM}})}; \tag{2.11}$$

$\mathrm{IE_{SC}}$ Supply-Chain Inventory Efficiency;
S_{Pd} Stock of products [0 pcs.; ∞ pcs.[;
S_{Ct} Stock of components [0 pcs.; ∞ pcs.[;
m_0 Average number of components per product [0 pcs.; ∞ pcs.[;
S_{WIP} Number of work-in-progress (WIP) stock;
C_{WW} Valuation parameter for WIP stock;
$\mathrm{Rev_{ttl}}$ Total revenue of all product variants [0 pcs.; ∞ pcs.[;
C_{GM} Addition factor of the relative gross margin to production costs [0; ∞[.

The second equation of the supply chain is focused on the buffer stocks of finished and unfinished components and is defined by the corresponding service degree. The formalization of the supply-chain efficiency according to Bohl (2015) is shown in Eq. (2.12):

$$\mathrm{EF_{SC}} = \frac{\sum_{i=1}^{u} \mathrm{QT_{FQ}}i}{\sum_{i=1}^{u} \mathrm{QUT_{ttl}}i} \approx \alpha \cdot \mathrm{SG_{SC}^{Pd}} + (1 - \alpha) \cdot \mathrm{SG_{SC}^{Bt}} \tag{2.12}$$

$\mathrm{EF_{SC}}$ Supply-Chain Effectiveness;
u Number of periods in the regarded time interval;
$\mathrm{QUT_{TQ}}i$ On time and in required quality delivered quantity in period i [pcs.];
$\mathrm{QUT_{ttl}}i$ Total quantity delivered in period i [pcs.];
α Degree of order processing type [0; 1];
$\mathrm{SD_{SC}^{Pd}}$ Service degree of finished products [0; 1];
$\mathrm{SD_{SC}^{Ct}}$ Service degree of unfinished components [0; 1].

The service degree is modeled depending on the order processing type that expresses which portion of the customer's needs is fulfilled with make-to-stock processing. SLM technologies are likely to reduce stocks since on-demand production is facilitated. Overall, effects that result from the integration of SLM technologies, like the higher flexibility of the supply chain, are likely to increase the effectiveness of the supply chain.

The consequent characteristic curves of the four dimensions "Product Program", "Product Architecture," "Production Structure" and "Supply Chain" for the formalizations presented are illustrated in the overall SLM-complemented PPS shown in Fig. 2.17.

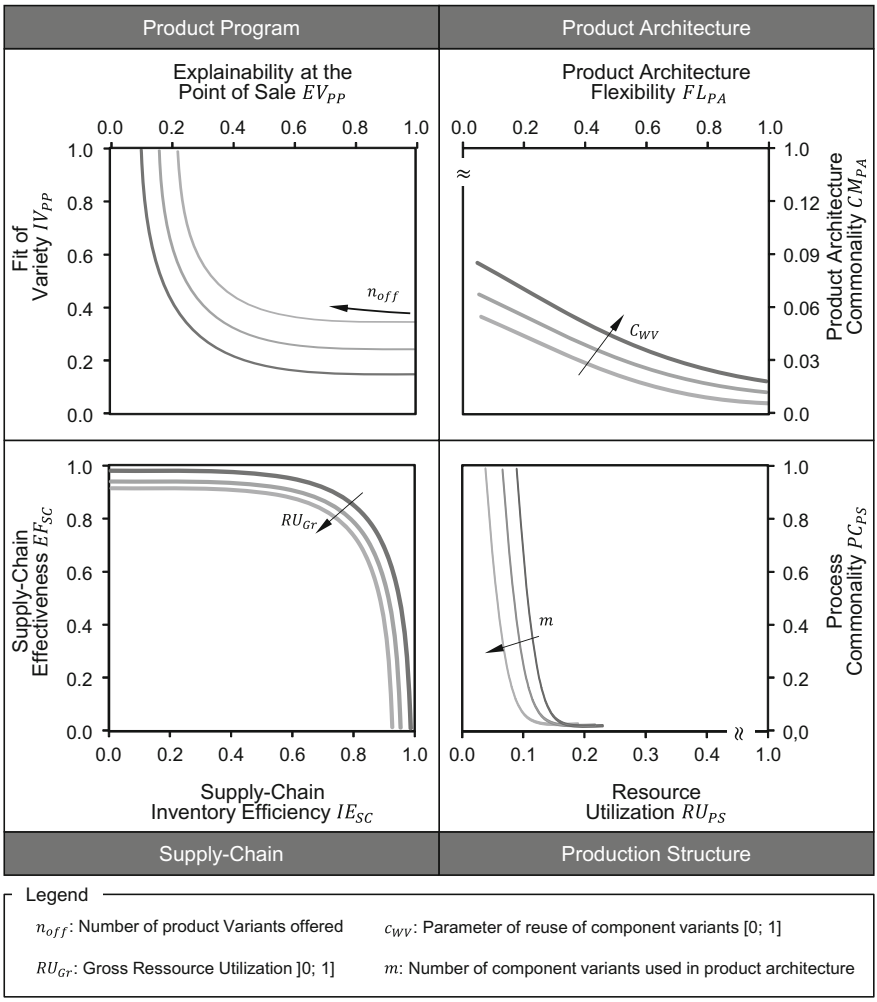

Fig. 2.17 Overall SLM-complemented product production system (PPS) based on Bohl (2015)

2.4.3 Machine-Specific Cost Drivers in Additive Manufacturing (AM) Technologies like Selective Laser Melting (SLM)

2.4.3.1 Approach

In this chapter, the approach for the cost estimation of SLM-manufactured parts is described. According to DIN 60300-3-3 (DIN 2005), a product life cycle comprises

Fig. 2.18 Life cycle phases of a product according to DIN 60300-1 (DIN 2005)

the life cycle phases concept and definition, design and development, manufacturing, installation, operation and maintenance, and disposal (see Fig. 2.18).

As mentioned in Sect. 2.3.3.2, the main costs of SLM-manufactured parts are caused by the machine costs. The machine costs are caused during the machine investment step. Further costs like the energy costs occur during operation of the SLM machine. This is why a life cycle-based cost analysis is performed. The total life cycle costs of a machine with a low initial investment cost can be higher if the operational costs during the years of operation are higher than in other machines. In this work, the product life cycle steps "Manufacturing" and "Operation & Maintenance" are considered in more detail. "Manufacturing" means the production of the considered SLM machine and not the SLM process itself.

The procedure of the life cycle-based evaluation of the cost estimation is shown in Fig. 2.19.

In a first step, a functional machine structure model is developed. This machine structure model constitutes the base for the following evaluation and ensures that the life cycle-based cost estimation is done on assembly and component level.

The next step comprises of showing a typical SLM machine reference process. Based on this process, a typical SLM manufacturing scenario can be described and modeled. Furthermore, the evaluation is performed considering different workpiece dimensions. The build envelope can be filled by big workpieces and small workpieces with a low filling degree. This directly influences the melting volume and hence the SLM manufacturing time.

Each process step linked with a definite time span can be connected with each SLM machine component from the machine structure model. This allows for identifying the time and performance drivers and thus the identification of the cost drivers on machine component level.

Optimization measures are deduced by sensitivity analysis by varying the input values considering the output of the cost and performance levels of each machine component.

Fig. 2.19 Structure and procedure of SLM life cycle costing methodology

2.4.3.2 Results

In this chapter, the basic machine structure model of a SLM machine on assembly and component level is presented. This model comprises of the mandatory components and assemblies that are incorporated in a SLM machine.

The main cost model and the interdependencies between input and output values are described in more detail. The SLM manufacturing costs in relation to the SLM build envelope size and the laser system used in one machine are presented. In addition, the resource consumption of SLM manufacturing is presented.

The following evaluation is based on different example scenarios. The SLM manufacturing costs of low-volume or high-volume components on different SLM machines with small or big build envelope sizes are evaluated.

2.4.3.3 Machine Structure Model

For the identification of cost drivers on assembly or component level, it is necessary to subdivide the considered SLM machine in its corresponding functional assemblies and components. This allows assigning all cost and performance elements to the functional assemblies and individual components.

For the analysis of existing SLM machines, the assembly's oriented structuring method is chosen. For the evaluation of SLM individual processes (such as the laser exposure process or the powder application process), the function-oriented structuring seems to be advantageous.

A SLM machine can be divided into the following main components: build platform, laser and optics system, powder management, process chamber, shielding gas system, software and control. For example, the build platform contains the linear drive for moving it in layer thickness steps in z-direction. It also comprises the heating elements for build platform preheating (Fig. 2.20).

2.4.3.4 SLM Reference Process

Each SLM process step presented in Table 2.2 can be allocated with individual time intervals. The total time for one SLM build job comprises the main time for the laser exposure, the auxiliary time for powder application, the machine setup time for CAD preparation and powder material change. The workpiece change comprises the manual activities for taking out the build platform, preheating and cooling down the build platform and the time for applying the shielding gas atmosphere. Some of the process steps are done with each workpiece layer, some are done with each build job, and others are done in special time intervals.

In addition to the SLM reference process, the production task has to be defined. For the evaluation of the cost model, four different workpiece geometries are considered (see Fig. 2.21). For workpiece B0, a cuboid of solid material is chosen with the same outer dimensions as the build envelope of a standard SLM machine

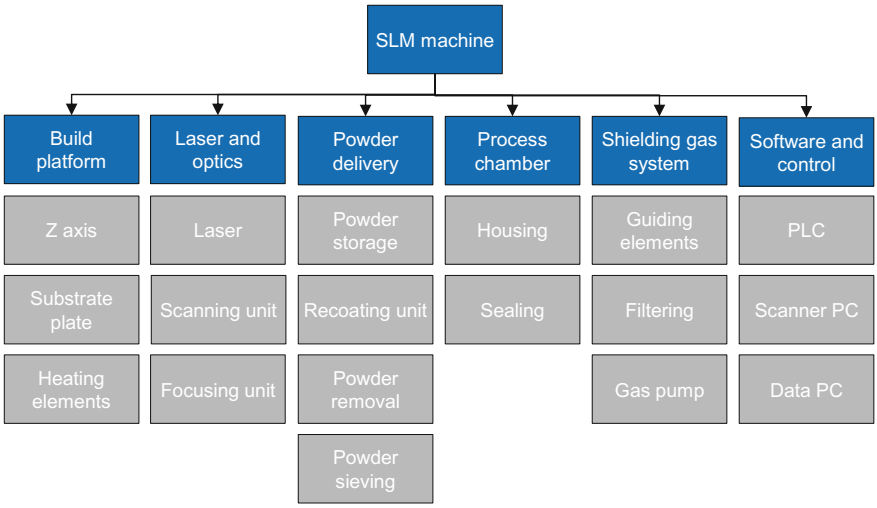

Fig. 2.20 Schematic illustration of a SLM machine structure model (Schrage 2016)

configuration ($V = 250 \times 250 \times 325$ mm^3). This means that the melted material volume equals the total build envelope in one SLM standard machine and only one workpiece of B0 can be manufactured in one build job. Workpiece B2 with an outer dimension of $25 \times 25 \times 25$ mm^3 can be manufactured multiple times in one build job. The small height leads to less powder application steps and reduces the auxiliary times. B3 with the same dimension as B2 has a filling degree of 20 % and equals a lattice structure.

By combining the machine structure model, the SLM reference process and the time components of the SLM build job, the displaying of all single-time contributions of each single machine component to the total SLM build time becomes possible (see Fig. 2.22).

2.4.3.5 Cost Model

In this chapter, the cost model for calculating the SLM manufacturing costs is presented. In particular, the interdependencies between machine- and process-specific input parameters and output are represented.

Main Time t_{Main}

The main time t_{Main} includes the time in that the powder material of a workpiece no. i with the volume V is melted by the laser radiation $t_{\mathrm{LaserExposure}}$ with the build-up rate $\dot{V}$. This time can be expressed by

Table 2.2 SLM reference process with time variables (Schrage 2016)

No.	Process step	Time
1	Machine setup	$t_{MachineSet\text{-}up}$
	• Preparation of CAD data	• t_{CAD}
	• Material change	• $t_{MaterialChange}$
	• Cleaning of process chamber	• $t_{Cleaning}$
	• Change of gas filter elements	• $t_{FlterChange}$
	• Setup of first powder layer	• t_{Layer0}
3	SLM process	$t_{SLMProcess}$
Iteration	Process step done each layer	
	• Powder delivery	• $t_{PowderDelivery}$
	• Powder application of layer n	• $t_{PowderApplication}$
	• Laser exposure of layer n	• $t_{LaserExposure}$
	• Lowering the build platform for one layer thickness	• $t_{BPM\ ovement}$
	• Backward movement of powder application unit	• $t_{SliderBackward}$
4	Work piece change	$t_{WorkPieceChange}$
	• Cool down of build platform	• $t_{BPcooldown}$
	• Removal of powder	• $t_{PowderOut}$
	• Removal of build platform incl. work pieces	• t_{BPout}
	• Mounting of new build platform	• t_{BPin}
	• Setup of shielding gas atmosphere inside the process chamber	• t_{SGin}
	• Heating of build platform	• $t_{BPpreheat}$

Workpiece	Dimension
B0	250*250*325 mm³
B1	75*75*75 mm³
B2	25*25*25 mm³
B3	25*25*25 mm³ (20% filling)

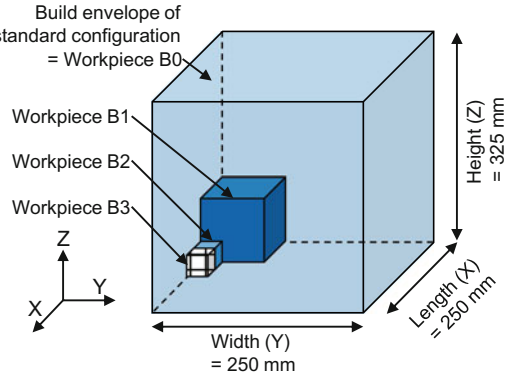

Fig. 2.21 Overview about the reference workpieces considered in the cost model (Schrage 2016)

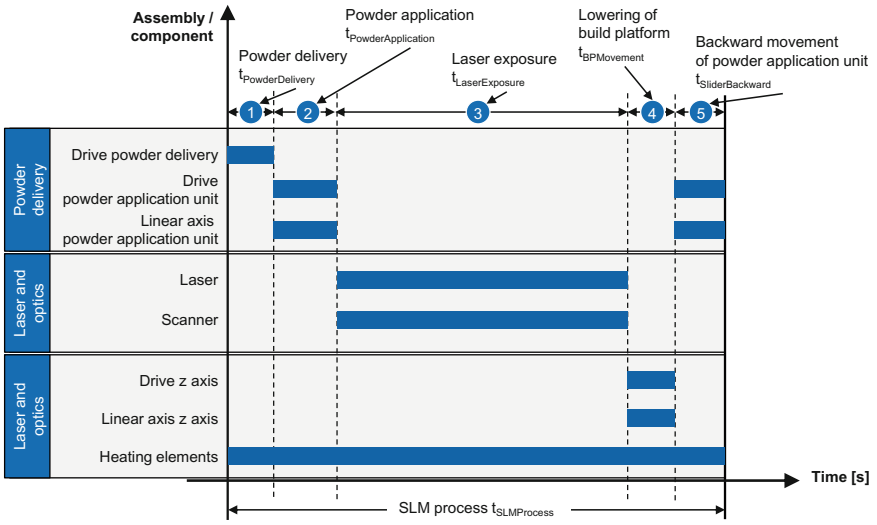

Fig. 2.22 Component-specific time drivers (Schrage 2016)

$$t_{\text{Main}} = \frac{V}{\dot{V}} = \frac{\sum_{i=1}^{N} V_i}{\dot{V}} = t_{\text{LaserExposure}}. \tag{2.13}$$

Volume V equals the total volume of all workpieces that are produced in one build job including the support structures of one workpiece. This volume can be expressed in terms of the build platform size $A_{\text{BuildPlatform}}$, the packing density of workpieces in one build job $f_{\text{BuildPlatform}}$ and the workpiece height $Z_{\text{WorkPiece}}$ [see Eq. (2.14)]:

$$V = A_{\text{BuildPlatform}} * f_{\text{BuildPlatform}} * Z_{\text{WorkPiece}}. \tag{2.14}$$

According to Meiners, the build-up rate $\dot{V}$ can be expressed by Eq. (2.15), where D_S is the layer thickness, Δy_S the scan line spacing, v_S the scanning speed, and n_{LSS} the number of laser–scanner systems that are installed in one SLM machine. (Meiners 1999). This equation

$$\dot{V} = D_S \cdot \Delta y_S \cdot v_S = f(P_L, n_{\text{LSS}}) \tag{2.15}$$

was previously introduced (see Sect. 2.3.4). Depending on the laser output power P_L and the powder material, the process parameters layer thickness D_S, scan line spacing Δy_S and scanning speed v_S have to be adapted to fully melt up the material and generate parts with a density up to 100 %. The scanning speed and the layer thickness are limited by the available laser power. The scan line spacing is limited by the focus diameter which typically equals approx. 0.7 times of the beam diameter (Meiners 1999). By using bigger beam diameters, the scan line spacing

can be increased while increasing the laser power up to a certain level (Brecher 2011; Schleifenbaum 2012).

The build-up rate is a function of laser power P_L and the number of laser and scanner systems n_{LSS}. While the maximum build-up rate is limited by material properties (e.g., spattering occurs at high laser powers and thus leads to an instable process), further increase of build-up rates can be done by parallelization of the SLM process. By using n_{LSS}, laser beam sources and scanner systems in one SLM machine, the build-up rate can be multiplied without the need for changing the process parameters.

Auxiliary Time $t_{Auxiliary}$

The auxiliary time $t_{Auxiliary}$ comprises the times for the powder application $t_{PowderApplication}$ and is dependent on the number of layers in one SLM build job n_L. It can be expressed by

$$t_{Auxiliary} = n_L * t_{PowderApplication} = \frac{Z_{WorkPiece}}{D_S} * t_{PowderApplication}. \quad (2.16)$$

The powder application has to be performed after the exposure and is thus dependent on the workpiece height $Z_{WorkPiece}$, respectively, on the number of layers n_L. Additionally, the time for the powder application depends on the travel distance of the powder application unit that is determined by the build platform size. Standard SLM machines are typically equipped with a square-shaped build platform in the size of, e.g., $X \cdot Y = 250\ mm \cdot 250\ mm$. This size determines the travel distance of the powder application unit $s_{BuildPlatform,X/Y}$. The time for the powder application $t_{PowderApplication}$ can be calculated by Eq. (2.17):

$$t_{PowderApplication} = \frac{s_{BuildPlatform,X/Y} + s_{Additional}}{v_{PowderApplication}}; \quad (2.17)$$

$s_{Additional}$ Additional distance for powder application (e.g., travel distance to powder storage) [mm];

$v_{PowderApplication}$ Speed of powder application unit [mm/s].

The powder application unit has to move the distance from the powder filling station to the build platform to lever the powder material and an additional distance to the powder overflow. This step is done once for each layer. Afterward, it is replaced from a backward movement to the starting position. The movement for the powder application is usually done with movement speeds $v_{PowderApplication}$ of 50–150 mm/s. During the backward movement, the build platform is lowered so that there is no contact between the powder application unit and the powder bed. Thus, backward movement can be performed with higher speeds (300–500 mm/s). Depending on the used powder application concept, another powder application process can be done during the backward movement. This would result in a shorter total time for powder application.

Time for Workpiece Change $t_{\text{WorkPieceChange}}$
The time for the workpiece change $t_{\text{WorkPieceChange}}$ comprises all single actions shown in Eq. (2.18). Table 2.2 comprises the explanation of each time component

$$t_{\text{WorkPieceChange}} = t_{\text{BPin}} + t_{\text{BPout}} + t_{\text{SGin}} + t_{\text{SGout}} + t_{\text{BPpreheat}} + t_{\text{BPcooldown}}. \quad (2.18)$$

The single actions for a workpiece change are the removal of the unmelted powder material, the removal of the build platform including the workpieces and afterward replacing and adjusting a new build platform into the process chamber. Before every build job, the process chamber has to be flooded with shielding gas to establish an inert process gas atmosphere to avoid oxidation during the melting process. This time depends on the process chamber size and is a SLM machine-dependent factor.

Machine Setup Time $t_{\text{MachineSet-up}}$
The machine setup time $t_{\text{MachineSet-up}}$ comprises the time for the CAD preparation t_{CAD} and the time for the material change $t_{\text{MaterialChange}}$ and can be expressed by

$$t_{\text{MachineSet-up}} = t_{\text{CAD}} + t_{\text{MaterialChange}}. \quad (2.19)$$

The time, which is required for the CAD data preparation, t_{CAD} strongly depends on the part complexity and the experience of the operator and can therefore only be estimated. The setup time includes the time for preparing the CAD data, the virtual attachment of the support structures and the virtual alignment of the components in the build envelope. The material change is only necessary if the next build job is to be performed with another powder material type. This would make an accurate process chamber cleaning necessary to avoid power contamination.

2.4.3.6 Unit Costs of SLM-Manufactured Parts

For determining the unit costs of SLM-manufactured workpieces, the activity-based costing method is (ABC) used in this cost model. The ABC allows allocating the costs that are induced by acquiring or running a SLM machine, and it allows to make a distinction between fixed and variable costs (Kaplan and Cooper 1999). The fixed costs are, for instance, the investment cost of the SLM machine. This makes it possible to identify cost drivers for using SLM machines.

Investment Costs of the SLM Machine
Fixed costs of the SLM manufacturing are thus the costs for the SLM machine and its accessories $C_{\text{SLMMachinePurchase}}$ like machine purchase price $C_{\text{SLMMachine}}$, the purchase price for the special SLM CAD preparation software $C_{\text{SLM-SW}}$ and costs for the machine maintenance and repair C_{Service} [see Eq. (2.20)]. These costs are often set in the context of service contracts, depending on the equipment purchase price:

$$C_{\text{SLMMachinePurchase}} = C_{\text{SLMMachine}} + C_{\text{SLM-SW}} + C_{\text{Service}}. \quad (2.20)$$

SLM Machine Costs

The costs caused by the machine can be described on the machine hour rate and the lifetime of the machine. The number of annual machine hours can be increased via raising machine utilization, for example, improvement of job scheduling and automating manual machine setup.

The general description and calculation of machine hour rate c_{MH} is shown in Eq. (2.21):

$$c_{\mathrm{MH}} = \frac{c_D + c_{\mathrm{Interest}} + c_{\mathrm{Facility}} + c_{\mathrm{Energy}} + c_{\mathrm{Maintenance}}}{t_{\mathrm{MachineUtilization}}}. \tag{2.21}$$

The machine hour rate comprises the depreciation c_D of the machine investment price over the whole machine life time, the annual interests c_{Interest}, the annual facility costs $c_{\mathrm{FacilityCost}}$, the annual energy costs $c_{\mathrm{EnergyCosts}}$, the annual maintenance costs $c_{\mathrm{Maintenance}}$ and the annual machine utilization time $t_{\mathrm{MaschineUtilization}}$.

The SLM machine costs $C_{\mathrm{SLMMachine}}$ which are caused during the SLM machine usage can be calculated according to Eq. (2.22):

$$\begin{aligned} C_{\mathrm{SLMMachine}} &= c_{\mathrm{MH}} \cdot t_{\mathrm{SLMJob}} = c_{\mathrm{MH}} \cdot \left(t_{\mathrm{Main}} + t_{\mathrm{Auxiliary}} \right. \\ &\quad \left. + t_{\mathrm{WorkPieceChange}} + t_{\mathrm{MachineSetup}}\right) \\ &= C_{\mathrm{SLMBasicMachine}} + C_{\mathrm{Laser}} + C_{\mathrm{Optics}}. \end{aligned} \tag{2.22}$$

The investment costs for a total SLM machine can be determined by the purchase price of commercially available SLM machines. These prices include, in addition to the investment costs, the profit margins and development cost of the system manufacturer. These rates may be used in the theoretical consideration of the productivity of these machines. The pricing of the series components, such as the laser beam source C_{Laser} or the scanner systems C_{Optics}, may be based on price consultation of offers and data sheets. The price of the basic machine structure $C_{\mathrm{SLMBasicMachine}}$ depends on the build envelope size $V_{\mathrm{BuildEnvelope}}$ [see Eq. (2.23)]. However, the cost for the manufacturing of the machine frame and base structure can only be estimated. Nonetheless, if different machine configurations (multi-laser and multi-scanner systems, different build envelopes) are examined and are not commercially available, the production costs for these machines must be estimated in greater detail. Proprietary analyses have shown that increasing the build envelope size $V_{\mathrm{BuildEnvelope}}$ in the build envelope height (in z-direction) is the most economical method, since less components and assemblies (like the powder application unit) have to be adjusted in the lateral directions (x- and y-directions) leading to less material and manufacturing effort:

$$C_{\mathrm{SLM\,Basic\,Machine}} = f\left(V_{\mathrm{Build\,Envelope}}\right). \tag{2.23}$$

Machine Price in Relation to the Build Envelope Size

For evaluating the influence of the SLM machine configuration on the workpiece costs, the most important cost driver is the cost of the basic machine structure neglecting the laser beam sources and the scanner systems integrated in one machine. So it is possible to reveal a relation between the build envelope sizes $V_{\text{BuildEnvelope}}$ and the investment price for the basic machine structure $C_{\text{SLMBasicMachine}}$. This relation is shown in Fig. 2.23.

The machine prices shown in Fig. 2.23 include the margins of the SLM machine manufactures. The build envelope size-dependent price of the basic machine can empirically be expressed by

$$C_{\text{SLMBasicMachine}} = f\left(V_{\text{BuildEnvelope}}\right) = 9.3542 \cdot V_{\text{BuildEnvelope}} + 185135. \qquad (2.24)$$

For a more detailed analysis of the machine price of each SLM machine configuration, a breakdown of the machine into the component level becomes necessary. When analyzing all machine-specific components and assemblies that are affected when increasing the build envelope size, the machine structure costs from manufacturer's point of view can be found. Therefore, self-initiated examinations regarding the cost influence of single machine component and assemblies are performed. These examinations were done analyzing the design drawings of a Trumpf Trumaform LF250 SLM machine that is installed at the Fraunhofer ILT. A cost estimation was carried out for each machine component which size would have to be changed if increasing or decreasing the build envelope size. The material

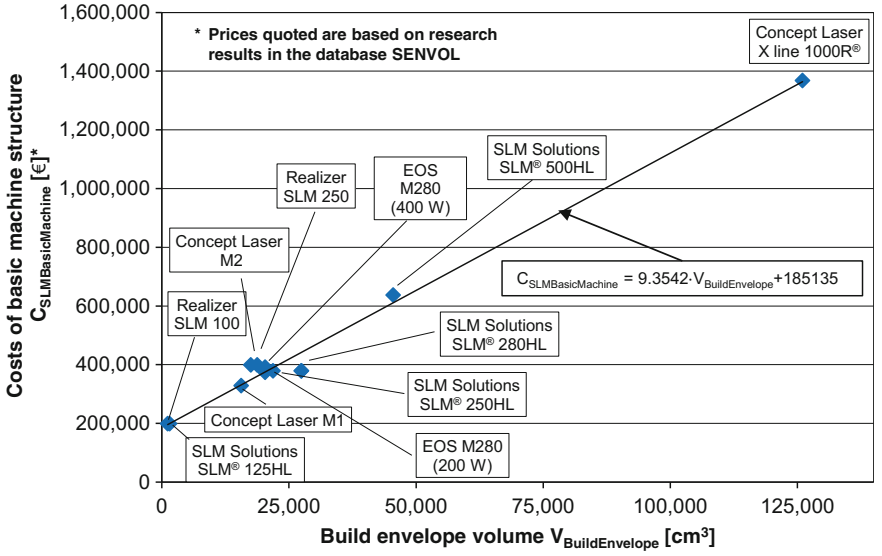

Fig. 2.23 Investment price for SLM machine structure in relation to the build envelope size (Schrage 2016)

price of each component directly relates to the component and its wrought part size. The manufacturing price of the machine component is also influenced by part complexity and number of machining operations necessary to finish the component. The higher the number of design drawings of each component and the number of views in one design drawing, the more complex the machine component. When changing the build envelope size, some specific machine components have to be changed in their sizes too. The build platform, for instance, has to be changed in two directions (in *x*- and in *y*-directions). The size of the powder application unit may only be changed in one direction that is perpendicular to the powder application direction (e.g., in *x*-direction if the powder application takes place in *y*-direction).

The build envelope can be influenced changing the build platform size in *x*- and *y*-directions or in *z*-direction. While changing the build platform size in *x*- or in *y*-direction, there is a steeper increase in costs of the machine structure than changing the build envelope size by varying the *z*-dimension (see Fig. 2.24). When increasing the build platform size in *x*- or in *y*-direction linear drives and some machine structure parts have to be enlarged as well, while the increase of the build envelope size in *z*-direction only affects the linear platform movement drive.

When considering the ratio of machine structure costs to build envelope size, a high cost decrease rate (especially at small build envelop volumes) can be obtained.

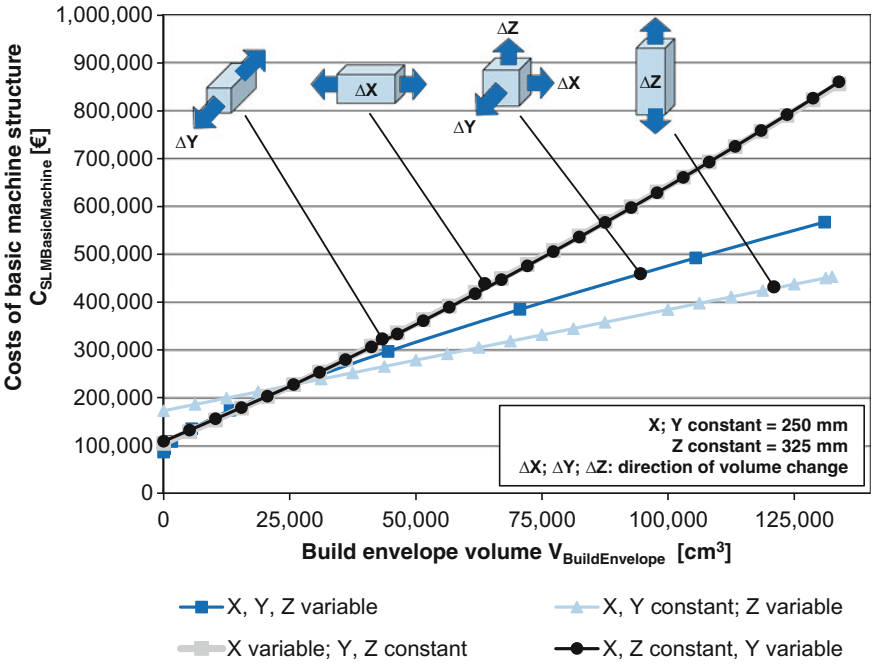

Fig. 2.24 SLM machine structure costs varying the build envelope in *x*-, *y*- and *z*-directions (Schrage 2016)

For higher build envelope sizes, the machine structure costs per build envelope size keep almost constant (see Fig. 2.25).

Depending on the build platform size, multi-laser beam sources and scanner systems have to be used in order to cover the complete build platform area or—at smaller platform sizes—the same scanner area should be laser exposed with multi-laser and scanner systems simultaneously. When increasing the number of laser beam sources and scanner systems in one SLM machine, the investment costs for the laser systems and scanner systems increase corresponding to the number of laser beam sources [see Eq. (2.22)].

The following costs are dependent on the number of SLM build jobs and thus belong to the variable costs:

- Material costs C_{Material} (powder material)
- Personnel costs $C_{\text{Personnel}}$
- Costs for electricity $C_{\text{Electricity}}$ and
- Costs for shielding gas $C_{\text{ShieldingGas}}$

Material Costs

Assuming a lossless use of the powder material during the SLM process, the powder consumption can be assessed by the workpiece volume $V_{\text{WorkPiece}}$ (including the volume of the support structures). The cost of the used powder material C_{Material} can be calculated by the material density ρ_{Material} and the powder price c_{Material} [see Eq. (2.25)]:

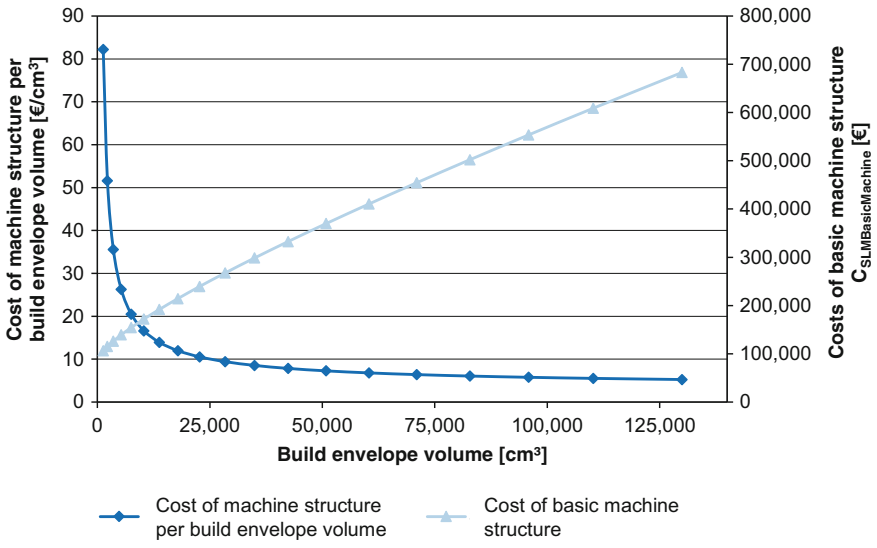

Fig. 2.25 SLM machine structure costs in relation to the build envelope (Schrage 2016)

$$C_{\text{Material}} = c_{\text{Material}} \cdot V_{\text{WorkPiece}} + C_{\text{Tool}} = c_{\text{Material}} \cdot \frac{m_{\text{WorkPiece}}}{\rho_{\text{Material}}} + C_{\text{Tool}}. \quad (2.25)$$

As tool costs are the purchase costs of new build platforms (they are reusable several times) and wear parts like the powder recoating lips.

Personnel Costs $C_{\text{Personnel}}$

Due to the fully automated SLM process, no manual intervention is necessary during the SLM build process. Personnel costs $C_{\text{Personnel}}$ occur in the time ranges between two SLM build jobs when manual activities for the machine setup and workpiece change are necessary. To take this into account, process monitoring shares a, b and c are defined:

$$C_{\text{Personnel}} = c_{\text{Personnel}} \cdot \left(a \cdot t_{\text{Main}} + b \cdot \frac{t_{\text{MachineSetup}}}{n_{\text{Job}}} + c.t_{\text{WorkPieceChange}} \right). \quad (2.26)$$

Costs for Electricity

The cost estimation for the electricity costs $C_{\text{Electricity}}$ is obtained by the energy price $c_{\text{Electricity}}$, the power consumption $E_{\text{Electricity}}$ at the associated time shares during the SLM process:

$$C_{\text{Electricity}} = c_{\text{electricity}} \cdot E_{\text{Electricity}} \cdot \left(t_{\text{Main}} + t_{\text{Auxiliary}} + t_{\text{BPpreheat}} \right). \quad (2.27)$$

Costs for Shielding Gas

The costs for shielding gas can be calculated using the shielding gas price c_{SG}, the shielding gas consumption $\dot{V}_{\text{SG}}$ and the associated time shares during the SLM process by Eq. (2.28):

$$C_{\text{SG}} = c_{\text{SG}} \cdot \dot{V}_{\text{SG}} \cdot \left(t_{\text{Main}} + t_{\text{Auxiliary}} + t_{\text{SGin}} + t_{\text{BPpreheat}} \right). \quad (2.28)$$

Shielding gas consumption occurs during the SLM process related process steps like the main time, the auxiliary time, during flooding the process chamber with shielding gas and during preheating the build platform.

Total Costs of One SLM Build Job

The number of SLM build jobs n_{SLMJob} can be expressed by Eq. (2.29), where m equals the lot size of the workpiece and m_{SLMJob} equals the number of workpieces that can be produced in one single SLM build job:

$$n_{\text{SLMJob}} = \left\lceil \frac{m}{m_{\text{SLMJob}}} \right\rceil. \quad (2.29)$$

The total cost of one SLM build job $C_{\text{SLMBuildJob}}$ can be calculated according to Eq. (2.30):

$$C_{\mathrm{SLMBuildJob}} = m \cdot C_{\mathrm{Material}} + n_{\mathrm{SLMJob}} \cdot (C_{\mathrm{SLMMachine}} + C_{\mathrm{Personnel}} + C_{\mathrm{Electricity}} + C_{\mathrm{SG}}). \tag{2.30}$$

Each single cost element C_i can be calculated by Eqs. (2.20)–(2.29).

2.4.3.7 Evaluation of Cost Drivers

In this chapter, the evaluation of the cost drivers in relation to the following input factors is described:

- Workpiece dimensions
- Filling degree of workpiece envelope
- Build envelope dimension
- Number and output power of lasers
- Number of scanner systems

2.4.3.8 Workpiece Dimension

Figure 2.26 shows the cost contribution for SLM manufacturing of different workpiece dimensions with a standard SLM machine configuration. Regardless of the workpiece dimension, the machine costs are the dominating share of costs. When reducing the workpiece size—and thus the workpiece height—less powder material has to be melted and the number of layers decreases. This leads to shorter build job times and increases the number of performed build jobs during the whole machine lifetime. The more the build jobs are performed, the more the manual

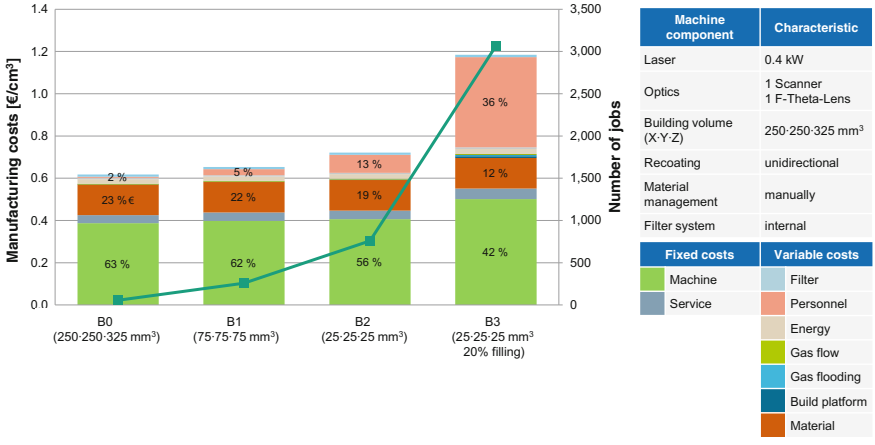

Fig. 2.26 Influence of part volume on workpiece costs (Schrage 2016)

activities have to be done, which directly leads to an increase of the personnel costs. Furthermore, the share of machine costs decreases due to increasing machine downtime.

The share of personnel costs as the dominating cost driver, for instance, machine preparation and setup activities, represents less than 2 % at workpiece B0 and 36 % at workpiece B3.

Material costs are high at workpiece B0, with about 23 %, and low when building workpiece B3 with 12 %.

When comparing the cost contribution of workpieces B2 and B3, the influence of the workpiece filling degree becomes clear. Both workpieces have the same envelope volume, height and thus the same number of layers. But when reducing the workpiece volume down to 20 % at constant workpiece envelope the number of build jobs increases significantly. This leads to increasing personnel costs from 13 % up to 36 %.

2.4.3.9 SLM Machine Build Envelope

Figure 2.27 shows the influence of the build platform size on the workpiece costs of SLM manufacturing workpiece B3. The increase of build platform size inducts an increase of machine costs (fixed costs). On the other hand, the bigger the build platform size is, the more the workpieces can be manufactured in one build job. This leads to a lower number of total build jobs due to longer build job times t_{SLMJob} and thus reducing the number of jobs and thereby the manual effort. This leads to decreased total costs up to an increase of the build platform size of 150 %. Further increase of build platform size leads to higher machine costs and higher total costs.

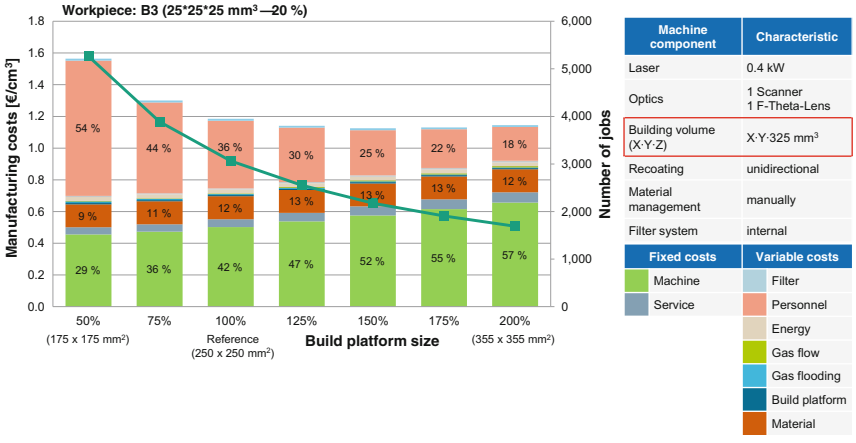

Fig. 2.27 Influence of build envelope size on workpiece costs (workpiece B3) (Schrage 2016)

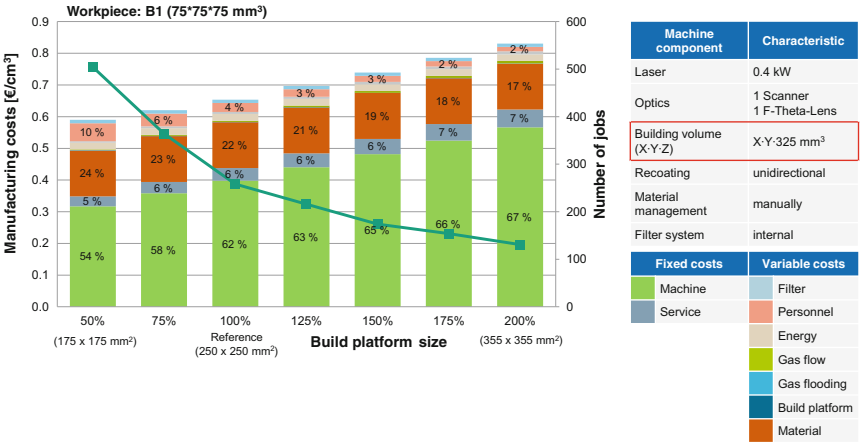

Fig. 2.28 Influence of build envelope size on workpiece costs (workpiece B1) (Schrage 2016)

The total build costs of workpiece B1 also increases when increasing the build platform size due to the increase of the machine costs (fixed costs) (see Fig. 2.28). The lower share of personnel costs compared to that of workpiece B3 is because of the lower number of build jobs due to the greater workpiece dimensions. The share of personnel costs also decreases when increasing the build platform size, but it has only small impact on total costs.

For relatively big workpiece dimensions like workpiece B1 and thus for a low number of build jobs, an increase of the work area size primary leads to an increase of the machine costs (fixed costs). For small workpieces, which induce a high number of build jobs, the high influence of the personnel costs and the high downtime of the machine during the machine setup times are shown. Depending on the manufacturing task, a cost optimization measure can be the increase of the build platform.

2.4.3.10 Laser Beam Sources and Scanner Systems

Figure 2.29 shows the influence of the total laser power, which is used in one single standard SLM machine on the manufacturing costs of workpiece B0. Using higher laser output powers, the build-up rate can be increased by increasing the scanning speed v_s or increasing the scan line distance Δy_S [see Eq. (2.15)]. High build-up rate that equals high machine productivity reduces the machine costs.

The lowest total costs of SLM manufacturing of workpiece B0 occur at using 3× 1 kW laser and 3× optics in one SLM machine.

The increase in total costs when using more than three laser and optical systems is caused from increasing energy costs. Parallelization of SLM processes at the same total laser output power leads to lower total costs (see Fig. 2.29). In this

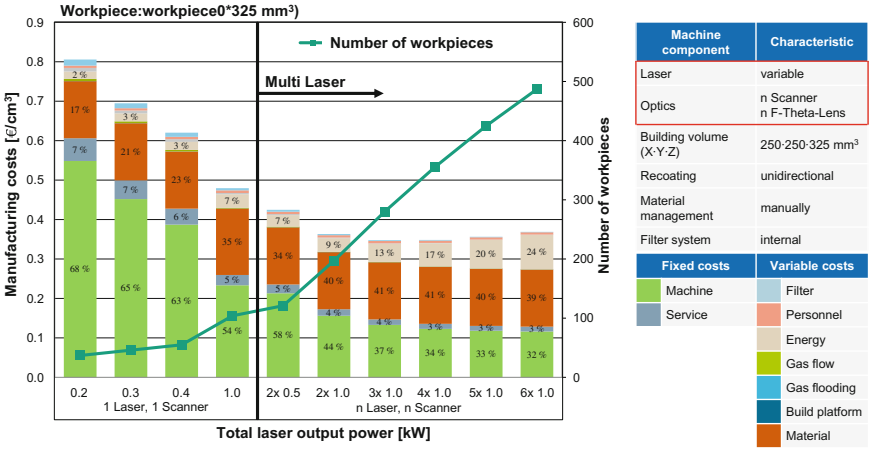

Fig. 2.29 Influence of the optical configuration on workpiece costs (Schrage 2016)

example, a SLM machine configuration with 2× 0.5 kW lasers creates lower total costs than a machine configuration with 1× 1.0 kW laser.

When considering the SLM manufacturing of workpiece B3, you can also find a cost optimum of the optical machine configuration (see Fig. 2.30). In this case, it lies at using 2× 1.0 kW lasers. By increasing the total laser output power from 0.2 kW up to 1 kW using one single-laser source and one optical system, the total costs decrease because of the increased build-up rate. The total costs decrease up to a total output power of 2 kW that is provided by two 1 kW laser beam sources. Further increasing of the number of laser beam sources and optical systems leads to an increase in energy costs that directly induces higher total costs.

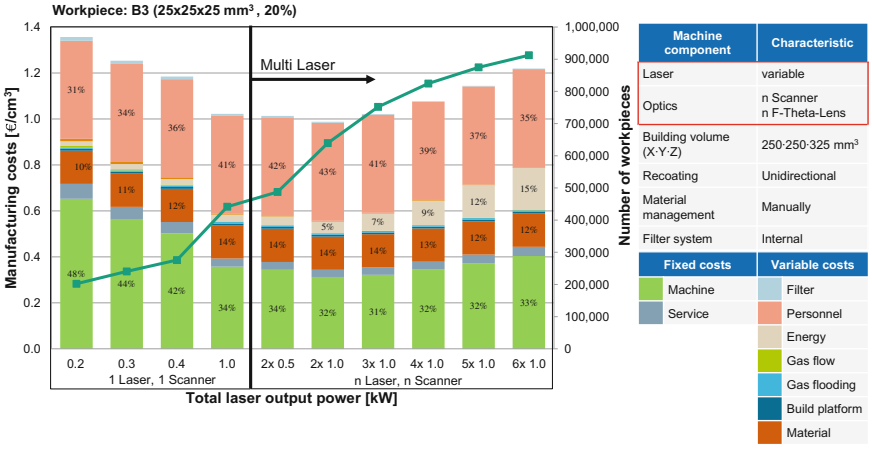

Fig. 2.30 Influence of optical configuration (number of laser beam sources and scanner systems) on workpiece costs (Schrage 2016)

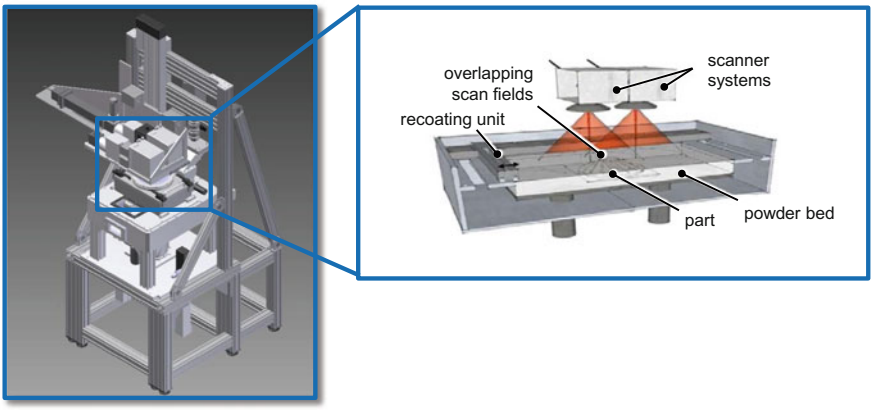

Fig. 2.31 CAD model of a multi-scanner SLM machine (*left*) and a schematic illustration of a multi-scanner process chamber (*right*)

2.4.3.11 Machine Development

In order to increase the productivity of SLM process, new SLM machine concepts are developed, constructed and tested. First, a multi-scanner system for simultaneous exposure of one scan field is built up. Second, a novel SLM machine concept is shown that works with a laser line generated by positioning multi-individual laser spots, produced by low-cost laser sources next to each other. This system is scalable in terms of its build area size and its total laser power.

Upscaling of build-up rate can be done via parallelizing two SLM processes using multi-laser beams and multi-scanner systems (see Fig. 2.31). This scaling allows for double, triple, etc., the achievable build-up rate. There is no need to develop new SLM process parameters; all process parameters (like laser power P_L, scanning speed v_s, layer thickness D_S) can be maintained. Using multiple laser and scanner systems also allows for increasing the build envelope by aligning each single scan field edge to edge. By aligning two adjacent scan fields with an overlap area in that both laser and scanner systems can perform the laser exposure, big workpieces can be manufactured. Providing multi-laser beams in one machine usually requires the integration of multi-laser beam sources and multi-laser scanner systems.

The upscaling of build-up rate and build envelope can be performed in the units of one laser scanner system. Disadvantageous is the increase in investment costs. Laser and scanner systems are the most expensive parts in SLM machines. By scaling process productivity by increasing the laser output power expenses for process development become necessary.

For scaling up both process productivity and machine build envelope, a new SLM machine concept has been developed at Fraunhofer ILT (Eibl 2014).

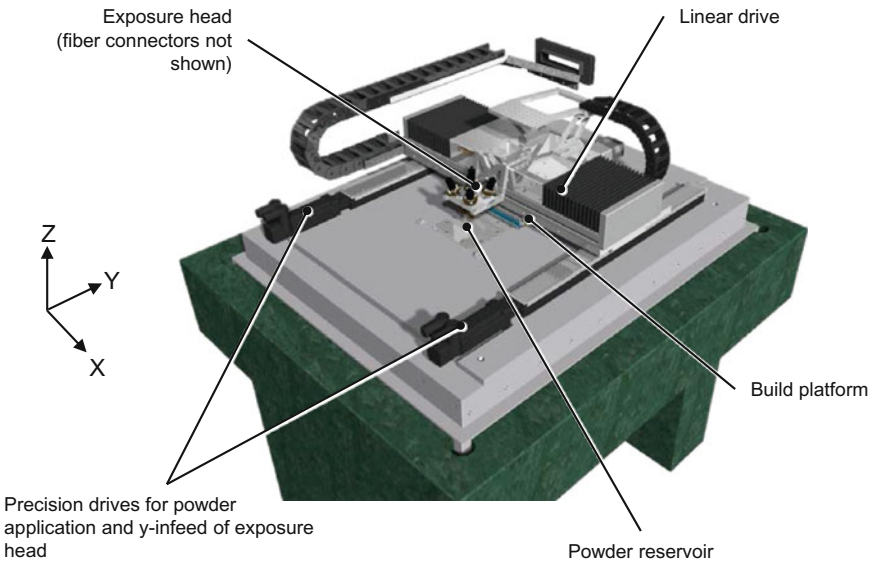

Fig. 2.32 CAD model of a multi-beam SLM machine

The basic machine setup of this new SLM machine concept is shown in Fig. 2.32. A print head-like processing head is equipped with several individually controllable diode lasers that move using linear axes. Each diode laser and its optics create a single spot aligned in one line. The advantage of multi-spot processing is that the build-up rate can be increased just by adding a virtually unlimited number of beam sources with no need for modifications to the system design, exposure control software or process parameters. The new machine and exposure design also make it possible to increase the build envelope simply by extending the travel lengths of the axis system and without changing the optical system. In addition, the processing head has a local shielding gas flow system that guarantees a constant stream of shielding gas at each processing point, regardless of the size of the installation space. This is essential for achieving position-independent, reproducible component quality.

Five diode lasers from DirectPhotonics with a laser output power of 170 W (each) are used. The build envelope is $150 \times 50 \times 180$ mm^3. The exposure head is moved by a linear drive in the direction of exposure (x-direction), and the in-feed and powder application takes place in y-direction by two precision drives. Each single laser spot can be switched on and off individually. The movements of the linear axes and the output power of the lasers are controlled with special controller software that allows developing various laser exposure strategies (see Fig. 2.33, down right).

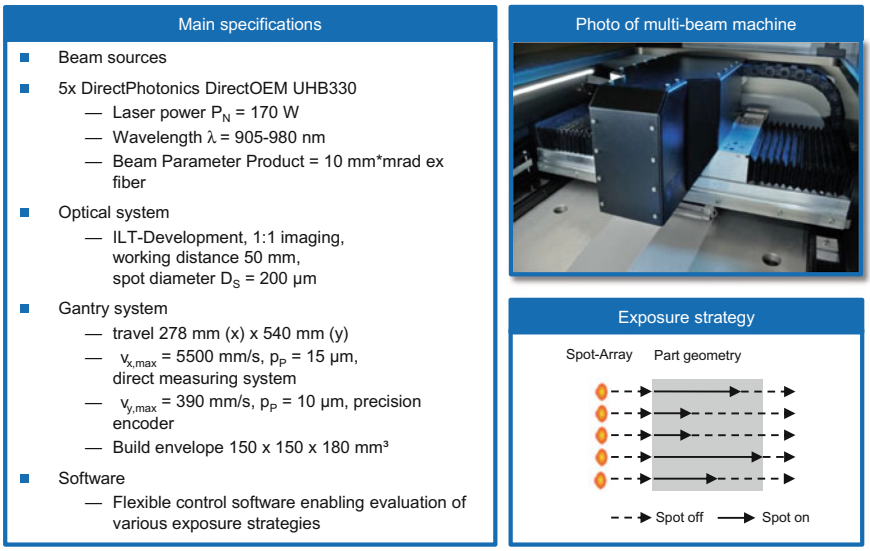

Fig. 2.33 Overview about the main specifications (*left*) a photograph (*top right*) and an example exposure strategy (*down right*) of the multi-beam SLM machine

2.4.4 High-Power Selective Laser Melting (HP SLM)

In order to give an answer to the two research questions presented in Sect. 2.3.4, a systematic procedure according to Fig. 2.34 is set up. First, a process window has to be examined, allowing the production of test samples with an average density $\geq$ 99.5 % and no cracks appearing. Therefore, the SLM machine from SLM Solutions type SLM 280HL is used. The machine is equipped with two laser sources, a single-mode fiber laser with a maximum laser power $P_L \leq$ 400 W (beamway 1) and a multi-mode fiber laser with a maximum laser power $P_L \leq$ 2 kW plane; the laser diameter for beamway 1 is d_{s1} = 80 µm and d_{s2} = 720 µm for beamway 2. The machine allows changing the active fiber in process by using a beamswitch unit. This beamswitch unit is a result of phase 1 of the Cluster of Excellence (Schleifenbaum 2012).

The powder material used for the research are the maraging tool steel 1.2709 (X3NiCoMoTi18-9-5) with a grain size between 15 and 45 µm. Maraging steels are iron nickel alloys with absence of carbon and contain additional alloying elements such as molybdenum, cobalt, titanium or aluminum. The structural hardening is obtained by intermetallic phases between nickel and the alloying components (Co, Mo, Ti). Thus, these steels are characterized by ultra-high strength, superior toughness, good weldability and low distortion (Jägle et al. 2014).

For the analysis of a process window, which enables the production of test specimen with an average density $\geq$ 99.5 % for HP SLM, test specimens, in accordance with Fig. 2.35, are manufactured. Afterward, the test specimens are cut

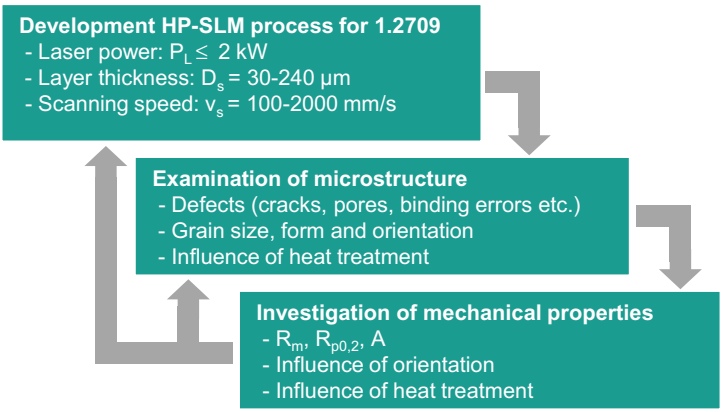

Fig. 2.34 Procedure for HP SLM of 1.2709

into two pieces, grinded, polished and examined with light microscopy to measure the density. The density is measured by arithmetic averaging of the results from five measurement fields per test specimen (see Fig. 2.35). The test specimen produced by beamway 1 using $P_L \leq 400$ W laser power is manufactured according to geometry. For the examination of a HP SLM process, window geometry 2 is used, whereby the part is divided into an outer skin (b = 2 mm) and an inner core. The skin is manufactured by beamway 1, and the core by the use of beamway 2.

In Fig. 2.36, the average density for cubic test specimen manufactured by beamway 1 is illustrated according to the employed scanning speed and an employed laser power P_L = 200–400 W. It can be observed that with increase of the scanning speed the density decreases, due to lower volume energy. Thereby,

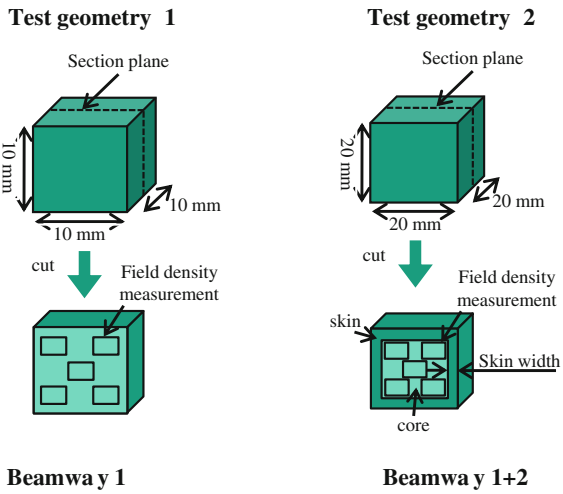

Fig. 2.35 Test specimen for the development of a process window for HP SLM

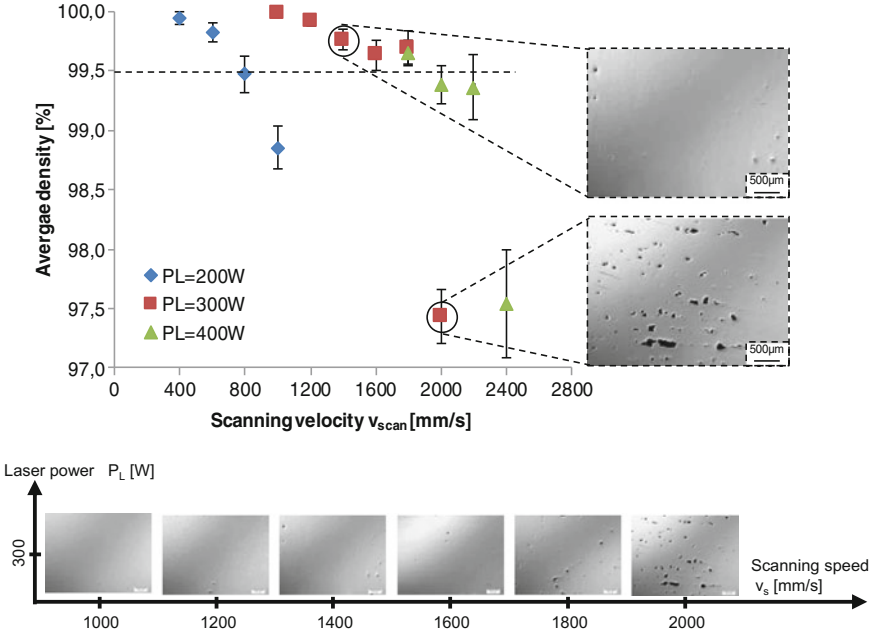

Fig. 2.36 Average density of cubic test specimen manufactured by beamway 1 (D_S = 30 µm)

binding errors appear because the powder material is not completely melted up. For beamway 1 using a scanning speed of v_s = 1400 mm/s, an average density of 99.76 % is achieved which results in a theoretical build-up rate of $\dot{V}$ = 2.94 mm^3/s and a volume energy of E = 102 J/mm^3 is needed. These values are used as a reference for the following analysis of a HP SLM process window.

For the development of a process window for HP SLM in a first step, cubic test specimens according to geometry 3 are manufactured with P_L = 1 kW laser power and a scan line spacing of Δy_s = 500 µm. The resulting density for a layer thickness D_S = 60–210 µm and a scanning speed v_s = 100–400 mm/s is illustrated in Fig. 2.37, right. It can be observed that a laser power of P_L = 1 kW can be used to manufacture test specimen with an average density $\geq$99.5 %. In addition, the results show that an increase of layer thickness from D_S = 60 µm up to D_S = 180 µm results in a significant increase of the build-up rate from $\dot{V}$ = 9 mm^3/s up to $\dot{V}$ = 18 mm^3/s. In comparison with conventional SLM employing a laser power of P_L = 300 W and D_S = 30 µm, the theoretical build-up rate can be increased by a factor of approximately 6.1.

With regard to process efficiency, the use of increased laser power of P_L = 1 kW and the adaption of layer thickness as well as scanning speed results in a decreased needed volume energy. At a layer thickness of D_S = 180 µm, a volume energy of E_V = 55.56 J/mm^3 is needed. In comparison with conventional SLM (P_L = 400 W,

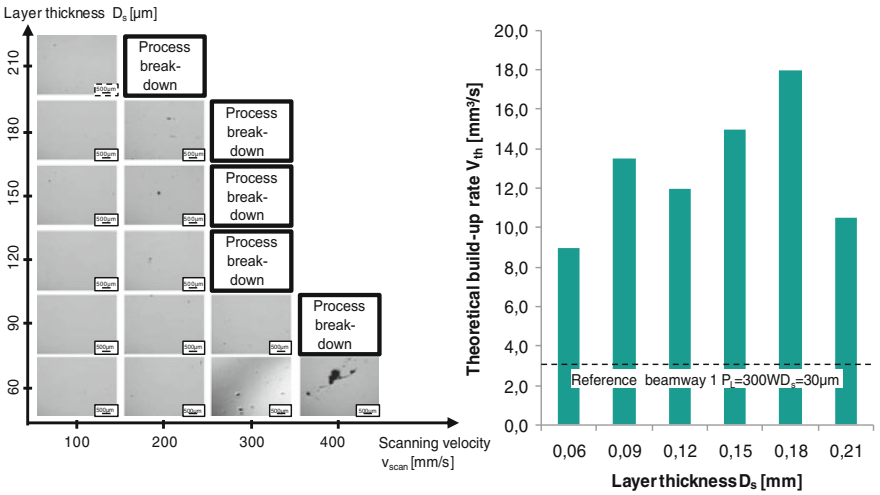

Fig. 2.37 Cross sections of cubic test specimen (P_L = 1 kW) according to D_S and V_s (*left*). Resulting theoretical build-up rate $\dot{V}$ according to D_S (*right*)

D_S = 30 µm) where a volume energy of E_V = 102 J/m^3 is needed, the process efficiency can be significantly increased.

In the next step, the laser power is increased up to P_L = 1.5 kW and P_L = 2 kW. It shall be examined whether a further increase of laser power can be used for a further increase in the theoretical build-up rate.

The achievable theoretical build-up rate for cubic test parts, with an average density $\geq$99.5 %, is shown in Fig. 2.38, according to the employed laser power. The results show that an increase of the laser powder allows the increase of the theoretical build-up rate. For example, at a layer thickness of D_S = 180 µm the increase of the laser power from P_L = 1 kW up to P_L = 2 kW results in an increase of the theoretical build-up rate from $\dot{V}$ = 18 mm^3/s up to $\dot{V}$ = 27 mm^3/s, which is an increase by a factor of 1.5. Considering the process efficiency, an increase of the laser power from P_L = 1 kW up to P_L = 2 kW leads to an increased needed volume energy E_V = 74.07 J/mm^3. In relation to the volume energy needed at P_L = 1 kW, the process efficiency declines.

In conclusion, the use of a laser power of P_L = 1 kW and the adaption of scanning speed as well as layer thickness results in increased theoretical build-up rates and a less-needed volume energy in comparison with the conventional SLM process (P_L = 400 W, D_S = 30 µm). A further increase of the laser power up to P_L = 1.5 kW and P_L = 2 kW leads to an increase of the theoretical build-up rate, but the process efficiency E_V is negatively influenced.

Microstructure

After the development of a process window for a laser power up to P_L = 2 kW, the microstructure of the test specimen is analyzed. Therefore, cross sections are

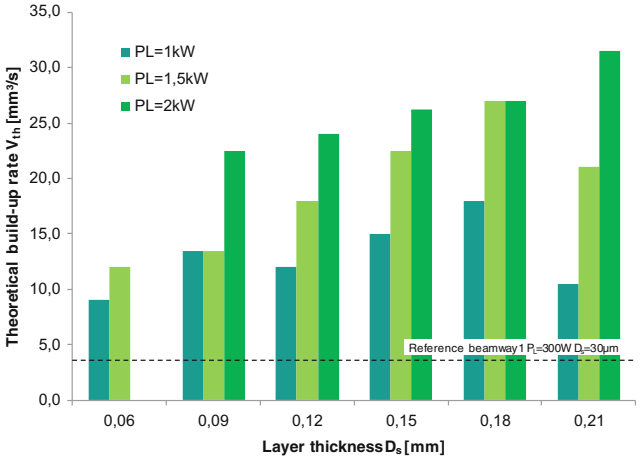

Fig. 2.38 Resulting theoretical build-up rate according to layer thickness for a laser power P = 1–2 kW

prepared and etched as well as scrutinized by light microscopy and electron backscatter diffraction (EBSD).

Figure 2.39 shows the microstructure of the conventional SLM (beamway 1) process with overlapping melt pools featuring colonies of columnar martensitic grains that exceed the melt pools because of the epitaxial growth of the former austenitic grains during solidification. Figure 2.39 shows the much larger melt pools of the high-power SLM process parameters in the core of the skin–core strategy sample featuring the same colonies of columnar martensitic grains exceeding multiple scan layers. With regard to the results of the EBSD analysis, it

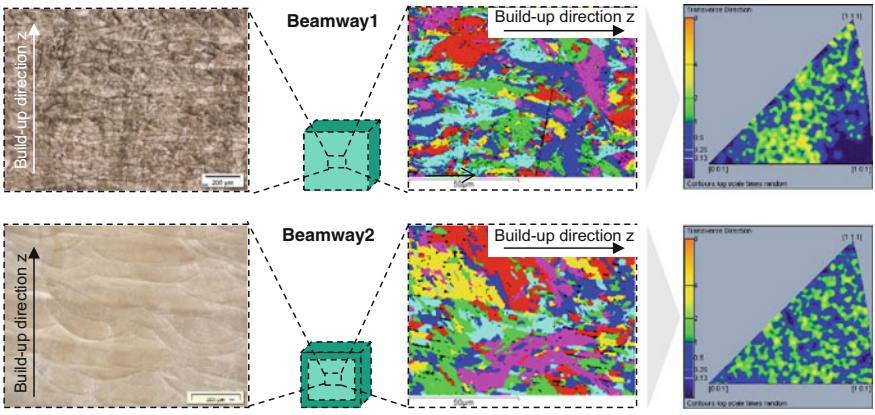

Fig. 2.39 Microstructure of SLM test specimen above: Conventional SLM below: HP SLM with skin–core strategy

can be observed that for beamway 1 smaller grains appear [equivalent circle diameter (ECD) = 3.3 µm] in comparison with the use of beamway 2 (ECD = 4.3 µm). The reason for this is the significant difference in cooling and solidification behavior in the melt pool caused by the different process parameters. The colonies of grains with the same orientation can be seen in both skin and core melt pools indicating that the former austenite grains grew from the smaller melt pools in the larger melt pools and vice versa forming a perfect metallurgical bond.

Mechanical Properties

The next step is to analyze the mechanical properties of the HP SLM-manufactured tool steel and compare the results with conventional SLM. Therefore, tensile test specimens according to DIN 50125 type B5x25 are manufactured with beamway 1 (P_L = 300 W, D_S = 30 µm) and beamway 2 (P_L = 1–2 kW, D_S = 90–180 µm). The orientation of these tensile test specimens is 90° to the platform (standing). After the SLM process, the test specimens are milled to their final dimensions and afterward heat-treated. For the heat treatment 2, different strategies are examined and compared with the resulting mechanical properties after the SLM process. The first heat treatment approach is a quenching at T = 510 °C for t = 6 h. The second approach is the use of a solution annealing at T = 900 °C for t = 1 h followed by the annealing at T = 510 °C for t = 6 h. The results according to the heat treatment are shown in Fig. 2.40.

The results in Fig. 2.40 show that after the SLM process the requirements for conventionally processed maraging tool steel 1.2709 after heat treatment strategy 1 (R_m = 1950 N/mm^2, A = 3 %) are not fulfilled. Therefore, the SLM-manufactured tensile test specimen is heat-treated with two different strategies. It can be observed

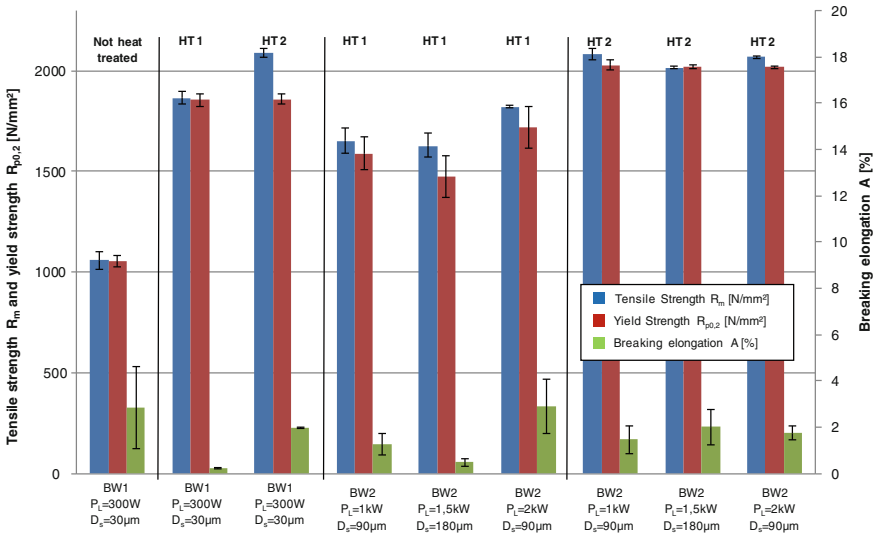

Fig. 2.40 Mechanical properties according to parameter set and heat treatment

that for heat treatment 1 (annealing T = 510 °C, t = 6 h) the mechanical properties can be increased. The tensile test specimens show a tensile strength of R_m = 1867 N/mm^2 and a breaking elongation of A = 0.3 %. The same results can be observed for tensile test specimen manufactured by beamway 2 and using increased laser power up to P_L = 2 kW. In the next step, the tensile test specimens are heat-treated with strategy 2, including a solution annealing and afterward an annealing step. The results in Fig. 2.40 show that the mechanical properties can be significantly improved. All test specimens show higher values for tensile strength and yield strength in comparison with the test specimens heat-treated with strategy 1.

One approach to explaining these differences concerning the mechanical properties according to the heat treatment can be the appearance of residual austenite. Figure 2.41 shows the results of the EBSD analysis for cubic test specimens exposed by the two heat treatment strategies. By the use of an additional solution annealing followed by quenching almost no residual austenite can be observed. In contrast, the microstructure after quenching shows residual austenite which exhibits lower mechanical properties.

As a result, it can be observed that increased laser power up to P_L = 2 kW can be used to significantly increase the productivity of the SLM process. Overall, the theoretical build-up rate is increased up to $\dot{V}$ = 27 mm^3/s, which is an increase by a factor of nine in comparison with the SLM state-of-the-art process for 1.2709. In addition, the mechanical properties of conventional and HP SLM-manufactured test

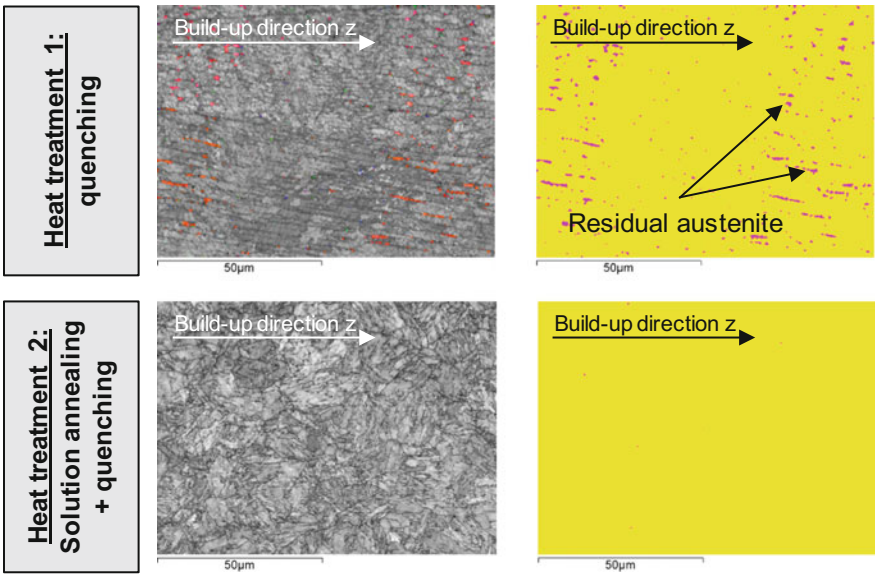

Fig. 2.41 Results of the EBSD analysis for residual austenite according to the heat treatment strategy

specimen are examined. The results show that by adapting the heat treatment the reference for the tool steel 1.2709 can be attained, although the theoretical build-up rate is significantly increased.

2.4.5 *Qualification of Lattice Structures Manufactured by Selective Laser Melting (SLM) for Custom Part Properties*

The qualification of lattice structures for custom part properties is performed on two different types of structures. To continue and extend the research on structure type f2cc,z, research on the influence of different scanning strategies on the mechanical properties of this type of anisotropic structure is carried out. To complement the research with a more isotropic structure, a hollow-sphere structure is developed considering the main restrictions of the SLM process. The hollow-sphere structure is composed of a hollow sphere with a predefined wall thickness and diameter. To remove the unmolten powder, every sphere contains four little holes. The spheres have a defined overlap of usually 5 % of the diameter. This guarantees the stable connectivity of the spheres. The holes of the inner spheres form little channels to enable a smooth removal of the powder through the outer spheres. The examined structure types and their main geometric parameters are illustrated in Fig. 2.42. The

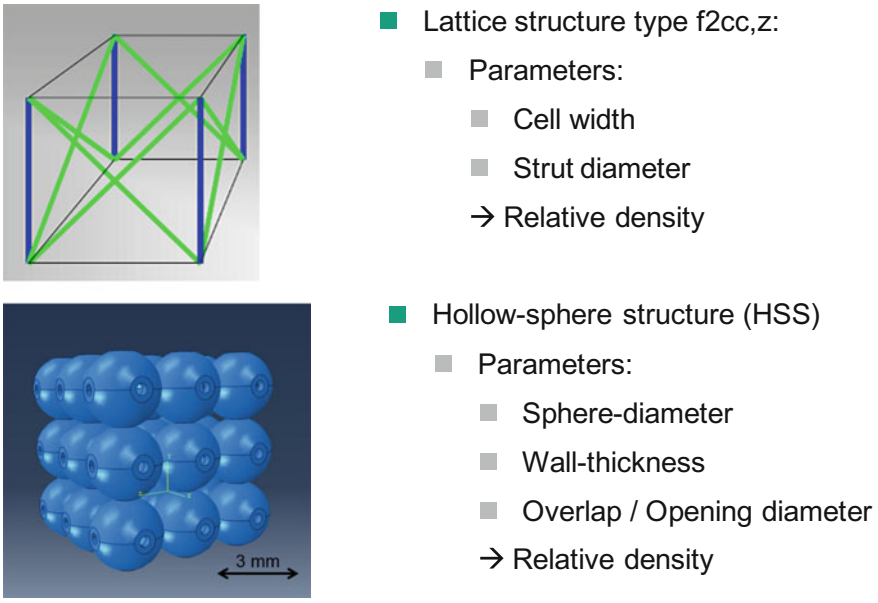

Fig. 2.42 Examined structure types and main geometric parameters (Merkt 2016)

aggregated parameter relative density is the most common parameter to allow a comparison of the mechanical properties of different structure types and the most common input parameter for the scaling laws.

There are two ways to manufacture cubic lattice structures by SLM: Point-like exposure and contour-hatch exposure. At the point-like exposure, single points are exposed with laser radiation. Layer by layer only single points are exposed until the final lattice structure is built. The size of the strut diameter is determined by exposure time at the single points and the melt pool propagation, which is determined by the material properties. Very small structures can be built by this exposure style. The main advantages of this scanning strategy are the reduction of process time and reduced amount of machine data. The complex geometry of lattice structures is fractionized into a set of points that causes only little amount of machine data. Currently, the PL exposure is not a machine standard in most of the industrial systems, which restrain the further distribution of this type of scanning strategy.

The second scanning strategy, which is used to manufacture lattice structures by SLM, is the conventional contour-hatch exposure. In contrast to the point-like exposure, the contour of the single struts is scanned with a little offset to consider the melt pool propagation. The inner volume of a strut is filled with the so-called hatch vectors. The main advantages of the contour-hatch scanning strategy are the freedom of geometries, which can be manufactured by this machine standard scanning strategy. In opposition to the point-like exposure, contour-hatch exposure is not limited to lattice structures and can be used for more volumetric geometries. The contour scan usually leads to better surface quality of the manufactured specimens. A disadvantage of this scanning strategy is the relatively high process time that is caused by the high number of scanning vectors and scanner delays that appear during the scanning of, for instance, round contours. The examined scanning strategies are illustrated in Fig. 2.43 with their main advantages and disadvantages.

To analyze the influence of different scanning strategies on the mechanical properties of lattice structures, blocks of lattice structures ($10 \times 10 \times 15$ unit cells, type f2cc,z) are built with both point-like and contour-hatch exposure. Before the mechanical tests, the process parameters of both scanning strategies are optimized regarding material density and geometric deviation from the CAD model. Three contour-hatch parameters (CH1–3) are chosen, resulting in material density higher than 99.90 % and geometric deviations smaller than 5 %. For the point-like exposure, one parameter set is chosen (PL). Quasi-static compression tests are carried out according to DIN EN ISO 50134 (DIN 2008) to compare the mechanical response of lattice structures manufactured by different scanning strategies. The results of the compression tests are shown in Fig. 2.44. If one compares the stress–strain curves of the specimens manufactured with different scanning strategies, it is clearly visible that the specimens manufactured by point-like exposure are less resistant against compressive loads.

The specimens manufactured by contour-hatch exposure outperform the point-like exposed specimens in terms of stiffness, yield stress R_{p1} and specific energy absorption E50 (see Table 2.3).

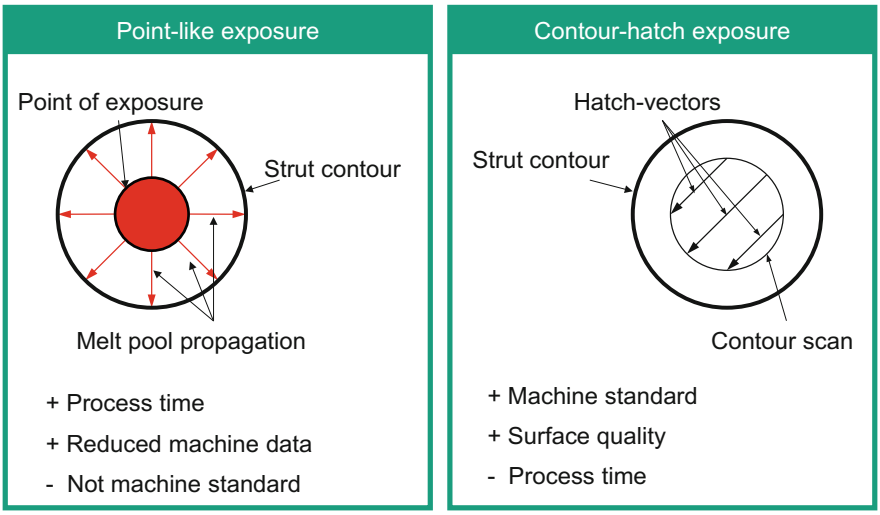

Fig. 2.43 Examined scanning strategies for the manufacture of lattice structures (Merkt 2016)

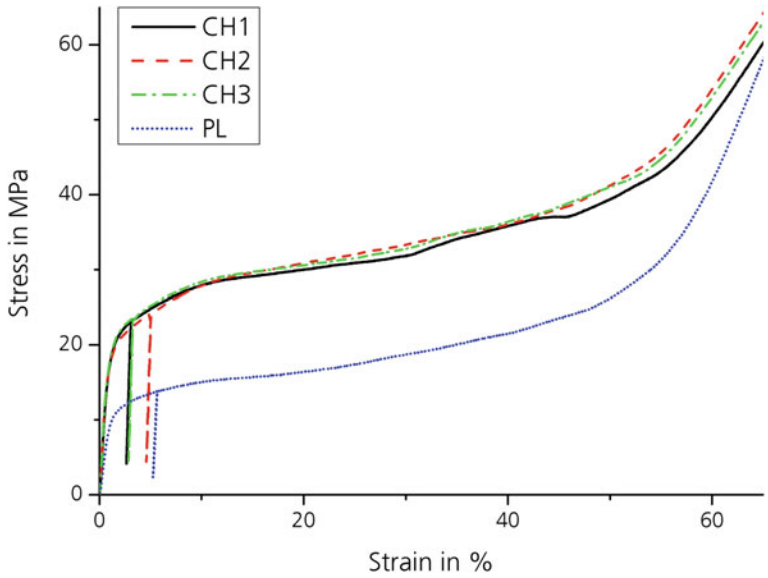

Fig. 2.44 Comparison of stress–strain curves for specimens manufactured by different scanning strategies (Merkt 2016)

The stiffness of the contour-hatch specimens is about 37 %, the yield stress R_{p1} about 50 % and the specific energy absorption E50 about 37 % higher than the point-like exposure specimens.

Table 2.3 Comparison of the main properties of lattice structure under compressive load (Merkt 2016)

Property	CH1	PL
Stiffness m (MPa)	4318	2695
Yield stress Rp1 (Mpa)	20.07	10.05
Specific energy absorption E50 (mJ/mm^3)	16.01	10.04

The reason for these differences can be found by examining the microstructure of the lattice structures. Therefore, EBSD analysis is performed that allows a detailed look on the crystalline structure and the size and orientation of the grains. The EBSD results show that both specimens exhibit the same gamma phase austenite. Differences can be found in the grain size and orientation. The point-like exposure specimens are composed of columnar grains and larger diameters, which are orientated toward the build-up direction. The contour-hatch exposure specimens exhibit a random and stochastic distribution of grains with smaller diameters. No clear orientation of the grains is visible (see Fig. 2.45).

The reason for the different microstructures can be found in the way laser energy is deposited into the powder bed. The cooling down rate for the point-like exposure specimens is much lower than for the contour-hatch exposure specimens, giving the material more time to form larger grains with a specific orientation. Another reason is the repeating re-melting of already exposed layers due to quite long exposure time at single spots at the point-like exposure.

In general, smaller grains lead to better mechanical properties than larger grains. This correlation can be transferred to the lattice structures and explain why

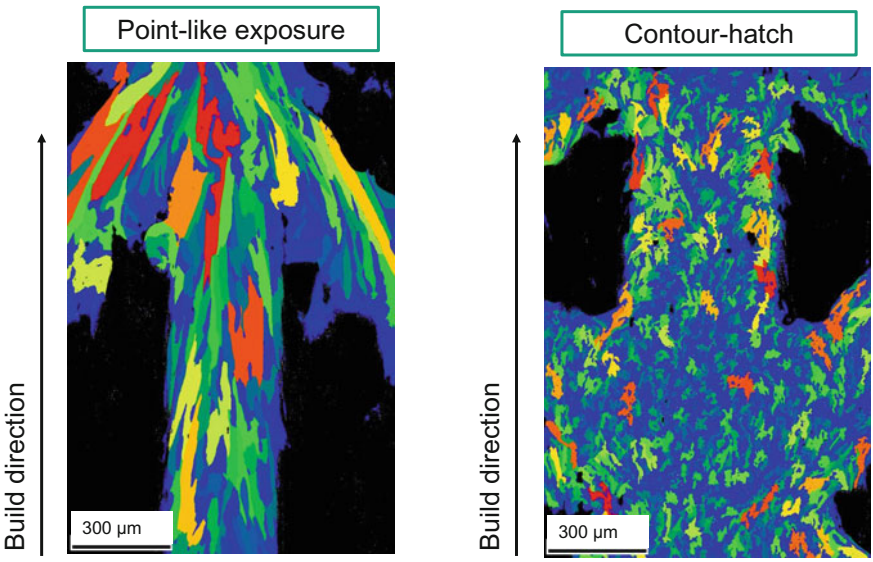

Fig. 2.45 Examination of grain size and orientation of lattice structures manufactured by different scanning strategies (Merkt 2016)

contour-hatch specimens show better results than point-like exposed specimens regarding the mechanical response under compressive load. These results lead to the conclusion that contour-hatch scanning strategy is more suitable for the manufacturing of lattice structures with SLM.

To manufacture the hollow-sphere structure, the contour-hatch scanning strategy needs to be applied due to the more volumetric design of hollow spheres. Again, specimens are manufactured to carry out quasi-static compression tests according to DIN EN ISO 50134 (DIN 2008). Figure 2.46 shows stress–strain curves of three samples from the same test series. All samples exhibit a wall thickness of 250 µm and a constant diameter of 3 mm. The reproducibility of the stress–strain curves within the test series is given (see Fig. 2.46).

One of the main advantages of cellular materials is the adjustment of mechanical properties through the modification of geometric parameters of the structures. Figure 2.47 shows the influence of different wall thicknesses from 250 to 350 µm on the stress–strain curve of hollow-sphere structures. The stiffness, yield strength and specific energy absorption can be adjusted by the wall thickness of the hollow-sphere structures.

Another test series was built to examine the influence of the build-up direction on the mechanical properties of the hollow-sphere structure. Therefore, hollow-sphere specimens were built in a lying and standing position on the substrate plate. To validate the isotropy of the hollow-sphere structures, specimens in two build-up directions are built and tested under compressive load. In Fig. 2.48, the stress–strain curves of these specimens are illustrated. The stress–strain curves

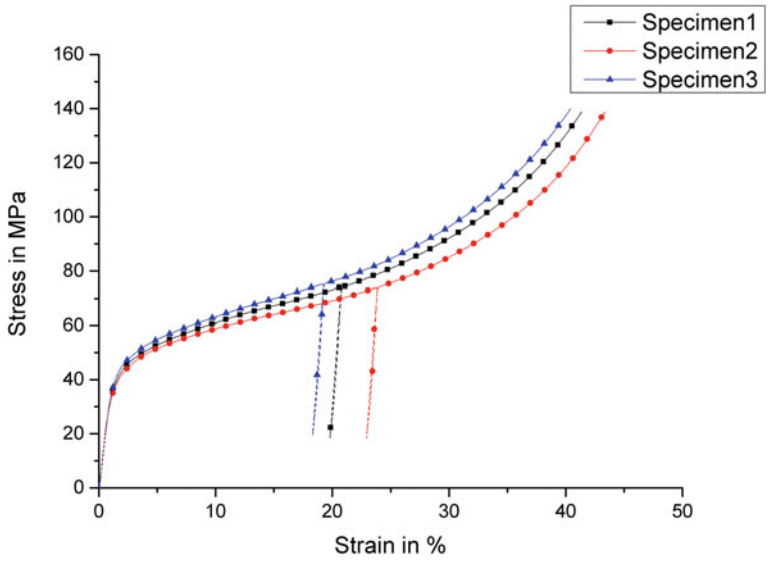

Fig. 2.46 Exemplary stress–strain diagram for hollow-sphere structures with a wall thickness of 250 µm (Merkt 2016)

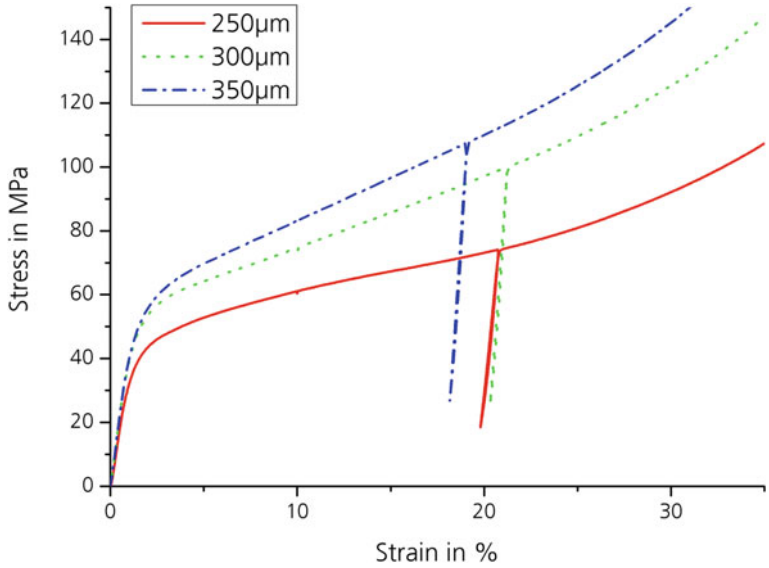

Fig. 2.47 Stress–strain diagram of hollow-sphere structures with different wall thicknesses (Merkt 2016)

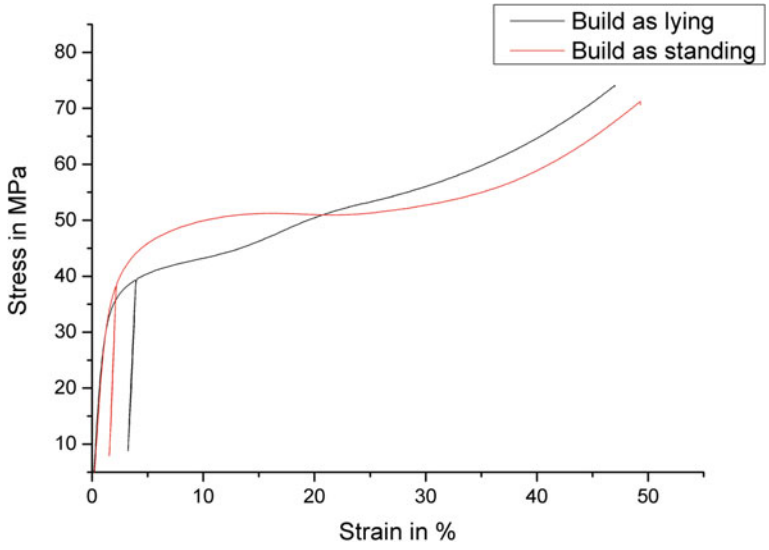

Fig. 2.48 Stress–strain diagram of hollow-sphere structures build in different directions (Merkt 2016)

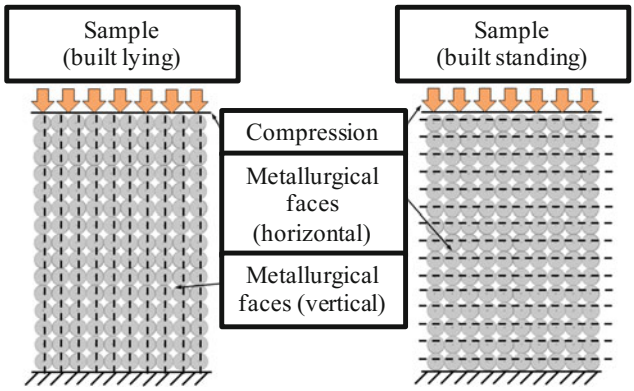

Fig. 2.49 Orientation of metallurgical faces for lying and standing samples (Merkt 2016)

do not exactly follow the same route. Compared to the anisotropic cubic lattice structures, the hollow-sphere structure can be seen as quasi-isotropic in the two examined directions. The reason for the deviations of the course of the lying and standing specimens can be found in the orientation of metallurgical faces inside the specimen's microstructure. For the lying samples, the compression direction is aligned to the metallurgical faces, which supports shearing along these faces. This results in a lower resistance against compressive loads and an earlier yielding and a lower stiffness of lying specimens (see Fig. 2.49). For the standing samples, the metallurgical faces are orientated perpendicular to the compression direction. This results in a higher resistance to the compressive loads.

The next step to qualify lattice structures for custom part properties is the development of scaling laws based on a large number of different types and configurations of lattice structures. Therefore, a large amount of lattice structures of type f2cc,z and hollow-sphere structures are built. Figure 2.50 shows an exemplary scaling law of a lattice structure of type f2cc,z for the specific energy absorption E50 in dependence of the cell width of the structures. Lattice structures with cell widths from 1.5 to 5 mm were built. To achieve a greater stiffness and energy absorption, the lattice structures are covered with skins of a thickness of 250 µm. Two groups of structures exist: one with only vertical skins (V) and one with vertical and horizontal skins (VH). The course of the stress–strain diagram of VH structures is shown in Fig. 2.50. As one can see, the specific energy absorption is decreasing with increasing cell widths. The strut diameter is fixed in this experiment, and as a consequence, the relative density is decreasing with increasing cell widths, resulting in lower energy absorption. Moreover, Fig. 2.50 shows that the specific energy absorption is scalable over a broad range from 180 mJ/mm^3 to below 10 mJ/mm^3. Depending on the application, the specific energy absorption can be customized through a variation of the cell width, respectively, relative

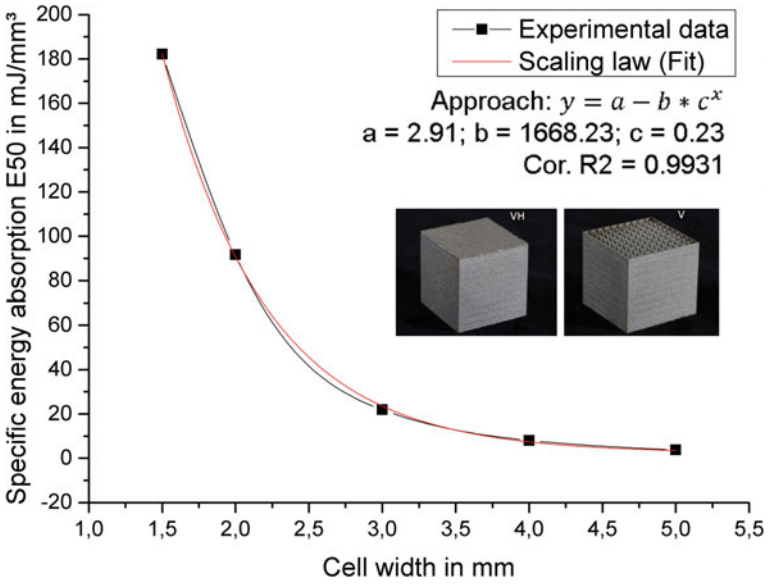

Fig. 2.50 Exemplary scaling law for specific energy absorption in dependence of cell width of lattice structures (type f2cc,z with skins)

density. The red line in Fig. 2.50 shows the fit for scaling law with power laws. The quality of the fit for scaling law is very high with a Cor.R2 of larger than 99 %. The scaling law can be used to determine the suitable structure configuration for specific applications, also between the experimentally determined values.

The benefit of scaling laws to find an appropriate set of structures will be discussed in the following for a crash box example. In formula student competitions there are clear guidelines for the designing of a crash box. The energy that needs to be absorbed is 7350 J. The deceleration must be lower than 20 g to avoid serious damages to the driver. To determine a structure configuration that enables the absorption of exactly 7350 J, the scaling law "Absorbable Energy" can be used. For different strain rates, this scaling law is illustrated in Fig. 2.51 for a lattice structure of type f2cc,z. Depending on the strain rate, three different cell widths are capable of absorbing the necessary amount of energy of 7350 J. The strain defines the deceleration distance that is important to fulfill the requirement of a deceleration lower than 20 g. For 50 % strain, a cell width of 4.1 mm is capable of absorbing the necessary energy. The length of the structure, respectively, the number of unit cells in impact direction, must be chosen to guarantee a deceleration lower than 20 g. A structure with a length of approx. 200 mm could fulfill this requirement.

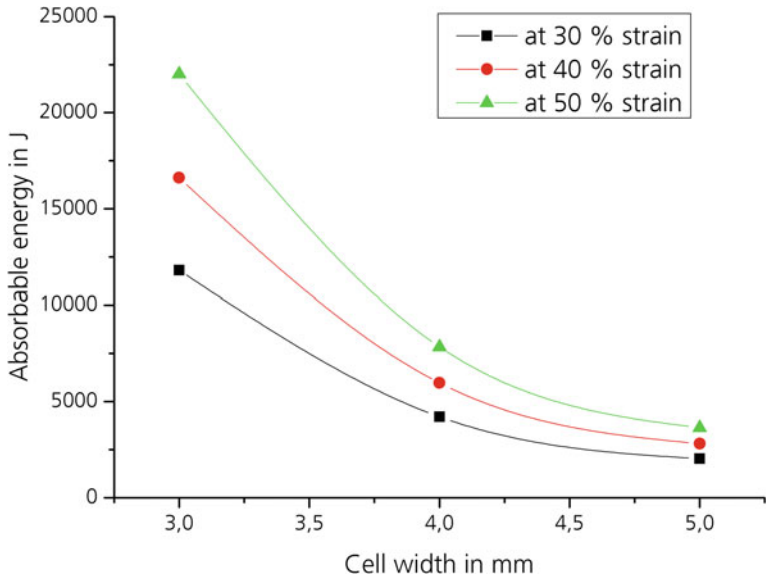

Fig. 2.51 Scaling law "Absorbable Energy" of structure type f2cc,z for different strains

A databank was developed that provides an interface to a design engineer to find suitable structures with respect to concrete requirements based on the above-presented scaling laws. The databank hosts all necessary information about the structural geometry, material, SLM system and process parameters used to manufacture the structures. A master table connects this information to the actual build job and the mechanical properties of these types of structures. This simplifies the designing of functional parts by assisting the design engineer during the selection of suitable structures for customized part functions and interpretation of the experimental results.

Finally, based on these results a design methodology (see Fig. 2.52) is proposed that systemizes the process of designing function components with custom part functions by integrating lattice structures to functional components.

The design methodology consists of four steps. The first step is the selection of a suitable lattice structure type depending on the application. For some applications, like the above-discussed crash box, a more anisotropic structure is needed. For other lightweight applications, a more isotropic structure like the hollow-sphere structure might be useful. The second step is the integration of the lattice structures with a suitable transition to the overall component design. The third step is the selection of a suitable lattice structure configuration using scaling laws. The structure database supports the design engineer during this process. Last is the assembly of the lattice structure to a customized, SLM-adapted component design.

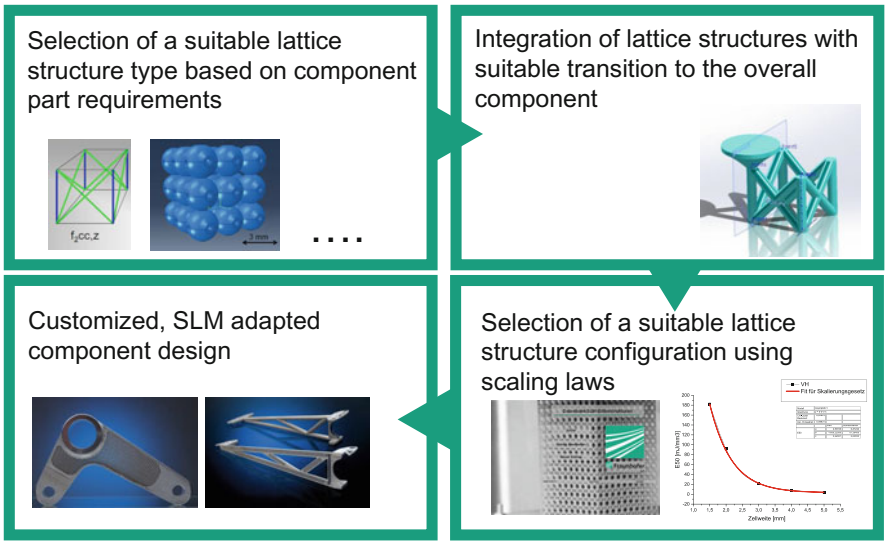

Fig. 2.52 Methodology for component design with customized component functions

2.4.6 High-Manganese Steel Fe-22Mn-0.3C in the Selective Laser Melting (SLM) Process

After the hot working steel X38CrMo5-1, the stainless steel X2CrNiMo17-12-2 and the maraging steel X3NiCoMoTi18-9-5, we introduced the high-manganese steel X30Mn22 to the SLM process for characterization.

High-manganese steels (HMnS) feature mechanical properties of high strength and good ductility. Because of the transformation-induced plasticity (TRIP) and twinning-induced plasticity (TWIP), they have extraordinary strain hardening even under impact conditions. By modifying the chemical composition and annealing parameters and therefore the microstructure, it is possible to adjust the mechanical properties within a wide range to fit specific applications. HMnS are believed to be insusceptible against inner material defects and so feature excellent properties for the AM (Grässel and Frommeyer 1998; Haase et al. 2016).

The X30Mn22 with 22 wt% manganese and 0.3 wt% carbon features a microstructure of metastable austenite and martensite. Under loading conditions, the metastable austenite transforms into martensite, leading to the transformation-induced plasticity of a TRIP steel (Saeed-Akbari et al. 2012).

The first step in characterizing new steel for SLM is an evaluation of process parameters to produce samples with a material density of almost 100 %. Small cubes as samples for the density measurements were manufactured with a M1 Cusing machine (Concept Laser GmbH) and SLM280HL machine (SLM Solutions GmbH). Both machines are equipped with an Yb fiber laser and argon atmosphere. Laser power P_L and focus diameter d_S were constant for all samples at 180 W and

60 µm, respectively. Additionally, the layer thickness D_S was kept constant at 30 µm. The scanning speed v_S varied from 350 to 3000 mm/s, and the scan line spacing Δy_S was varied from 30 to 100 µm. According to the constant and varied process parameter, the build-up rate $\dot{V}$ varied from round about 1–5 mm^3/s and the energy density from 37.5 to 175 J/mm^3.

Figure 2.53 shows exemplarily some micrographs for the density evaluation. Higher density values of almost 100 % are achieved at low scanning speed and small scan line spacing, leading to high energy density values. It was found that the energy density should be between 70 and 110 J/mm^3 to achieve samples of a density higher than 99.9 %. A high scanning speed leads to a smaller energy density and therefore to a smaller melt pool and a thinner scan line, but a high scan line spacing requires a large melt pool for a good bonding between the scan lines.

When scan line spacing and scanning speeds are too high for the deployed laser power, there are gaps between the scan lines and especially between the intersections of the hatching of the layers, leading to a tessellated order of the defects.

As Fig. 2.54 shows, the as-built microstructure features large colonies of fine columnar grains of the same orientation. Because of the rapid solidification of the melt pools and the oriented heat transfer into the already solidified layers below during the process, the colonies are oriented in build direction and exceed the melt

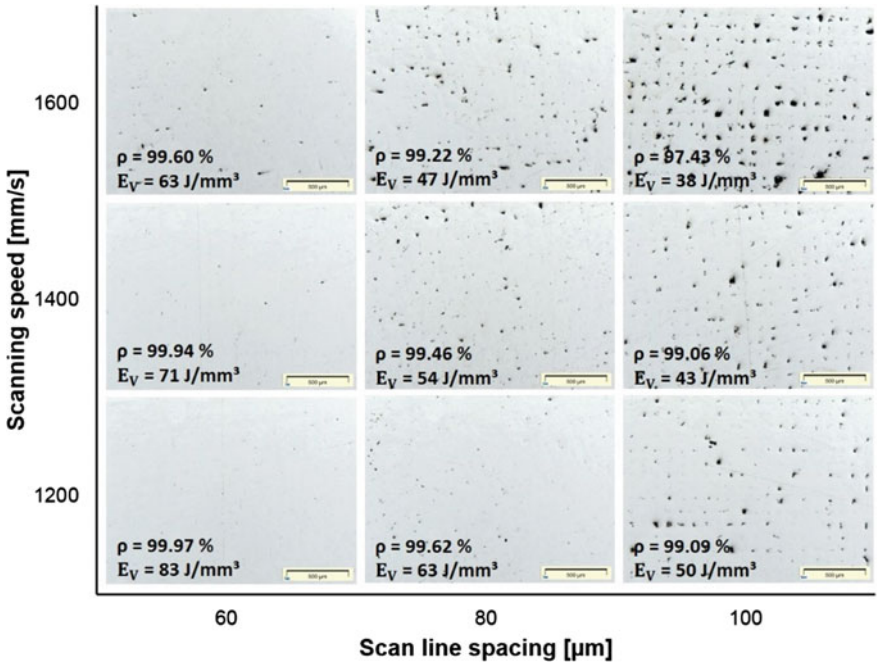

Fig. 2.53 Exemplary micrographs of polished but not etched samples for density measurements sorted by scanning speed and scan line spacing, including the material density ρ and energy density Ev

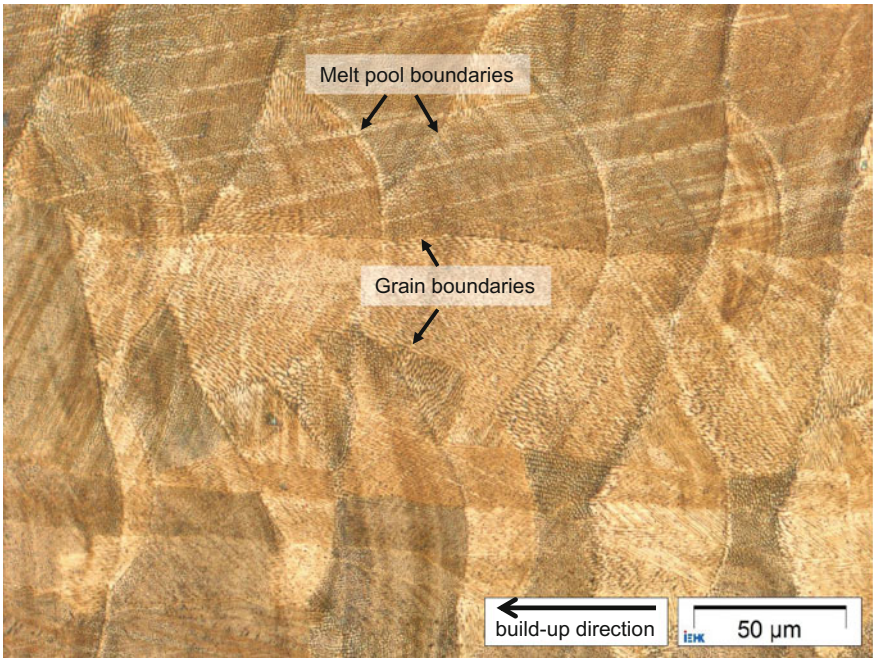

Fig. 2.54 Optical micrograph of melt pool overlap and grain structure of a sample with a material density ρ = 99.98 % and energy density E_v = 105 J/mm^3

pools through multiple layers. No microcracks are visible, and all melt pools and layers form a good metallurgical bond. These structures are found in other SLM-manufactured steels and other metals as well (Yasa et al. 2010; Shifeng et al. 2014; Ma et al. 2015).

Figure 2.55 shows the mechanical properties of the X30Mn22 obtained from tensile tests with DIN EN ISO 6892 B4x20 tensile test samples manufactured in the SLM process. For the tensile test samples, process parameters were used with material density ρ = 99.98 % in density evaluation tests. The samples were generated horizontally (0°), diagonally (45°) and vertically (90°) to accommodate the build direction dependency of the mechanical properties in the SLM process.

The reference is an EN 10002 A30 2.4-mm-thick hot-rolled sheet steel sample of the X30Mn22 along rolling direction (Saeed-Akbari et al. 2012).

The vertical samples with build direction and loading direction being parallel and the diagonal samples reach 1200 MPa before rupture. The horizontally generated samples with build direction and loading direction being perpendicular are the strongest samples with a true stress of circa 1400 MPa like the reference. Total elongation is between 0.2 and 0.3. The vertically generated samples feature the best elongation, while the diagonally are the shortest. The reference exceeds the SLM samples and reaches almost 0.5 of logarithmic strain.

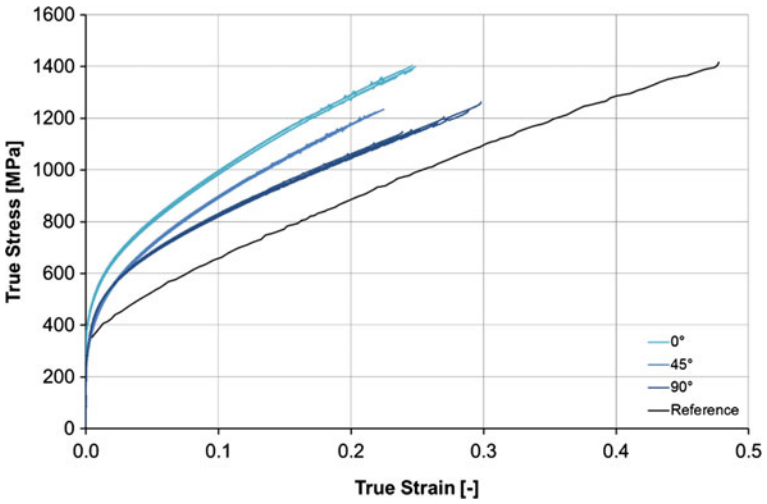

Fig. 2.55 Results of tensile tests of samples with a material density ρ = 99.98 % and energy density E_v = 105 J/mm^3 in three build directions and a sheet steel reference sample of the X30Mn22

The results show the X30Mn22 good excellent mechanical properties like high strength and good ductility in the as-built state after SLM process. But with an additional heat treatment after the SLM process, these properties might be increased even further, and this will be topic of further research.

Distortion in the SLM process is prevented by supporting structures between the component and the substrate plate. Because of the freedom of geometry of the SLM process and thus the possible complexity of the product building the supporting structures is time-consuming and it is not always practicable in providing all the parts of a product with supporting structures or to remove them later—depending on how accessible the product is. The material and process parameter-dependent distortion can be measured with twin cantilever samples (Buchbinder et al. 2011; Leary et al. 2014; Papadakis et al. 2014).

The twin cantilever samples were built with a length of 100 mm and a cantilever thickness of 0.5 and 3 mm, respectively. After cutoff from the substrate plate, the deviation of each cantilever was measured in steps of 10 mm starting in the middle of the samples. Cantilever with a thickness of 3 mm showed only small distortion of less than 1 mm at a length of 50 mm. The 0.5-mm-thick cantilever reached values of almost 2.5 mm. By changing the scanning strategy from 10-mm-long stripes to a 4-mm checkerboard hachure, the deviation of the 0.5-mm cantilevers could be reduced to values of around 1 mm (see Fig. 2.56).

So by altering the scanning strategy, the high deviation of the X30Mn22 could be reduced to tolerable values, making it possible to build complex geometries with without an increased amount of support structures.

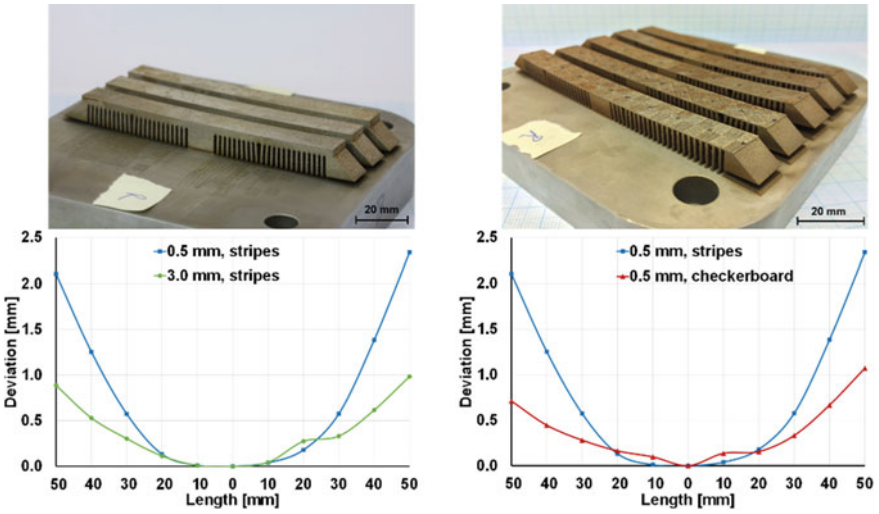

Fig. 2.56 Pictures of twin cantilever samples for distortion measurements of the X30Mn22 after cutoff from the substrate plate and diagrams of the measurements for different cantilever thicknesses and different scanning strategies

2.5 Profitability Assessment as a Contribution to the Theory of Production

SLM is an AM technology that is classified as a primary shaping technology. One major advantage of SLM is the tool-less manufacturing. Only the CAD model of the workpiece and the material in powder state are needed. This directly leads to elimination of tooling costs that belong to the primary drivers of profitability (see Fig. 2.57). The starting material used in the SLM process is a metal powder, which is applied to a build platform in a thin layer (approx. 30–50 µm). According to the CAD information of the workpiece, this powder layer is selectively melted with laser radiation and binds metallurgically with the lower layer. Since the use of series-identical material, functional prototypes and end products can be manufactured in a short amount of times. This directly influences the time-to-market.

Since SLM allows for manufacturing prototypes and end products near-net shape, the effort for additional workpiece finishing processes like machining can be reduced as well. This directly influences the secondary drivers like the main process time. At current state, the material prices for metal powders are higher than for wrought material. SLM allows for saving a high amount of material consumption due its high resource efficiency, which counters the increase in material costs.

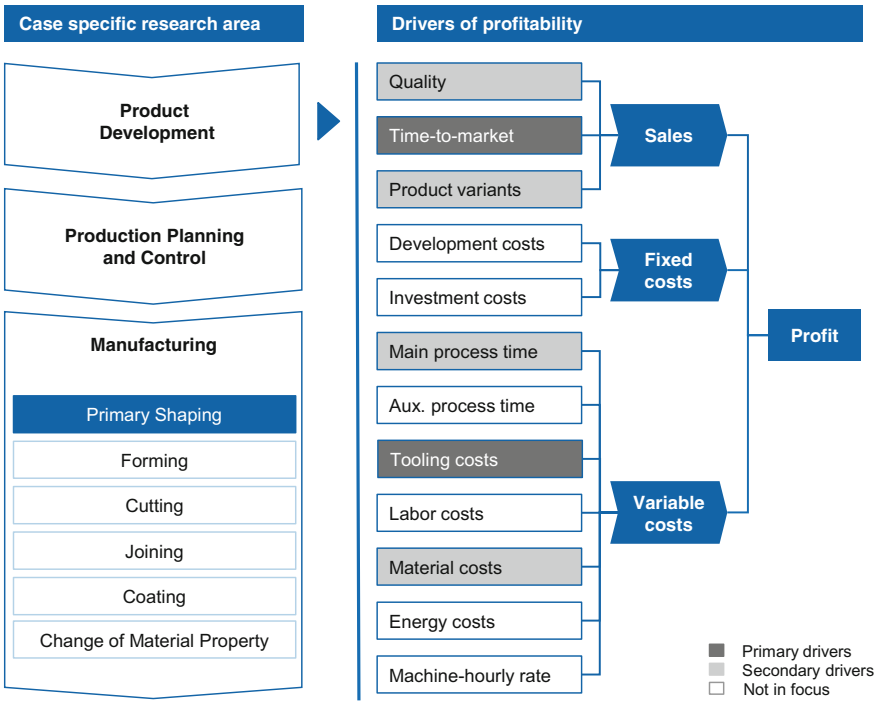

Fig. 2.57 Drivers of profitability within ICD A2 SLM

2.5.1 *Time-to-Market*

SLM has a great influence on the whole product design and development process. In Fig. 2.58, a product lifecycle of conventional manufacturing is displayed against a product lifecycle, which is shortened by means of SLM manufacturing.

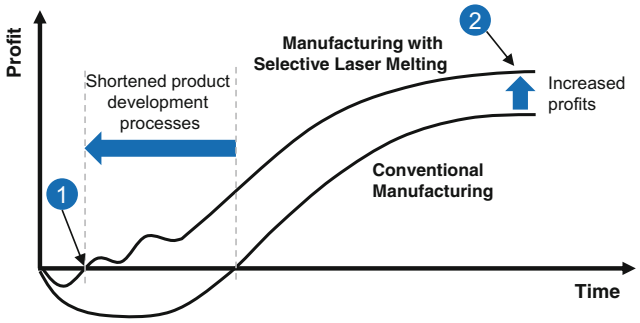

Fig. 2.58 Product life cycles of conventional and SLM manufacturing [modeled after (Schuh et al. 2014)]

The graph of conventional manufacturing begins with high investment during product introduction stage, then grows steeply and finally approaches to a maximum in the stage of maturity. The latter, which refers to SLM production, starts with the alternation of smaller investments, then starts to grow at an earlier point of time and ends with an even higher maximum of profit.

SLM manufacturing allows lower initial investment costs during the introduction stage due the expendability of any tool. Tool-making is a very cost- and time-intensive step in manufacturing, which can be reduced or even displaced by SLM.

Product manufacturing with SLM allows the market entry with many product variants. This enables meeting the customer's demands to a greater degree. Even product design changes proposed by the customers after the product market launch can be implemented into the product.

As a result of the improved customer satisfaction and concurrent product functionality as well as customer demands for integration, a significant increase in profits can be achieved toward the end of the product life cycle.

When using SLM for prototyping during the product design and development process, all experiences gained during this stage can be reused during the real product manufacturing. The effort for SLM process development is the same. This learning rate directly leads to a faster market entry in an early state of the product life cycle [see spot (1) in Fig. 2.58] and ends with higher product maturity, thus leading to higher profits [see spot (2) in Fig. 2.58].

2.5.2 Tooling Costs

The cost of tools, such as for injection molding, makes up a great share of the primary investment costs. They are mainly determined by the tool's geometric complexity, thus leading to high costs and effort for manufacturing this tool. The tool costs consist of personnel costs (design, NC programming, mounting, etc.), material costs (base form), machine hour rates and overhead expenses. The tool investment costs are distributed between the final products (e.g., products produced via injection molding). In conventional manufacturing, the product complexity directly leads to higher costs (see Fig. 2.59, right) as a result of more manufacturing steps and machining operations. Speaking of manufacturing of products—which also can be the tools as a tool manufacturer—the costs of a single SLM-manufactured tool can be more cost-efficient than conventionally manufactured ones (see left graph in Fig. 2.59).

While in the conventional tool-making process, several manufacturing technologies are necessary to shape the final product, SLM manufacturing enables the reduction of the number of needed manufacturing technologies to a minimum. Only functional surfaces of the tool have to be machined after the SLM process. This leads to a reduction of interfaces, like those between the tooling and production department inside the manufacturing company.

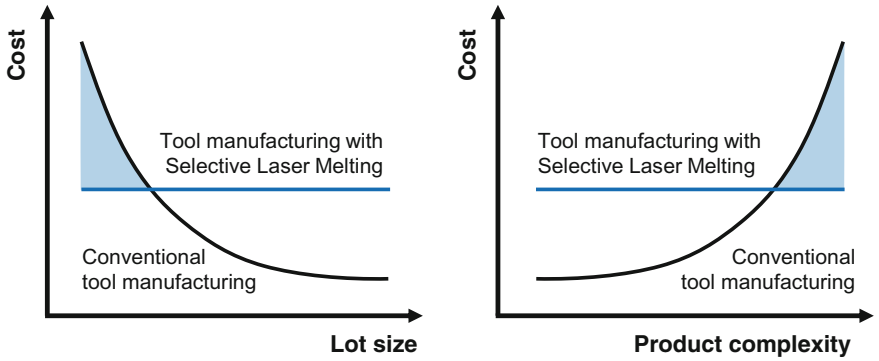

Fig. 2.59 Impact of lot size and product complexity on tool costs

Furthermore, SLM enables the reduction of the number of single parts a tool comprises of. An integral design of tools by means of SLM can replace the modular and layered construction of tools in the future. The number of interfaces can be reduced and allows for manufacturing of integral and monolithic parts, which leads to less or no mounting steps necessary to finish the product. Furthermore, new functionalities can be adapted in the same tool. One example is the integration of geometry and surface-adapted cooling channels, which cannot be produced conventionally (see Fig. 2.60). The conformal cooling channels can improve the heat dissipation during an injection molding process, which directly leads to reduced cycle times and higher lifetimes of tools.

The above-mentioned advantages that SLM-manufactured tools could lead to lower tooling costs.

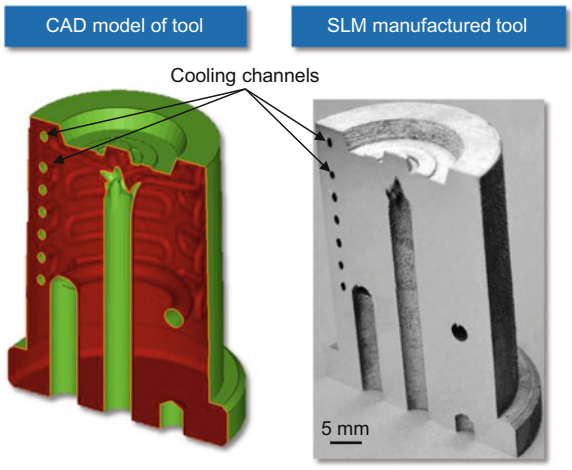

Fig. 2.60 CAD model and photograph of a SLM-manufactured injection molding tool (Bremen et al. 2012)

2.6 Industrial Relevance

Numerous managerial implications arise from the research highlighted in this chapter. Since AM technology is a new manufacturing technology in both an industrial and consumer context, management has to continuously monitor this field and keep learning in order to make well-informed decisions. In our research paper on "Economic Implications of 3D Printing" (Weller et al. 2015a), we thoroughly assessed potential implications on a firm's payoff function when it invests in AM technology. Thus, we could highlight that when prospective market entrants invest in AM technology, they can manufacture with greater flexibility, which, in turn, enables them to offer specific products tailored to individual customers' needs. In summary, we derived patterns of market settings in which AM can best unfold its benefits of individualization, flexibility and complexity at little or no cost at all. In our research papers on WTP [see Weller et al. (2015b) and Weller (2015)], we evaluated whether or not there is a value creation potential for highly customized products ("full customization") while comparing them to standard products and conventional (modular) MC offerings.

The underlying studies provided empirical evidence on how to maximize perceived product value from a consumer's perspective. Practitioners would need to carefully decide on several parameters for designing the solution space in order to maximize value. First, target customer segments (niches) would need to be identified. Then, full customizers would need to carefully choose the products, the type of attributes (i.e., style vs. fit) and the specific continuous options they can customize. Our empirical results highlight that targeting specific customer segments enables additional value upsides of 50–90 %. Further, we could highlight that full customization (vs. conventional modular MC) was valued higher in the case of the espresso cup (Weller et al. 2015b) compared to the kitchen knife (Weller 2015). This suggests that full customization is not a value in itself since the success of customization offerings is highly dependent on the right market (niches) and the product it is offered for. Altogether, we can stress, in line with Piller (2004, p. 316), that "[…] setting the solution space becomes one of the foremost competitive challenges of a mass customization company." This challenge is likely to be even more relevant when co-design freedom is enlarged with a continuous solution space enabled by AM technology.

By complementing their manufacturing processes with SLM, users will likely be able to manufacture complex and individualized components or product variants profitably. The outcomes described here build the practical foundation of the controlling methodology for users so that they can purposefully dimension product development, production and the supply chain. The added value of this approach affects the manufacturing industry in its entirety. Among others, component manufacturers, medical technologies or engine manufacturers can profit from systematically integrating SLM into production, since these branches are characterized by exceptional individualization of demand. Additionally, potential can be derived for

innovative business models based on the models of integrative description of interdependencies within the PPS.

The cost model developed here provides SLM machine operators with a guide to choosing a suitable SLM machine for their intended use, single or (small) series production. In addition to considering the construction space needed for SLM, we have also factored in the laser power and overall productivity of the machine. For SLM machine manufacturers, this cost model can be used to assess and compare current SLM machine generations with each other. From this, further measures can be derived to optimize future and new machine designs.

The novel multi-scanner and multi-beam SLM machines are mainly used in industrial applications that demand high productivity and flexibility with regard to component size, all of which cannot be accomplished with conventional machines.

The productivity gains achieved by HP SLM and the skin–core process control serve, in particular, to produce large-volume components quickly and economically. The main application area is the tool and mold-making industry, in which tool inserts of large dimensions and/or with integrated cooling channels can be generally manufactured additively.

When the mechanical properties and power laws of additively manufactured lattice structures have been qualified, these structures can be used for lightweight construction. These lightweight components are commonly found in, for example, the aerospace and automotive industries. Integrating lattice structures makes it possible to configure the mechanical properties of the components to suit the load.

Under component load, high-manganese steels possess not only great tensile strength, but also high ductility. Due to their robustness against internal component defects, these materials are ideally suited for AM. As a result, new areas for applying AM can be exploited, for example, in the automobile industry as it can put these additively manufactured components to good use thanks to their excellent material-specific properties.

2.7 Future Research Topics

There are several possible avenues which future research on the economic impact of AM could take. For example, analysis is needed on how AM technology will influence different areas, not only in manufacturing, but also on the economy and society as a whole. Key drivers and specific areas for future development should be examined in order to develop what the future of AM holds.

Innovation management would gain a great benefit from better understanding how extant business models are affected by and how new business models can be composed with AM technology. Entrepreneurs can create new concepts of value creation as conventional barriers for accessing manufacturing resources diminish.

Increasingly, more users are gaining access to decentralized production resources (e.g., their own 3D printer, or a digital manufacturing workshop such as a FabLab or TechShop) with a standardized interface: a product's 3D design data. This trend may generate a shift in value creation activities and revenue streams, constituting a promising field for future research (Piller et al. 2015). Rather than selling finished products, firms may concentrate their value-adding activities on offering digital product designs while production occurs locally at the consumer's premises or digital manufacturing workshops close by. In this regard, innovating (lead) users can play an interesting role in future developments of AM. With relatively inexpensive access to local manufacturing resources, lead users (von Hippel 2006) can (i) develop important innovations more easily and turn them into physical products ("user manufacturing") and (ii) commercialize their product innovations ("user entrepreneurs") with AM technology. Hence, such user entrepreneurs may have superior local market knowledge, which allows them to better adjust products to individual needs (Kleer and Piller 2013).

Another interesting question is if there are structural effects that would lead to a shift in value creation activities and revenue streams. By taking into account the whole ecosystem AM technology is involved in, researchers will reap great benefits from an interdisciplinary approach that combines theories from engineering, economics, business management and social sciences.

At this time, manufacturers have little experience making use of AM technologies within their production systems. Therefore, research is currently focused on the qualitative effects that the upcoming integration of SLM into manufacturing will have on the product program, the product architecture, the supply chain and the production structure. With respect to this integration, research regarding the related production systems will benefit from the technology itself as it develops over the next couple of years. The developed PPS builds the theoretical foundation for users so that they can actively facilitate product development as well as dimension production and supply-chain metrics. The theoretical framework for adding SLM into existing manufacturing environments needs to be developed by providing evidence, empirical data, of the complex relationships. Also, since SLM possesses diverse technological development potential, future research should focus on the development of alternative production models based on the approach presented in Sect. 2.4.1 to take substantial changes of the manufacturing system into account. Therefore, the system should also factor in the extensively changing future business models, ones that influence, e.g., the customer's requirements, the product program or the potential markets in terms of the needed complexity.

The cost model used to represent the life cycle manufacturing costs of SLM components should be supplemented with an exact calculation of construction time. The production times listed in the featured cost model result from a number of simplified assumptions of geometry in order to estimate the scanning times and, thus, the construction time. In particular, as components become more complex, the

assumed construction time can deviate from the actual construction time. This is due to the laser–scanner-related delay times, which can account for a large proportion of the total production time. These delay times are dependent on the number and orientation of the individual scan vectors. When the pure scanning time is determined exactly, the unit cost can be calculated more accurately. Likewise, the model should be expanded by adding the ability to calculate the scanning time for innovative exposure concepts, for example, by a multi-spot strategy.

In machine and plant development, in particular, the process development for the multi-spot system stands in the foreground as a further research field. Here, research is focusing on examining the process control for producing dense test samples. In particular, suitable scanning strategies need to be explored, ones that are entirely new because of the individual spots are arranged in a line. Further intensive research is required to understand how both the modulated laser power of each individual spot and the degree of overlap of the individual laser spots influence the melting process. Also, the SLM process development of the multi-scanner system constitutes another focal point of research. Here, novel process control strategies emerge from the specific control of the deflection and energy input of the laser radiation of each laser scanner unit. In particular, the targeted heating and cooling speeds from the leading or trailing laser spot can have a specific influence on the component's characteristics.

The mechanical properties of additively manufactured skin–core components were determined by tensile tests. Other properties, such as the fatigue strength under cyclic loading of skin–core components, must be determined in order to make more comprehensive statements about the probability of failure and load-carrying capacity in real component use.

In addition, research will be testing additively manufactured lattice structures under shear, bending and fatigue loads and analyzing them to determine their failure mechanisms. Furthermore, standardized test methods need to be developed further to augment scaling laws for these types of loads, which can be applied to study the mechanical behavior of additively manufactured lattice structures. Moreover, the mechanical properties of graded materials should be included in further research. The developed hollow spherical structure opens up the field of graded materials due to its structure-specific advantages for flowing variation of its density. To encourage the use of additively manufactured lattice structures components in the industry, research needs to consider non-mechanical properties, such corrosion resistance, as another prospective research field.

By specifically developing the materials used in SLM, researchers need to determine how the alloy can influence the SLM process and what the resulting mechanical properties of the component are. To this end, in addition to targeted materials development, an investigation is needed for suitable heat treatment cycles in order to adjust the mechanical properties of the SLM-generated components by adapting the microstructure.

References

Anderson C (2008) The long tail: Why the future of business is selling less of more, 1, paperback edn. Hyperion, New York, NY

Ashby M (2006) The properties of foams and lattices. Philos Trans R Soc A Math Phys Eng Sci 364(1838):15–30. doi:10.1098/rsta.2005.1678

ASTM International (2015) Standard terminology for additive manufacturing technologies

Baumers M (2012) Economic aspects of additive manufacturing: benefits, costs and energy consumption

Baumers M, Dickens P, Tuck C, Hague R (2016) The cost of additive manufacturing: Machine productivity, economies of scale and technology-push. Technol Forecast Soc Chang 102:193–201

Bechthold L, Fischer V, Greul A, Hainzlmaier A, Hugenroth D, Ivanova L, Kroth K, Römer B, Sikorska E, Sitzmann V (2015) 3D printing—a qualitative assessment of applications, recent trends and the technology's future potential: Studien zum deutschen innovations system. EFI, Berlin

Berman B (2012) 3-D printing: the new industrial revolution. Bus Horiz 55(2):155–162. doi:10.1016/j.bushor.2011.11.003

Bogers M, Hadar R, Bilberg A (2016) Additive manufacturing for consumer-centric business models: Implications for supply chains in consumer goods manufacturing. Technol Forecast Soc Chang 102:225–239. doi:10.1016/j.techfore.2015.07.024

Bohl A (2015) Kennlinien der Produkt- und Produktionskomplexität. Ergebnisse aus der Produktionstechnik, Band 8/2015. Apprimus Verlag, Aachen

Brecher C (ed) (2011) Integrative Produktionstechnik für Hochlohnländer. Springer, Heidelberg (u.a.)

Brecher C (ed) (2012) Integrative production technology for high-wage countries. Springer Berlin Heidelberg, Berlin, Heidelberg

Bremen S, Buchbinder D, Meiners W, Wissenbach K (2011) Mit Selective Laser Melting auf dem Weg zur Serienproduktion? LTJ 8(6):24–28. doi:10.1002/latj.201190072

Bremen S, Meiners W, Diatlov A (2012) Selective laser melting: a manufacturing technology for the future? LTJ 9(2):33–38. doi:10.1002/latj.201290018

Brynjolfsson E, Hu Y, Simester D (2011) Goodbye pareto principle, hello long tail: the effect of search costs on the concentration of product sales. Manag Sci 57(8):1373–1386. doi:10.1287/mnsc.1110.1371

Buchbinder D, Schilling G, Meiners W, Pirch N, Wissenbach K (2011) Untersuchung zur Reduzierung des Verzugs durch Vorwärmung bei der Herstellung von Aluminiumbauteilen mittels SLM. RTejournal—Forum für Rapid Technologie. Online J 8:15

Bültmann J, Merkt S, Hammer C, Hinke C, Prahl U (2015) Scalability of the mechanical properties of selective laser melting produced micro-struts. J Laser Appl 27(S2):S29206. doi:10.2351/1.4906392

Casalino G, Campanelli SL, Contuzzi N, Ludovico AD (2015) Experimental investigation and statistical optimisation of the selective laser melting process of a maraging steel. Opt Laser Technol 65:151–158. doi:10.1016/j.optlastec.2014.07.021

Coelho PS, Henseler J (2012) Creating customer loyalty through service customization. Eur J Mark 46(3/4):331–356. doi:10.1108/03090561211202503

Concept Laser GmbH (2015) Laser melting metal systems. http://www.concept-laser.de/en/industry/automotive/machines.html. Accessed 19 May 2016

DIN (2005) Zuverlässigkeitsmanagement - Teil 3-3: Anwendungsleitfaden – Lebenszykluskosten (60300-3-3)

DIN (2008) Prüfung von metallischen Werkstoffen - Druckversuch an metallischen zellularen Werkstoffen DIN 50134 (50134)

Eibl F (2014) Annual report 2014 Fraunhofer institute for laser technology 2014: SLM exposure design for easy scaling of productivity and building space, Aachen

Eisenhut M, Langefeld B (2013) Additive manufacturing—a game changer for the manufacturing industry?. Roland Berger Strategy Consultants, München

Elberse A (2008) Should you invest in the long tail? Harvard Bus Rev 86(7/8):88–96

EOS GmbH (2015) EOS M 400: product information sheet. http://www.eos.info/m-solutions/download/system_datasheet_EOS_M_400.pdf. Accessed 19 May 2016

Forbes (2013) Full text: president Obama's 2013 state of the union address. http://www.forbes.com/sites/beltway/2013/02/12/full-text-president-obamas-2013-state-of-the-union-address/. Accessed 29 Oct 2015

Franke N, Keinz P, Steger CJ (2009) Testing the value of customization: when do customers really prefer products tailored to their preferences? J Mark 73(5):103–121. doi:10.1509/jmkg.73.5.103

Franke N, Piller F (2004) Value creation by toolkits for user innovation and design: the case of the watch market. J Prod Innov Manage 21:401–415

Franke N, Schreier M (2010) Why customers value self-designed products: the importance of process effort and enjoyment*. J Prod Innov Manage 27(7):1020–1031. doi:10.1111/j.1540-5885.2010.00768.x

Franke N, Schreier M, Kaiser U (2010) The "i designed it myself" effect in mass customization. Manage Sci 56(1):125–140. doi:10.1287/mnsc.1090.1077

Gausemeier J (2013) Thinking ahead the future of additive manufacturing—innovation roadmapping of required advancements: Studie, Paderborn

Gebhardt A (2012) Understanding additive manufacturing: rapid prototyping, rapid tooling, rapid manufacturing. Hanser, Munich

Gebhardt A (2013) Generative Fertigungsverfahren: additive manufacturing und 3D Drucken für prototyping—tooling—Produktion. Carl Hanser Verlag GmbH & Co, KG, München

Gibson I, Rosen D, Stucker B (2015) Additive manufacturing technologies: 3D printing, rapid prototyping, and direct digital manufacturing, 2nd edn. Springer, New York, NY

Gibson LJ, Ashby MF (1999) Cellular solids: structure and properties, 2nd ed, 1st pbk. ed with corr. Cambridge solid state science series. Cambridge University Press, Cambridge, New York

Gobrecht J (2009) Werkstofftechnik - Metalle, 3., überarb. Aufl. Oldenbourg Lehrbücher für Ingenieure. Oldenbourg, R, München

Gordon ME, McKeage K, Fox MA (1998) Relationship marketing effectiveness: the role of involvement. Psychol Mark 15(5):443–459. doi:10.1002/(SICI)1520-6793(199808)15:5<443:AID-MAR3>3.0.CO;2-7

Grässel O, Frommeyer G (1998) Effect of martensitic phase transformation and deformation twinning on mechanical properties of Fe–Mn–Si–AI steels. Mater Sci Technol 14(12):1213–1217. doi:10.1179/mst.1998.14.12.1213

Guan K, Wang Z, Gao M, Li X, Zeng X (2013) Effects of processing parameters on tensile properties of selective laser melted 304 stainless steel. Mater Des 50:581–586. doi:10.1016/j.matdes.2013.03.056

Gümrük R, Mines R (2013) Compressive behaviour of stainless steel micro-lattice structures. Int J Mech Sci 68:125–139. doi:10.1016/j.ijmecsci.2013.01.006

Haase C, Ingendahl T, Güvenç O, Bambach M, Bleck W, Molodov DA, Barrales-Mora LA (2016) On the applicability of recovery-annealed twinning-induced plasticity steels: potential and limitations. Mater Sci Eng A 649:74–84. doi:10.1016/j.msea.2015.09.096

Hao L, Raymont D, Yan C, Hussein A, Young P (2012) Design and additive manufacturing of cellular lattice structures. In: Bártolo P (ed) Innovative developments in virtual and physical prototyping: proceedings of the 5th international conference on advanced research and rapid prototyping, Leiria, Portugal, 28 September-1 October, 2011. CRC Press, Boca Raton, pp 249–254

Holzweissig MJ, Taube A, Brenne F, Schaper M, Niendorf T (2015) Microstructural characterization and mechanical performance of hot work tool steel processed by selective laser melting. Metall and Materi Trans B 46(2):545–549. doi:10.1007/s11663-014-0267-9

Hopkinson N, Hague RJM, Dickens PM (2006) Rapid manufacturing: an industrial revolution for the digital age. John Wiley, Chichester, England

Huffman C, Kahn BE (1998) Variety for sale: mass customization or mass confusion? J Retail 74 (4):491–513. doi:10.1016/S0022-4359(99)80105-5

Jägle EA, Choi P-P, van Humbeeck J, Raabe D (2014) Precipitation and austenite reversion behavior of a maraging steel produced by selective laser melting. J Mater Res 29(17):2072–2079. doi:10.1557/jmr.2014.204

Kaplan RS, Cooper R (1999) Prozesskostenrechnung als Managementinstrument. Campus-Verl, Frankfurt/Main, New York

Kieviet A (2015) Implications of additive manufacturing on complexity management within supply chains in a production environment. Dissertation, University of Louisville

Kleer R, Piller F (2013) Welfare effects of a radical process innovation: benefits of local production by users via 3D printing. Presented at the 73rd annual meeting of the academy of management, Orlando, FL

Lampel J, Mintzberg H (1996) Customizing customization. Sloan Manag Rev 38(1):21–30

Leary M, Merli L, Torti F, Mazur M, Brandt M (2014) Optimal topology for additive manufacture: a method for enabling additive manufacture of support-free optimal structures. Mater Des 63:678–690. doi:10.1016/j.matdes.2014.06.015

Lindemann U, Reichwald R, Zäh M (2006) Individualisierte Produkte – Komplexität beherrschen in Entwicklung und Produktion. Springer-Verlag, Berlin Heidelberg, Berlin, Heidelberg, VDI-Buch

Lipson H, Kurman M (2013) Fabricated: the new world of 3D printing. John Wiley & Sons, Indianapolis, Indiana

Ma M, Wang Z, Gao M, Zeng X (2015) Layer thickness dependence of performance in high-power selective laser melting of 1Cr18Ni9Ti stainless steel. J Mater Process Technol 215:142–150. doi:10.1016/j.jmatprotec.2014.07.034

Meiners W (1999) Direktes selektives Laser-Sintern einkomponentiger metallischer Werkstoffe. Als Ms. gedr. Berichte aus der Lasertechnik, Shaker, Aachen

Merkt S (2016) Qualifizierung von generativ gefertigten Gitterstrukturen für maßgeschneiderte Bauteilfunktionen, RWTH Aachen

Merle A, Chandon J-L, Roux E, Alizon F (2010) Perceived value of the mass-customized product and mass customization experience for individual consumers. Prod Oper Manag 19(5):503–514. doi:10.1111/j.1937-5956.2010.01131.x

Mertens A, Reginster S, Contrepois Q, Dormal T, Lemaire O, Lecomte-Beckers J (2014) Microstructures and mechanical properties of stainless steel AISI 316L processed by selective laser melting. MSF 783–786:898–903. doi:10.4028/www.scientific.net/MSF.783-786.898

Milgrom P, Roberts J (1990) The economics of modern manufacturing: technology, strategy, and organization. Am Econ Rev 80(3):511–528

Mohles V, Facchini L, Vicente N, Lonardelli I, Magalini E, Robotti P, Molinari A (2010) Metastable Austenite in 17-4 precipitation-hardening stainless steel produced by selective laser melting. Adv Eng Mater 12(3):184–188. doi:10.1002/adem.200900259

Murr LE, Martinez E, Hernandez J, Collins S, Amato KN, Gaytan SM, Shindo PW (2012) Microstructures and properties of 17-4 PH stainless steel fabricated by selective laser melting. J Mater Res Technol 1(3):167–177. doi:10.1016/S2238-7854(12)70029-7

Niendorf T, Brenne F (2013) Steel showing twinning-induced plasticity processed by selective laser melting—an additively manufactured high performance material. Mater Charact 85:57–63. doi:10.1016/j.matchar.2013.08.010

Over C (2003) Generative Fertigung von Bauteilen aus Werkzeugstahl X38CrMoV5-1 und Titan TiAl6V4 mit "Selective Laser Melting". Berichte aus der Lasertechnik, Shaker, Aachen

Papadakis L, Loizou A, Risse J, Schrage J (2014) Numerical computation of component shape distortion manufactured by selective laser melting. Procedia CIRP 18:90–95. doi:10.1016/j.procir.2014.06.113

Piller F, Schoder D (1999) Mass customization und electronic commerce: Eine empirische Einschätzung zur Umsetzung in deutschen Unternehmen. Zeitschrift für Betriebswirtschaft 69 (10):1111–1136

Piller FT (2004) Mass customization: reflections on the state of the concept. Int J Flex Manuf Syst 16(4):313–334
Piller FT, Weller C, Kleer R (2015) Business models with additive manufacturing—opportunities and challenges from the perspective of economics and management. In: Brecher C (ed) Advances in production technology. Springer, Cham, pp 39–48
Pine JB (1993) Mass customization. The new frontier of business competition. Harvard University Press, Boston, MA
Rayna T, Striukova L (2014) The impact of 3D printing technologies on business model innovation. In: Benghozi P, Krob D, Lonjon A, Panetto H (eds) Digital enterprise design & management, vol 261. Springer International Publishing, Cham, pp 119–132
Rayna T, Striukova L (2016) From rapid prototyping to home fabrication: How 3D printing is changing business model innovation. Technol Forecast Soc Chang 102:214–224
Rehme O (2007) Cellular design for laser freeform fabrication, Stuttgart
Rehme O (2009) Cellular design for laser freeform fabrication, 1. Aufl. Schriftenreihe Lasertechnik, Bd. 4. Cuvillier, Göttingen
Rehme O (2011) Additive manufacturing zellularer metallischer Strukturen
Rickenbacher L, Spierings A, Wegener K (2013) An integrated cost-model for selective laser melting (SLM). Rapid Prototyping J 19(3):208–214. doi:10.1108/13552541311312201
Roland Berger Strategy Consultants (2013) Additive manufacturing: a game changer for the manufacturing industry? Roland Berger Studie
Saeed-Akbari A, Schwedt A, Bleck W (2012) Low stacking fault energy steels in the context of manganese-rich iron-based alloys. Scripta Mater 66(12):1024–1029. doi:10.1016/j.scriptamat.2011.12.041
Schleifenbaum H, Diatlov A, Hinke C, Bültmann J, Voswinckel H (2011) Direct photonic production: Towards high speed additive manufacturing of individualized goods. Prod Eng Res Devel 5(4):359–371. doi:10.1007/s11740-011-0331-0
Schleifenbaum JH (2012) Verfahren und Maschine zur individualisierten Produktion mit high power selective laser melting, Zugl.: Aachen, Techn. Hochsch
Schrage J (2016) Maschinenspezifische Kostentreiber bei der additiven Fertigung mittels Laser-Strahlschmelzen (LBM). In: Kniffka W, Eichmann M, Witt G (eds) Rapid.Tech—international trade show & conference for additive manufacturing: proceedings of the 13th Rapid.Tech conference erfurt, Germany, 14–16 June 2016. Hanser, Carl, München
Schreier M (2006) The value increment of mass-customized products: an empirical assessment. J Consum Behav 5(4):317–327. doi:10.1002/cb.183
Schuh G, Arnoscht J, Bohl A (2013) Integriertes controlling von Produkt- und Produktionskomplexität. Controlling : Zeitschrift für erfolgsorientierte Unternehmenssteuerung 8(25):450–457
Schuh G, Behr M, Brecher C, Bührig-Polaczek A, Michaeli W, Schmitt R, Arnoscht J, Bohl A, Buchbinder D, Bültmann J, Diatlov A, Elgeti S, Herfs W, Hinke C, Karlberger A, Kupke D, Lenders M, Nußbaum C, Probst M, Queudeville Y, Quick J, Schleifenbaum H, Vorspel-Rüter M, Windeck C (2012) Individualised production. In: Brecher C (ed) Integrative production technology for high-wage countries. Springer, Berlin Heidelberg, Berlin, Heidelberg, pp 77–239
Schuh G, Potente T, Wesch-Potente C, Weber AR, Prote J-P (2014) Collaboration mechanisms to increase productivity in the context of industrie 4.0. Procedia CIRP 19:51–56. doi:10.1016/j.procir.2014.05.016
Shen Y, Cantwell WJ, Mines RA, Ushijima K (2012) The properties of lattice structures manufactured using selective laser melting. AMR 445:386–391. doi:10.4028/scientific5/AMR.445.386
Shifeng W, Shuai L, Qingsong W, Yan C, Sheng Z, Yusheng S (2014) Effect of molten pool boundaries on the mechanical properties of selective laser melting parts. J Mater Process Technol 214(11):2660–2667. doi:10.1016/j.jmatprotec.2014.06.002

SLM Solutions Group AG (2015) SLM 500 HL selective laser melting system: product information sheet. http://slm-solutions.com/sites/default/files/attachment/page/2016/01/slm_500_english.pdf. Accessed 19 May 2016

Steiner F (2014) Solution space development for mass customization: Impact of continuous product change on production ramp-up. Schriftenreihe innovative betriebswirtschaftliche Forschung und Praxis, vol 413. Kovač, Hamburg

The Economist (2011) Print me a stradivarius: how a new manufacturing technology will change the world. The Economist

Thomas DS, Gilbert SW (2014) Costs and cost effectiveness of additive manufacturing. National Institute of Standards and Technology

Ulrich KT (2011) Design: creation of artifacts in society. University of Pennsylvania, Pennsylvania

Von Hippel E (2006) Democratizing innovation, 1. MIT Press paperback ed. MIT Press, Cambridge, Mass

Wang Z, Chen L, Zhao X, Zhou W (2014) Modularity in building mass customization capability: the mediating effects of customization knowledge utilization and business process improvement. Technovation 34(11):678–687. doi:10.1016/j.technovation.2014.09.002

Wei Q, Li S, Han C, Li W, Cheng L, Hao L, Shi Y (2015) Selective laser melting of stainless-steel/nano-hydroxyapatite composites for medical applications: Microstructure, element distribution, crack and mechanical properties. J Mater Process Technol 222:444–453. doi:10.1016/j.jmatprotec.2015.02.010

Weller C (2015) Economic perspectives on 3D printing. Dissertation, RWTH Aachen University

Weller C, Kleer R, Piller FT (2015a) Economic implications of 3D printing: market structure models in light of additive manufacturing revisited. Int J Prod Econ 164:43–56. doi:10.1016/j.ijpe.2015.02.020

Weller C, Kleer R, Piller FT (2015b) Economic value of digitized manufacturing: product customization with 3D printing. Presented at the 75th annual meeting of the academy of management, Vancouver, BC

Wohlers T (2015) Wohlers Report 2015: 3D printing and additive manufacturing state of the industry; annual worldwide progress report. Fort Collins, Wohlers Associates

Yadroitsev I, Smurov I (2010) Selective laser melting technology: from the single laser melted track stability to 3D parts of complex shape. Phys Procedia 5:551–560. doi:10.1016/j.phpro.2010.08.083

Yasa E, Kempen K, Kruth J-P, Thijs L, van Humbeeck J (2010) Microstructure and mechanical properties of maraging steel 300 after selective laser melting. In: SFF symposium, Solid Freeform Fabrication, 2010, Austin

Zaichkowsky JL (1985) Measuring the involvement construct. J Consum Res 12(3):341. doi:10.1086/208520

Zhang B, Dembinski L, Coddet C (2013) The study of the laser parameters and environment variables effect on mechanical properties of high compact parts elaborated by selective laser melting 316L powder. Mater Sci Eng, A 584:21–31. doi:10.1016/j.msea.2013.06.055

http://www.springer.com/978-3-319-47451-9

Integrative Production Technology
Theory and Applications
Brecher, C.; Özdemir, D. (Eds.)
2017, XXXIX, 1100 p. 651 illus., 482 illus. in color.,
Hardcover
ISBN: 978-3-319-47451-9